DISSERTATION

SAND DISPERSION IN A LABORATORY FLUME

Submitted by

Tsung Yang

In partial fulfillment of the requirements

for the Degree of Doctor of Philosophy

Colorado State University

Fort Collins, Colorado

May 1968

ABSTRACT OF DISSERTATION

SAND DISPERSION IN A LABORATORY FLUME

This study is concerned mainly with the longitudinal dispersion of sand particles along the bed of an alluvial channel under conditions of steady, uniform flow. Attention is focussed on developing a general one-dimensional stochastic model to describe and predict the longitudinal dispersion process. The method of approach used by Sayre and Conover (1967) for a two-dimensional stochastic model, which described the movement of sand particles along an alluvial bed, is adapted here for the development of a general one-dimensional stochastic model. The parameters used in this general one-dimensional stochastic model can be obtained either from longitudinal dispersion and transport data, or from bed configuration data, or from a combination of both. The statistical analysis of ripple bed configurations indicates that the distribution of bed elevation closely follows a normal distribution, and may possess the ergodic property.

The Aris moment equations are used to solve the problem of sand dispersion along an alluvial bed as a special case of the problem of dispersion of suspended sand particles near the bed. The Aris moment equations used in this study are modified forms of the conservation of mass equations for the transport, deposition, and re-entrainment of suspended sediment. When appropriate initial and boundary conditions are used, there is excellent agreement between solutions of the Aris moment equation and results given by the general one-dimensional stochastic model.

Fine, medium, and coarse sized radioactive sand grains were used as tracer particles in experiments at two different flow conditions, namely, ripple and dune conditions. In spite of the irregularities of the experimental longitudinal dispersion curves caused by the irregularities of the bed configurations, the mean longitudinal displacement and the variance of the longitudinal distribution of the tracer particles were found to increase linearly with time, as required by the stochastic model. The shape of the experimental longitudinal dispersion curves could also be fairly well represented by the general one-dimensional stochastic model.

Tsung Yang
Department of Civil Engineering
Colorado State University
Fort Collins, Colorado
May 1968

ACKNOWLEDGMENTS

With sincere gratitude, the writer acknowledges all the assistance he has received in his research. Special thanks are due to Dr. W. W. Sayre of the U.S. Geological Survey for his helpful guidance, advice and encouragement throughout the experimental work and in the analysis and interpretation of the results.

Acknowledgment is due to Mrs. L. J. Niemann for the many hours she has devoted to helping the writer in developing the computer programs used in this study. Appreciation is also expressed to the members of the Graduate Committee, Professor H. W. Shen, the writer's major professor, and Professors D. B. Simons, E. V. Richardson, V. A. Sandborn and P. W. Mielke, for their review and constructive criticism of the dissertation. Dr. C. F. Nordin's suggestions and Mr. D. K. Collins' editorial assistance are also appreciated.

Gratitude is also expressed to those people who helped in the collection of the data. They are: Dr. R. E. Rathbun, Mr. J. P. Bennett, Mr. W. E. Gaskill, Mr. N. S. Grigg, Mr. Z. K. Mughrabi, Mr. C. H. Neuhauser, and Mr. C. A. Ramirez.

The writer thanks the U.S. Geological Survey for the financial support which made this study possible.

TABLE OF CONTENTS

TABLE OF CONTENTS - Continued

TABLE OF CONTENTS - Continued

LIST OF TABLES

LIST OF FIGURES

LIST OF FIGURES - Continued

LIST OF FIGURES - Continued

LIST OF SELECTED SYMBOLS

Symbol	Definition	Dimensions
C	Concentration of sediment at a point in weight per unit volume	F/L^3
C_p	p'th moment of longitudinal concentration distribution taken about $\xi = 0$	F/L^3
D	Coefficient of diffusion averaged over the depth of flow	L^2/T
d	Average depth beneath the surface of the bed through which tracer particles are distributed	L
$f( )$	Probability-density function	
$\{f( )\}^{n*}$	n-fold convolution of the probability-density function	
$F( )$	Distribution function (cumulative probability-density function)	
i	Number of steps or rest periods associated with the movement of a sand particle	
i_c	Fraction, by volume, of bed material particles within the size range of the tracer particles	
k_1	Parameter in concentration-distribution and related functions	L^{-1}
k_2	Parameter in concentration-distribution and related functions	T^{-1}
n	Particular number of steps or rest periods associated with the movement of sand particle	
$P( )$	Probability	
r	Parameter in concentration-distribution and related functions	
S	Skew coefficient for longitudinal concentration distribution curves and related functions	
t	Dispersion time	T

LIST OF SELECTED SYMBOLS - Continued

Symbol	Definition	Dimensions
T	Random variable denoting the duration of a rest period	T
U	Time-averaged local velocity of flow in the x-direction	L/T
$\overline{U}$	Cross-sectional average of U	L/T
U_s	Time-averaged local velocity of sediment particle	L/T
$\overline{U}_s$	Cross-sectional average of U_s	L/T
U_τ	Shear velocity in a wide, open channel defined as $\sqrt{gy_n S_e}$	L/T
V_s	Settling velocity of a sediment particle in water	L/T
W	Amount of sediment stored per unit area of bed surface	F/L^2
W_p	p'th moment of longitudinal distribution of W, taken about $\xi=0$	F/L^2
w	A subscript, denoting the deposited sand	
x,y,z	Distance coordinates in the longitudinal, vertical and lateral directions, respectively	L
y_n	Normal depth of flow in an open channel	L
α	Bed absorbency coefficient representing the probability that a particle of sediment coming into contact with the bed is deposited	
β	Dimensionless fall velocity parameter, defined as $V_s/\kappa U_\tau$	
γ	Dimensionless entrainment-rate coefficient, defined so that γW is the mean rate of entrainment	
γ_s	The specific weight of the bed material	F/L^3

LIST OF SELECTED SYMBOLS - Continued

Symbol	Definition	Dimensions
$\varepsilon_x, \varepsilon_y, \varepsilon_z$	Local diffusion coefficient in the longitudinal, vertical and lateral direction, respectively	L^2/T
η	Dimensionless vertical distance coordinate, defined as y/y_n	
κ	von Karman turbulence coefficient	
λ	The fraction of volume of bed material, in place, not occupied by particles (porosity)	
μ	Dimensionless mean velocity of flow defined as $\bar{U}y_n/D$	
$\mu\chi$	Dimensionless local velocity of flow	
ν_s	Dimensionless settling velocity of sediment in water, defined as $V_s y_n/D$	
ξ	Dimensionless longitudinal distance coordinate, defined as $(x - \bar{U}t)/y_n$	
σ_w^2	Dimensionless variance of longitudinal concentration distribution of sediment	
σ_x^2	Variance of longitudinal concentration distribution of sediment	L^2
τ	Dimensionless dispersion time, defined as Dt/y_n^2	
χ	Weighting function for the local velocity, defined as $(U-\bar{U})/\bar{U}$	
ϕ	Conversion factor, defined as $\frac{6y_n}{\kappa U_\tau}$	
ψ	Weighting function for the local diffusion coefficient, defined as ε_y/D	
ψ_3	Parameter, defined as $\frac{r+2}{r+1} \quad \frac{1}{S\sqrt{t}}$	$T^{-\frac{1}{2}}$

Chapter I

INTRODUCTION

The behavior of sediment in an alluvial channel has long been a research subject for both engineers and geologists. The movement of sediment combines the action of rolling, sliding, jumping and sometimes even suspension. Regardless of the mode of movement, when a sediment particle is deposited and stays on the bed surface, it will usually be covered by other sediment particles that are deposited later. This buried particle will be re-exposed and move again only after all the particles covering it have been scoured away. Since each particle deposits at a different location on the bed, the time duration that particles remain buried will differ. As a result of this phenomenon, and since the particles do not all move the same distance when they move, the particles move at different average rates. This is the main mechanism which causes sediment particles to disperse. The application of sedimentation theories can be found in various areas, such as in the determination of geometrical shape of a channel cross section, in the determination of river meandering, and in the effects of sediment transportation on hydraulic structures.

A recent application of the theories of movement and dispersion of sediment is in the water pollution problem. Together with the increase in population and industrial prosperity, the demand of usable

water increases rapidly. It is an engineer's responsibility to use every practical method to satisfy these growing demands on the water supply. However, if pollution is not controlled, the availability of usable water may be sharply curtailed. The permissible limit of the concentration of contaminants in a river depends on its ability to transport and disperse these contaminants. Most of the dispersion studies so far have been concerned with those contaminants which can be dissolved or suspended in water and move at the same velocity as the water. Less work has been done with those contaminants which can be absorbed by bed material and move with the bed material.

Due to the complex nature of the movement of sediment in alluvial channel flow, different investigators tackle this problem from different angles. Some start from the mechanics point of view to explain the movement of sediment, some classify this movement according to the bed configurations, and some make judgments from experience alone. No satisfactory agreement among these methods of investigation has ever been achieved. Since the movement of sediment in an alluvial channel is so irregular and random, the stochastic approach has recently been adopted by a few mathematicians and engineers to give a more realistic description of this movement.

In order to understand the movement and dispersion process of those contaminants which move with the bed material, the movement and dispersion process of the sand along an alluvial channel should be studied first. This report starts with a review of the theories

related to the movement and dispersion of sand along the bed of an alluvial channel. A general one-dimensional stochastic model is developed to simulate this process. For the purpose of testing the assumptions made in this stochastic model and comparing this stochastic model to actually measured longitudinal concentration distributions, some supplementary investigations were also made. These supplementary investigations include some preliminary studies of the step length and rest period of a single plastic particle, the bed configurations, the vertical concentration distribution of tracer particles in the sand bed along the flume, and the total sediment discharge. A numerical solution of Aris' moment equations, which is used in this study as a modified form of the conservation of mass equations for the transport, deposition, and re-entrainment of suspended sediment, is also compared with the stochastic model.

This investigation is restricted to a consideration of the dispersion of sand in an alluvial channel with a uniform, two-dimensional, turbulent shear flow. The initial condition is a line source of radioactive sand tracer particles distributed on the bed across the flume. Fine, medium, and coarse size sand tracer particles are used for ripple bed conditions. Only the results for the medium and coarse size sand tracer particles are reported for dune bed conditions to avoid the problem of significant quantities of tracer particles being transported in suspension. This study was supported by the Water Resources Division of the U.S. Geological Survey in Fort Collins, Colorado.

Chapter II

REVIEW OF LITERATURE

A. The Movement of Sand Along an Alluvial Bed

The behavior of sediment moving along an alluvial bed is very complicated. It combines the action of rolling, sliding, jumping and sometimes even suspension. The basic requirement to start a sediment particle moving is that the drag force and the intensity of turbulence in the vicinity of that particle must be sufficient to overcome the inertial and frictional forces acting on that particle.

In order to have a better understanding of this kind of movement, it is necessary to study the bed configurations, because they are closely related to the movement of sediment. Simons and Richardson (1960) classified the bed forms of alluvial channels into ripples, dunes, plane bed, standing waves and antidunes.

For the ripple case, the suspended load is small, and the velocity of water is low. Most of the grains on the bed surface roll and slide; a few grains make short jumps.

For the dune bed, more grains make jumps which are longer than in a ripple bed, and the suspended load is increased. If the velocity is increased, a plane bed may develop.

In the plane bed condition, the grains in the upper layer of the bed are in almost continuous movement. In the standing waves or antidune case, intense turbulence is created, so that the concentration of

the suspended load is very high. This kind of classification gives only a qualitative description of the movement of sand along an alluvial bed. This is usually not sufficient for engineering purposes.

B. The Concept of Entrainment and Deposition

Regardless of the kind of bed form, the movement of grains starts with entrainment into the flow and stops with deposition on the bed. Thus, entrainment includes all kinds of movement of sand along and above the bed surface, such as rolling, sliding, jumping and suspension. The concept of entrainment has been discussed by Lane and Kalinske (1939) among others. They hypothesized that grains are picked up from the bed surface and kept in suspension by turbulent eddies. The rate of pickup (entrainment) is proportional to the intensity of the vertical velocity components due to the turbulent eddies. For an equilibrium condition, the rate of entrainment of sediment must be equal to the rate of deposition on the bed surface. O'Brien (1933) assumed that the rate of pickup of a given type of sediment depends only upon the characteristics of the flow, and so for steady uniform flow under equilibrium condition, the rate of pickup equals the rate of deposit and is a constant expressed mathematically as

$$\varepsilon_y \left(\frac{\partial C}{\partial y}\right)_{y=0} = -V_s \, C_{y=0} \qquad (2\text{-}1)$$

where ε_y is the exchange coefficient or the coefficient of eddy diffusivity in y direction, $C = C(y)$ is the concentration of sediment

in suspension, and V_s is the fall velocity of sediment in water. The minus sign indicates that the net transport by diffusion is in the direction of decreasing sediment concentration.

Hubbell and Sayre (1964) described the movement of bed material particles as consisting of an alternating sequence of steps and rest periods, where both the step lengths and rest periods are random variables. Physically, a particle may roll along the bed or be entrained temporarily in the flow and then rest on the bed where it will remain, usually becoming covered by other particles until it is re-exposed and takes another step. Thus, the motion of a grain can be described in terms of step lengths and rest periods provided that the aggregate resting time is large in comparison to the aggregate time spent in motion.

C. One-Dimensional Stochastic Model

After realizing the complexity of the movement of sediment and introducing the concept of step lengths and rest periods, the development of a statistical model to describe the displacement, x, of sediment along an alluvial bed at a particular time, t, is needed. Hubbell and Sayre (1964) presented a one-dimensional stochastic model for the transport of bed-material sediment particles in an alluvial channel wherein the transport of a particle is described as an alternating sequence of step lengths and rest periods. The assumptions are:

1. The flow condition is steady and uniform.
2. Both the step lengths and rest periods are exponentially and independently distributed with mean step length $1/k_1$ and mean rest period $1/k_2$.

3. The time spent in moving is so short in comparison to the rest period that it can be neglected.

Under these assumptions and using the concepts of joint and conditional probability, the density function for the probability that a particle has traveled a distance x in time t was found to be

$$f_t(x) = k_1 e^{-(k_1 x + k_2 t)} \sum_{n=1}^{\infty} \frac{(k_1 x)^{n-1}}{\Gamma(n)} \frac{(k_2 t)^n}{n!} \quad , x > 0 \qquad (2\text{-}2)$$

Equation (2-2) applies only to particles that have taken at least one step. This result was identical to one obtained by Einstein (1937) by a different method.

Todorović (1967) started with a more general proposition where the time a particle spent in traveling is not neglected, and he obtained Eq. (2-2) as the upper boundary, i.e., a special case where the time spent in traveling can be neglected.

D. Total Sediment Discharge Equation

When the flow condition is in equilibrium and the tracer particles have the same properties as sand of the same size, a continuity equation based on the tracer study can be used to calculate the total sediment discharge. Hubbell and Sayre (1964) used a continuity equation

$$(Q_s)_c = i_c (\gamma_s)_c (1-\lambda) \, Bd \left(\frac{\bar{x}}{t}\right)_c \qquad (2\text{-}3)$$

to calculate the total sediment discharge of a certain characteristic. In Eq. (2-3), Q_s is the total sediment discharge, i_c is the ratio of the volume of particles possessing the characteristic to the volume of bed material particles in the zone of particle movement, γ_s is the specific weight of the bed material, λ is the porosity, B is the width of the channel, d is the average depth of zone in which particle movement occurs, $\overline{x}/t$ is the average rate of movement during a total elapsed time and c is a subscript that denotes terms associated with the particles possessing the characteristics. Combining Eq. (2-3) with the result from the Hubbell-Sayre one-dimensional stochastic model gives the total amount of sediment discharge for all the sizes in the channel as

$$Q_s = \sum_c i_c (\gamma_s)_c (1-\lambda)\, Bd \left(\frac{k_2}{k_1}\right)_c . \qquad (2\text{-}4)$$

E. The Dispersion of Suspended Particles

The general equation for dispersion in open-channel flow is

$$\frac{\partial C}{\partial t} + U \frac{\partial C}{\partial x} = \frac{\partial}{\partial x}\left(\varepsilon_x \frac{\partial C}{\partial x}\right) + \frac{\partial}{\partial y}\left(\varepsilon_y \frac{\partial C}{\partial y}\right) + \frac{\partial}{\partial z}\left(\varepsilon_z \frac{\partial C}{\partial z}\right) \qquad (2\text{-}5)$$

where ε_x, ε_y and ε_z are the coefficients of eddy diffusivity in the x, y and z direction, respectively, and $U = U(y,z)$ is the velocity of flow. Equation (2-5) is valid when the foreign particles used in the dispersion study have the same density as the fluid and are

completely responsive to the turbulent motion of the fluid. When the particles are dense and large enough to have a terminal settling velocity V_s, which cannot be neglected in comparison with the eddy velocities, the plume of particles as a whole tends to settle toward the bottom of the channel. In the study of the movement and dispersion of sand along an alluvial channel, the fall velocities of sediment particles are large enough so that most of the sediment particles are moving along the bed. If the sediment particles are suspended at all, they are suspended only very near the bed surface. In this limiting case the study of dispersion of suspended particles relates to the study of dispersion of sand along an alluvial bed.

The effect of fall velocity can be accounted for in the diffusion equation by introducing a convective term $V_s C$. For a uniform two-dimensional flow in the x direction with $\frac{\partial U}{\partial z} = 0$ and $\frac{\partial C}{\partial z} = 0$. Eq. (2-5) becomes, for suspended sediment,

$$\frac{\partial C}{\partial t} + U_s \frac{\partial C}{\partial x} = \varepsilon_{s_x} \frac{\partial^2 C}{\partial x^2} + \frac{\partial}{\partial y}\left(\varepsilon_{s_y} \frac{\partial C}{\partial y}\right) + V_s \frac{\partial C}{\partial y} \quad . \qquad (2\text{-}6)$$

Here, the subscript s refers to sediment particles, and $U_s = U_s(y)$. Brush (1962) and Sayre (1968) concluded that the reduction in response of a sediment particle to eddy motion due to its inertia decreases with decreasing particle size, and may be neglected when the diameter of sediment particles is less than about 0.2 mm. Thus, for such particles at any particular point in the fluid, it may be assumed that $\varepsilon_{s_x} = \varepsilon_x$, $\varepsilon_{s_y} = \varepsilon_y$ and $U_s = U$. However, the average velocity of all the

suspended sediment is not the same as that of the fluid. The average velocity of sediment over the depth of flow is

$$U_s = \frac{\int_0^{y_n} UC \, dy}{\int_0^{yn} C \, dy} \tag{2-7}$$

where y_n is the normal depth of the flow. Whenever there is entrainment and/or deposition, there must be an exchange existing between the boundary of flow and the alluvial bed. Equation (2-6) is valid only for the sediment particles that are entrained in the flow.

F. De Vries' Diffusion Theory

In 1966, De Vries developed a diffusion model for the dispersion of bed material particles with the following assumptions:

1. The transport condition is homogeneous in time and space.
2. Variations perpendicular to the main current will be neglected.
3. The bed material is uniform.
4. The tracer material has the same transport characteristics as the bed material.
5. The amount of input of tracer material is small, and the tracer concentrations are small compared to unity, so they do not influence the transport phenomenon.

De Vries started with the equation of continuity and the equation of motion to get

$$\frac{\partial \overline{C}}{\partial t} - D \frac{\partial^2 \overline{C}}{\partial x^2} + w \frac{\partial \overline{C}}{\partial x} = 0 \tag{2-8}$$

where $\overline{C}$ is the average concentration over a cross section

D is the coefficient of diffusion in L^2/T

w is the horizontal sand velocity in L/T .

The initial condition is

$$\overline{C}\ (x\ ,\ 0) = 0 \tag{2-9}$$

and the two boundary conditions are: (1) the concentrations are finite for every x and t , and (2) there is an instantaneous source, namely,

$$\overline{C}\ \ (\infty,\ t) = 0 \tag{2-10}$$

and

$$w\overline{C}\ (0,\ t) - D\ \frac{\partial \overline{C}(0,t)}{\partial x}\ = \delta(t)\ \ \frac{W_*}{Bd} \tag{2-11}$$

where W_* is the total weight of tracer particles released from the source, B is the width of the channel and d is the average depth beneath the bed surface to which the tracer particles are distributed, $\delta(t)$ is a Dirac delta function in T^{-1}.

The solution of Eq. (2-8) with these initial and boundary conditions is

$$\overline{C}(x,t) = \frac{W_*}{Bd}\left\{ \frac{1}{\sqrt{\pi Dt}}\ \exp\left[-\left(\frac{x-wt}{2\sqrt{Dt}}\right)^2\right] - \frac{w}{2D}\exp\left(\frac{xw}{D}\right)\operatorname{erfc}\left[\frac{x+wt}{2\sqrt{Dt}}\right]\right\} \tag{2-12}$$

which is De Vries' one-dimensional diffusion model.

G. The Comparison Between Stochastic Model and Diffusion Model

Having reviewed Hubbell and Sayre's one-dimensional stochastic model and De Vries' one-dimensional diffusion model, it is interesting to consider the similarities and differences of these two approaches.

From Eq. (2-2), the concentration of tracer particles, defined as the weight of tracer particles per unit volume of bed material, is

$$\overline{C}\ (x,t) = \frac{W_*}{Bd}\ f_t\ (x)$$

$$= \frac{W_*}{Bd}\ k_1 e^{-(k_1 x + k_2 t)} \sum_{n=1}^{\infty} \frac{(k_1 x)^{n-1}}{\Gamma(n)}\ \frac{(k_2 t)^n}{n!}\ ,\ x > 0 \qquad (2\text{-}13)$$

De Vries (1965) found the following asymptotic relationships between Eq. (2-12) and (2-13):

$$w = \frac{k_2}{k_1} \quad \text{for every } x \text{ and } t \qquad (2\text{-}14)$$

and

$$D = \frac{k_2}{k_1} \qquad (2\text{-}15)$$

The similarities between these two models are:

1. The location of the mode of the concentration curve described by both models is similar for $k_2 t \geq 200$.
2. The decay of the relative peak concentration for both models is almost the same when $k_2 t \geq 5$.
3. Neither model can be expected to apply near the source.

The differences between these two models are:

1. The difference in the decay of the relative peak concentration between two models increases with decreasing $k_2 t$ value when $k_2 t < 5$. At $k_2 t = 2$, the relative peak concentration obtained from the stochastic model equals 1.15 times the value obtained from the diffusion model.

2. The mode of the concentration curve described by the diffusion model moves faster than the stochastic model at small values of k_2t.
3. For the diffusion model, an artifical boundary condition, Eq. (2-11), was applied which acted as a reflecting barrier at the source that did not permit particles diffusing in the upstream direction to pass the source but reflects them back in the downstream direction. For the stochastic model, no such assumption was made.

The method of approach in both models is good. The diffusion model is more familiar to most engineers, but the boundary condition, Eq. (2-11), is not true in actuality. The stochastic model is more realistic, but the assumption that the step length and rest period both follow the exponential function is open to question.

Chapter III

ANALYTICAL INVESTIGATIONS

A. General One-Dimensional Stochastic Model for the Transport and Dispersion of Bed-Material Sediment Particles

As mentioned at the end of the preceding chapter, Hubbell and Sayre's (1964) assumption of exponentially distributed step lengths and rest periods is open to question. Because of this, a set of preliminary experiments for the step length and rest period was made with colored lightweight plastic particles in the summer of 1966 (unpublished) at the Engineering Research Center, Colorado State University. Attention was focused on individual particles, and step lengths and rest periods were actually measured. The results of these experiments indicated that the distribution of rest periods followed the exponential function, but the step lengths can be represented better by the gamma distribution than by the exponential function. Therefore, a modified stochastic model is developed here.

In order to make the model more general to fit any distribution function, the method of approach used by Sayre and Conover (1967) for a two-dimensional model is adopted here for our one-dimensional model. As mentioned before, a sediment particle moves along an alluvial bed in an alternating sequence of steps and rest periods. Let us define

$\{X_i: i=1,2,3, \ldots\}$ as a set of random variables describing step lengths which are independently and identically distributed according to the probability density function $f_X(x)$, and $\{T_i: i=1,2,3 \ldots\}$ as a set of random variables describing rest period durations which are independently and identically distributed according to the probability density function $f_T(t)$. If the initial condition is that the process starts with a rest period, then the total displacement for a particle after n steps from the origin is

$$x(n) = \sum_{i=0}^{n} X_i = \sum_{i=1}^{n} X_i \quad . \tag{3-1}$$

The probability that the particle has traveled a distance equal to or less than x at time t is

$$F_t(x) = \sum_{n=0}^{\infty} P\left[\sum_{i=0}^{N(t)} X_i \leq x, \; N(t) = n \right] \tag{3-2}$$

where $P[\ ]$ denotes probability, and N(t) is the number of steps taken by the particle in time t.

By using the definition of conditional probability, Eq. (3-2) becomes

$$F_t(x) = \sum_{n=0}^{\infty} P\left[\sum_{i=0}^{N(t)} X_i \leq x \;\middle|\; N(t) = n \right] P\left[N(t) = n \right] \tag{3-3}$$

which is equivalent to

$$F_t(x) = \sum_{n=0}^{\infty} P\Big[\sum_{i=0}^{n} X_i \leq x\Big] \; P\Big[N(t) = n\Big]$$

$$= \sum_{n=1}^{\infty} P\Big[\sum_{i=1}^{n} X_i \leq x\Big] \; P\Big[N(t) = n\Big]$$

$$+ P\Big[X_0 \leq x\Big] \; P\Big[N(t) = 0\Big] . \qquad (3\text{-}4)$$

Since the step lengths are independently and identically distributed, by the addition theorem for independent, identically distributed random variables,

$$P\Big[\sum_{i=1}^{n} X_i \leq x\Big] = \Big\{F_X(x)\Big\}^{n^*} = \int_0^x \Big\{f_X(x')\Big\}^{n^*} dx' , \qquad (3\text{-}5)$$

where $\{f_X(x')\}^{n^*}$ is the n-fold convolution of the probability density function for the length of a single step length. This is equal to the probability density function for the distance traveled by the particle in n steps. Similarly, because the rest periods are also independently and identically distributed,

$$P\Big[N(t) = n\Big] = P\Big[N(t) \geq n\Big] - P\Big[N(t) \geq n + 1\Big]$$

$$= P\Big[\sum_{i=1}^{n} T_i \leq t\Big] - P\Big[\sum_{i=1}^{n+1} T_i \leq t\Big]$$

$$= \int_0^t \Big[\Big\{f_T(t')\Big\}^{n^*} - \Big\{f_T(t')\Big\}^{n+1^*}\Big] dt' . \qquad (3\text{-}6)$$

where $\{f_T(t')\}^{n*}$ is the n-fold convolution of the probability density function for the duration of a single rest period which is equal to the probability density function for the duration of n successive rest periods. Since $x \geq 0$ and $X_0 = 0$, so $P\,[X_0 \leq x] = 1$, combining Eqs. (3-4) and (3-5) gives

$$F_t(x) = \sum_{n=1}^{\infty} \int_0^x \left\{ f_X(x') \right\}^{n*} dx' \; P\left[N(t) = n \right] + P\left[N(t) = 0 \right] \tag{3-7}$$

where $P\left[N(t) = n\right]$ is as defined in Eq. (3-6). The desired density function can be obtained by differentiating Eq. (3-7) with respect to x, i.e.,

$$f_t(x) = \frac{\partial}{\partial x} F_t(x)$$

$$= \sum_{n=1}^{\infty} \left\{ f_X(x) \right\}^{n*} P\left[N(t)=n \right] . \tag{3-8}$$

Equation (3-8) is the general density function for a particle that has moved a distance x from the origin in time t. It should be noted that $f_t(x)$ is not a true probability density function because

$$\int_0^{\infty} f_t(x)dx = 1 - P\left[N(t) = 0 \right] < 1, \tag{3-9}$$

where P [N(t) = 0] is the probability that the particle has not moved from its initial position. Thus, Eq. (3-8) is valid only after the particle has moved from its initial position.

If the step lengths are gamma distributed, then

$$f_X(x) = \frac{k_1}{\Gamma(r)} (k_1 x)^{r-1} \quad e^{-k_1 x} \tag{3-10}$$

where r is a parameter, $\Gamma(r)$ is a gamma function and the mean step length is

$$\overline{X} = \frac{1}{n} \sum_{i=1}^{n} X_i = \frac{r}{k_1} \quad . \tag{3-11}$$

If the rest periods follow the exponential distribution

$$f_T(t) = k_2 \; e^{-k_2 t} \tag{3-12}$$

then the mean rest period is

$$\overline{T} = 1/k_2 \quad . \tag{3-13}$$

The n-fold convolution of a gamma probability function with parameters r and k_1 is also a gamma probability function with parameters nr and k_1 (Parzen, 1962). Thus,

$$\left\{ f_X(x) \right\}^{n*} = \frac{k_1}{\Gamma(nr)} (k_1 x)^{nr-1} \quad e^{-k_1 x} \quad . \tag{3-14}$$

The n-fold convolution of the exponential probability function is a special case of the n-fold convolution of the gamma probability function with r = 1. Thus,

$$\left\{f_T(t)\right\}^{n*} = \frac{k_2}{\Gamma(n)} (k_2 t)^{n-1} e^{-k_2 t} \quad . \tag{3-15}$$

Putting Eqs. (3-14) and (3-15) into (3-8), we have

$$f_t(x) = \sum_{n=1}^{\infty} \frac{k_1}{\Gamma(nr)} (k_1 x)^{nr-1} e^{-k_1 x} \int_0^t \left[\frac{k_2}{\Gamma(n)} (k_2 t')^{n-1} e^{-k_2 t'} - \frac{k_2}{\Gamma(n+1)} (k_2 t')^{n} e^{-k_2 t'}\right] dt' \quad . \tag{3-16}$$

Integrating by parts, we have

$$\int_0^t \left[\frac{k_2}{\Gamma(n)} (k_2 t')^{n-1} e^{-k_2 t'}\right] dt' = 1 - e^{-k_2 t} \sum_{i=0}^{n-1} \frac{(k_2 t)^i}{i!} \tag{3-17}$$

and

$$\int_0^t \left[\frac{k_2}{\Gamma(n+1)} (k_2 t')^{n} e^{-k_2 t'}\right] dt' = 1 - e^{-k_2 t} \sum_{i=0}^{n} \frac{(k_2 t)^i}{i!} \quad . \tag{3-18}$$

By substituting Eqs. (3-17) and (3-18) into (3-16), the probability density function for x at time t can be written as

$$f_t(x) = k_1 e^{(-k_1 x + k_2 t)} \sum_{n=1}^{\infty} \frac{(k_1 x)^{nr-1}}{\Gamma(nr)} \frac{(k_2 t)^n}{n!} \quad , x > 0 \qquad (3\text{-}19)$$

The k_1, k_2 and r values may be obtained from a set of experimental concentration-distribution curves with respect to x for various values of t. If r = 1, then Eq. (3-19) becomes Eq. (2-2) which was obtained by Einstein (1937), Hubbell and Sayre (1964) and Todorović (1967) under the assumption that both the step lengths and rest periods are exponentially distributed. Some of the significant statistical parameters of the density function described by Eq. (3-19) are given as follows:

1. Area under curve:

$$\int_0^{\infty} f_t(x)\, dx = 1 - e^{-k_2 t} \qquad (3\text{-}20)$$

2. Mean:

$$\bar{x} = \int_0^{\infty} x f_t(x)\, dx = \frac{k_2 t r}{k_1} \qquad (3\text{-}21)$$

3. Mean rate of movement of tracer particles:

$$\frac{d\bar{x}}{dt} = \frac{k_2 r}{k_1} \qquad (3\text{-}22)$$

4. Variance:

$$\sigma_x^2 = E(x^2) - E^2(x)$$

where E( ) is the expected value defined as

$$E(x^2) = \int_0^\infty x^2 f_t(x)\, dx$$

$$= \frac{k_2 tr}{k_1^2}(k_2 tr + r + 1)$$

$$E^2(x) = \overline{X^2} = \left(\frac{k_2 tr}{k_1}\right)^2 .$$

Thus, the variance is

$$\sigma_x^2 = \frac{k_2 tr}{k_1^2}(r+1) \qquad (3\text{-}23)$$

5. Skew coefficient

$$S = \frac{\int_0^\infty x^3 f_t(x)dx - 3\bar{x}\int_0^\infty x^2 f_t(x)dx + 2(\bar{x})^3}{(\sigma_x^2)^{3/2}}$$

$$= \frac{r+2}{\sqrt{(r+1)\, rk_2 t}} . \qquad (3\text{-}24)$$

B. The Statistical Characteristics of the Bed Form

Since the movement of sand particles along an alluvial bed is closely related to the bed configurations which are very irregular and vary randomly, a study of the statistical characteristics of the bed form is necessary. Figure 3-1 is a definition sketch of the bed form. Crickmore and Lean (1962) found that the distribution of surface area with depth is approximately Gaussian. Similar results have been observed (1967) in the two-foot flume in the Engineering Research Center of Colorado State University. Most studies of the statistical properties of bed forms have emphasized the variation in elevation but neglected the variation along the direction of flow. Usually, a sand particle starts a step length on a positive slope, such as AB or CD in Fig. 3-1; the distance it travels depends on the local, instantaneous flow condition, but when it is deposited and buried by other particles, this sand particle is usually deposited on a negative slope, such as BC or DE on Fig. 3-1. It is, therefore, logical to assume that the step length of a moving particle is closely related to the distance between peaks of ripples or dunes, or the distance between zero crossings. If the step lengths of a single particle follow the gamma distribution, it is reasonable to assume that the zero-crossings of the bed form may also follow a gamma distribution or vice versa.

C. The Mean Rest Period and the Mean Step Length

Since the rest periods are closely related to the level where particles are deposited on the bed, and hence the variation of

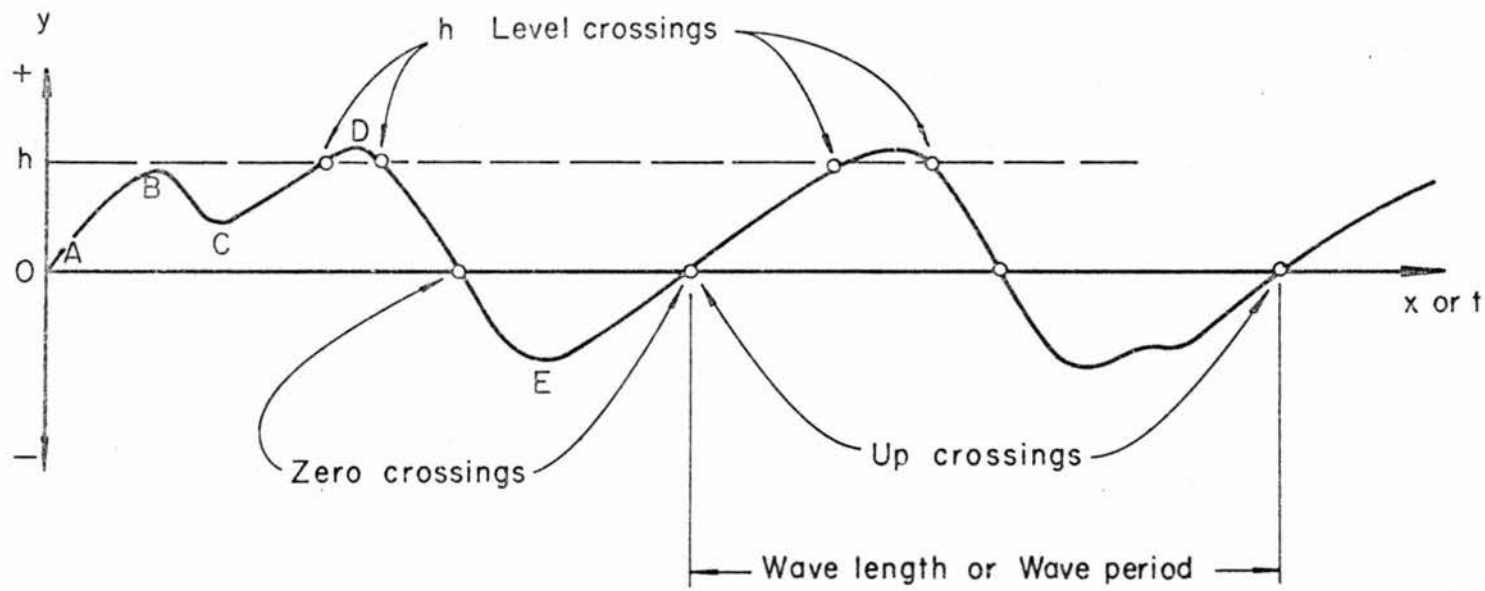

Figure 3-1. Definition sketch of the bed form.

bed elevation, it should be possible to find the mean rest period from the bed form data without measuring the longitudinal concentration distribution. When the bed elevation is statistically stationary in time, Hubbell and Sayre (1965) suggested that the unconditional probability density function for the duration of a rest period,

$$f_T(t) = \int_{-\infty}^{\infty} f_{T|Y}(t|y)\, f_Y(y)\, dy, \tag{3-25}$$

could be obtained from sufficiently long continuous records of bed elevation in the time domain measured from a stationary reference point, and along the direction of flow at an instant. The function $f_T(t)$ corresponds to the assumed exponential distribution for rest periods as stated in Eq. (3-12). $f_{T|Y}(t|y)$ is the conditional probability density function for the rest period duration, T, of a particle given the elevation, Y, at which it was deposited. $f_{T|Y}(t|y)$ relates to the variation of bed elevation measured from a stationary reference point. $f_Y(y)$ is the probability density function that a particle is deposited on the bed at elevation Y. $f_Y(y)$ relates to the variation of bed elevation with respect to distance x along the direction of flow. If it is assumed that the sand particles are equally likely to deposit anywhere on the negative slope of the bed surface, $f_Y(y)$ is equal to the probability density function of bed elevation of negative slope obtained from a record of variation of y with respect to distance x along the direction of flow. If there is no significant difference

between the probability density function of bed elevation along the direction of flow by considering either both positive and negative slopes or just the negative slopes, $f_Y(y)$ is equal to the probability density function of the bed elevation obtained from a record of y with respect to x. Although there are grounds for supposing that $f_T(t)$ and $f_Y(y)$ are respectively exponential and normal probability density functions, the nature of the conditional probability density function $f_{T|Y}(t|y)$ has not yet been determined.

The mean value of the rest period or the unconditional expected value of rest periods can be obtained from

$$E[T] = \int_{-\infty}^{+\infty} E[T|Y=h]\, f_Y(h)\, dh \quad . \tag{3-26}$$

Nordin (1968), in his study of statistical properties of the bed form, has assumed that the elevation h was measured in terms of the standard deviation of bed elevation σ_y . Thus, it was found that the ratio of the expected value of rest period of a particle, which was deposited at elevation h, to the expected value of rest period of a particle deposited at zero elevation, i.e. mean bed elevation, is

$$\frac{E[T|Y=h]}{E[T|Y=0]} = 2\{P[Y(0) > h]\}e^{\left(\frac{h}{\sigma_y}\right)^2/2} \tag{3-27}$$

where $P[Y(0) > h]$ is the probability that the elevation Y at t=0, i.e. at the beginning of the rest period, is greater than h. The value of $P[Y(0) > h]$ can easily be found from bed form data along the direction of flow. The expected value of a rest period of a particle which was

deposited at zero elevation should be a constant, T_o, for a given flow and sediment condition. When all the particles are equally likely to deposit anywhere on the negative slope of the bed surface, T_o is equal to the mean value of the duration of burials (rest period) at zero elevation obtained from a sufficiently long continuous record of bed elevation measured from a stationary reference point. Combining Eq. (3-26) and Eq. (3-27), the mean rest period is

$$\overline{T} = 2\, T_o \int_{-\infty}^{+\infty} e^{\left(\frac{h}{\sigma_y}\right)^2 \Big/ 2} f_Y(h)\, P[Y(0) > h]\, dh \quad . \qquad (3\text{-}28)$$

Because $P[Y(0) > h]$ and $f_Y(h)$ are related by the quality

$$P[Y(0) > h] = 1 - \int_{-\infty}^{h} f_Y(y)\, dy \quad , \qquad (3\text{-}29)$$

Eq. (3-28) can be simplified still further to

$$\overline{T} = 2\, T_o \int_{-\infty}^{+\infty} e^{\left(\frac{h}{\sigma_y}\right)^2 \Big/ 2} f_Y(h)\, \left[1 - \int_{-\infty}^{h} f_Y(y)dy\right] dh \qquad (3\text{-}30)$$

Equations (3-28) and (3-30) can be integrated either analytically or graphically using information based on the actual bed form data.

The most direct way of finding the step lengths of a particle is to actually follow that particle and measure its step lengths. If this method is not possible, then an indirect method can be applied to find the mean step length. This method is based on the mean rest period. In a dispersion study, in which n tracer particles are used,

suppose that the j'th particle (j = 1,2,3 ..., n) requires N_j steps to travel a distance x in time t. If the time spent in motion can be neglected, then the time, t, required for all the tracer particles to travel an average distance, $\bar{x}$, from the origin is

$$t = \overline{N_j \bar{T}_j} = \frac{1}{n} \sum_{j=1}^{n} \sum_{i=1}^{N_j} T_{ij} \quad , \tag{3-31}$$

where the subscript i, i=1,2,3, ..., N_j is the number of steps taken by the j'th particle during the process. Since the steps and rest periods follow each other in successive cycles, the total number of steps should be equal to the total number of rest periods in a finite traveling distance. The average distance, $\bar{x}$, traveled by all the tracer particles from the origin in time t is

$$\bar{x} = \overline{N_j \bar{X}_j} = \frac{1}{n} \sum_{j=1}^{n} \sum_{i=1}^{N_j} X_{ij} \quad . \tag{3-32}$$

When the number of tracer particles, n, is large, the average velocity of tracer particles should be

$$\bar{U}_s = \frac{\bar{x}}{t} = \frac{\overline{N_j \bar{X}_j}}{\overline{N_j \bar{T}_j}} = \frac{\bar{N}\,\bar{X}}{\bar{N}\,\bar{T}} = \frac{\bar{X}}{\bar{T}} \quad , \tag{3-33}$$

where $\bar{N}$ is the average number of steps required by all the tracer particles to travel a mean distance, $\bar{x}$, from the origin in time t. When the average depth of the zone in which particle movement occurs

can be determined from bed configuration data, $\overline{U}_s$ can also be obtained from Eq. (2-3), either by actual measurement of the sediment discharge or calculation of the sediment discharge by some known formulas. Thus, the mean step length should be

$$\overline{X} = \overline{U}_s \overline{T} \quad . \tag{3-34}$$

D. Aris' Moment Equation

For sand particles that have been entrained into the flow, the theory of dispersion of suspended particles can be applied. Sayre (1968) suggested the possibility that the probability density function for the longitudinal distribution of deposited tracers for the initial condition that all particles are concentrated near the bed might turn out to be closely related to the step length distribution function. Sayre further stated that if for this initial condition, the probability density function for the deposited tracer with respect to the dimensionless longitudinal distance is an exponential function, it is more than likely that the Hubbell-Sayre stochastic model can be obtained as a particular solution of an appropriate system of dispersion equations and boundary conditions for suspended particles. The methods used in this and the next two sections will provide us with some theoretical background in comparing the gamma distributed step lengths to the distribution function of step length obtained from solving the Aris moment equations for the initial condition that all the particles are concentrated near the bed. This also makes it possible to compare

the general one-dimensional stochastic model with the solution of the Aris moment equations to see if it is a particular solution of the dispersion equation for suspended particles with the initial condition that all the tracer particles are in the bed at the beginning of the process, but where entrainment into the flow is permitted.

Following Aris (1956), let us define the velocity of flow in the x direction as a function of y by

$$U(y) = \overline{U}[1+\chi(y)] \tag{3-35}$$

where $\chi(y)$ defines the variation of velocity relative to the mean velocity in the vertical $\overline{U}$, and let the local diffusion coefficient be

$$\varepsilon_x = \varepsilon_y = D\psi(y) \tag{3-36}$$

where D is the mean value of the diffusion coefficient in the vertical, and $\psi(y)$ defines the variation of the diffusion coefficient. Combining Eqs. (2-6), (3-35) and (3-36) gives us

$$\frac{\partial C}{\partial t} + \overline{U}(1+\chi)\frac{\partial C}{\partial x} = D\psi\frac{\partial^2 C}{\partial x^2} + D\frac{\partial}{\partial y}\left(\psi\frac{\partial C}{\partial y}\right) + V_s\frac{\partial C}{\partial y} \tag{3-37}$$

which is the basic two-dimensional dispersion equation for sedimentation in open channel flow.

Sayre (1968) used Aris' moment equation to solve the longitudinal dispersion problem in open channel flow. Sayre's initial

condition was an instantaneous uniformly-distributed plane source over the depth of flow at the origin. A coordinate system moving at the mean velocity of flow was adopted by Sayre. In this study, Sayre's notation is adopted. To simulate the problem in which we are interested, the initial condition is a line source of marked sand particles on the bed across the flume at the origin. Since the average rate of movement of the sediment is much slower than the mean velocity of the flow, a fixed coordinate system at the origin is used. To solve the problem, it is necessary to consider the total amount of tracer particles as made up of two separate parts. The concentration of the entrained part is denoted by C, and W is used for the deposited part. The exchange between C and W occurs at the interface between the bed surface and flow by the processes of entrainment and deposition. Once the particles are entrained into the flow, the dispersion theory of suspended particles can be applied. Introducing the dimensionless parameters

$$\left.\begin{aligned} \xi &= x/y_n \\ \eta &= y/y_n \\ \tau &= Dt/y^2_n \\ \mu &= \overline{U}\, y_n/D \\ \nu_s &= V_s\, y_n/D \end{aligned}\right\} \qquad (3\text{-}38)$$

Equation (3-37) becomes

$$\frac{\partial C}{\partial \tau} + (\mu + \mu\chi)\frac{\partial C}{\partial \xi} = \frac{\partial}{\partial \eta}\left(\psi \frac{\partial C}{\partial \eta} + \nu_s C\right) + \psi \frac{\partial^2}{\partial \xi^2} \quad . \qquad (3\text{-}39)$$

The equation of conservation of mass for the deposited particles is

$$\frac{dW}{d\tau} = \alpha v_s C(\xi,0^+,\tau) - \gamma W \tag{3-40}$$

where

α = bed absorbency coefficient, which represents the probability that a tracer particle settling to the bed is deposited,

$W = W(\xi,\tau)$ which represents the amount of tracer particles stored per unit area of bed surface, and

γ = entrainment-rate coefficient such that γW represents the average rate of entrainment.

The boundary condition existing between the flow and the bed is

$$\eta = 0 \quad : \quad \psi \frac{\partial C}{\partial \eta} + (1-\alpha)\, v_s C + \gamma W = 0 \ . \tag{3-41}$$

Equation (3-41) allows the bed to behave either as an absorbing or reflecting barrier and also permits temporary storage of the tracers on the bed. Since there can be no transport of tracers across the water surface, the relation

$$\eta = 1 \quad : \quad \psi \frac{\partial C}{\partial \eta} + v_s C = 0 \tag{3-42}$$

must exist at the upper boundary.

By using the Aris' moment transformations

$$\left.\begin{aligned} C_p &= \int_{-\infty}^{\infty} \xi^p \, C \, d\xi \\ \text{and} \\ W_p &= \int_{-\infty}^{\infty} \xi^p \, W \, d\xi \end{aligned}\right\} \qquad (3\text{-}43)$$

where C_p and W_p are the p'th moments about $\xi = 0$ of the longitudinal distribution of C and W, respectively. These moment transformations eliminate one variable in the longitudinal direction, i.e. ξ. Thus, Eq. (3-39) becomes

$$\frac{\partial C_p}{\partial \tau} = \frac{\partial}{\partial \eta}\left(\psi \frac{\partial C_p}{\partial \eta} + \nu_s C_p\right) + p(\mu+\mu\chi)C_{p-1} + p(p-1)\psi C_{p-2} \qquad (3\text{-}44)$$

and Eq. (3-40) becomes

$$\frac{dW_p}{d\tau} = \alpha\nu_s \, C_p(0^+,\tau) - \gamma W_p \quad . \qquad (3\text{-}45)$$

The boundary conditions are

$$\eta = 1 \; : \; \psi \frac{\partial C_p}{\partial \eta} + \nu_s C_p = 0 \qquad (3\text{-}46)$$

$$\eta = 0 \; : \; \psi \frac{\partial C_p}{\partial \eta} + (1-\alpha)\,\nu_s C_p + \gamma W_p = 0 \quad . \qquad (3\text{-}47)$$

Although the number of variables has been reduced by Aris' moment transformation, no analytical solutions have been obtained except for a few special cases as summarized in Table 3-1.

E. Finite Difference Equation and Computer Program

In order to solve the dispersion equation given in the previous section, a finite difference equation and computer program were developed by Sayre (1968) in his Ph.D. dissertation. Following Sayre's notation and method of approach, a similar set of finite difference equations and computer programs can be obtained. Sayre gave the definition sketch of the variables in the finite difference equations as shown in Fig. 3-2. The depth of flow is divided into N equal increments of thickness DY = $\Delta\eta$. The number of time intervals of duration, DT = $\Delta\tau$, counted from the beginning of the dispersion process, is indicated by J, starting with J = 1 at $\tau = 0$ so that $\tau = (J-1)DT$. The average value of $C_p(\eta,\tau)$ in the increment between I and I+1 after J-1 time intervals is defined as $C_p(I,J)$.

TABLE 3-1. KEY TO ANALYTICAL SOLUTIONS OF ARIS EQUATIONS

Case	Variables for which solution obtained	Velocity distribution	β	α	γ	Range of τ
1	$C_1(\eta,\tau)$	parabolic	0			all
2	$C_1(\eta,\infty)$	logarithmic	0			$\tau\to\infty$
3	$C_0(\eta,\tau)$	parabolic	all	1	0	all

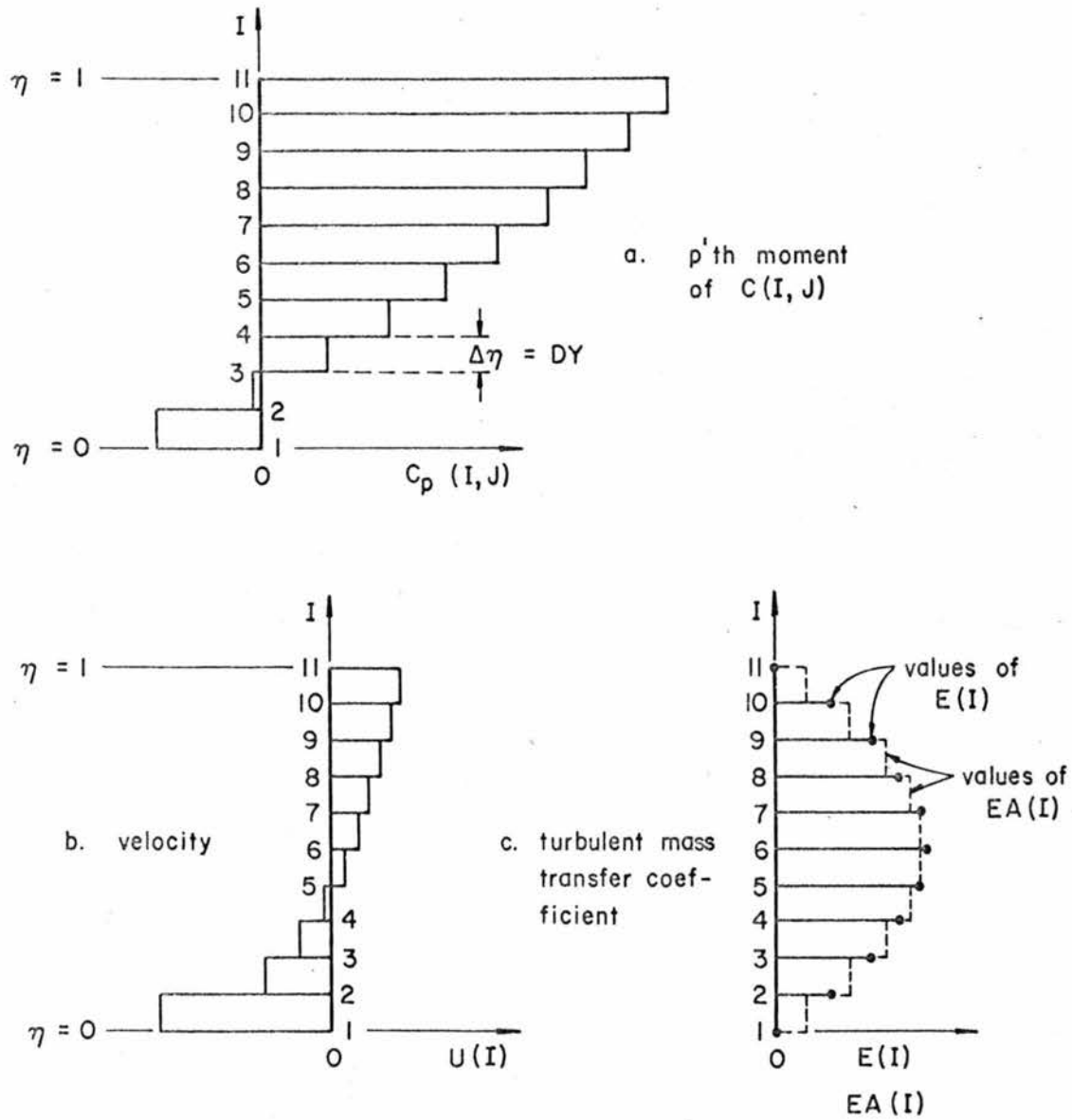

Figure 3-2. Definition sketch of variables in finite difference equations.

The von Karman-Prandtl logarithmic velocity distribution function

$$\frac{U-\overline{U}}{U_\tau} = \frac{1}{\kappa} (1n\eta + 1) \tag{3-48}$$

is employed in this study, where κ is the so-called von Karman turbulence coefficient and U_τ is the shear velocity. However, in alluvial channels, κ has been found to vary with the flow condition, the concentration of sediment and the bed form. By applying Reynold's analogy for the equivalence of momentum and mass transfer, the vertical turbulent mass transfer coefficient (vertical diffusion coefficient) is

$$\varepsilon_y = \frac{U_\tau^2 \, y_n (1-\eta)}{\frac{dU}{d\eta}} \quad . \tag{3-49}$$

From Eq. (3-48)

$$\frac{dU}{d\tau} = \frac{U_\tau}{\kappa\eta} \tag{3-50}$$

then Eq. (3-49) becomes

$$\varepsilon_y = \kappa y_n \, U_\tau \, \eta(1-\eta) \tag{3-51}$$

which is distributed parabolically with respect to η, and

$$D = \int_0^1 \kappa\, y_n\, U_\tau\, \eta(1-\eta)d\eta = \frac{\kappa}{6}\, y_n\, U_\tau \ . \tag{3-52}$$

Combining Eqs. (3-35), (3-38), (3-48) and (3-52), we have

$$\mu\chi = \frac{6}{\kappa^2}(1n\eta+1) \tag{3-53}$$

and

$$\psi = \frac{\varepsilon_y}{D} = 6\eta(1-\eta) \ . \tag{3-54}$$

With all these dimensionless parameters obtained, we can further define the velocity, $\frac{6}{\kappa^2}[U(I) + \kappa UA]$, and the diffusion coefficient, EA(I), as the average values of $\mu + \mu\chi$ and ψ in the increment between I and I + 1 so that

$$\frac{6}{\kappa^2}[U(I) + \kappa UA] = \frac{1}{DY}\int_{(I-1)DY}^{(I)DY} (\mu + \mu\chi)\, d\eta \tag{3-55}$$

and

$$EA(I) = \frac{1}{DY}\int_{(I-1)DY}^{(I)DY} \psi\, d\eta \ . \tag{3-56}$$

The vertical component of the eddy diffusivity, E(I), is defined as the value of ψ at the boundary between the increments in question so that $E(I) = \psi(\eta)$, where $\eta = (I-1)DY$.

With the above definitions, the finite difference equation corresponding to Eq. (3-44) can be written as

$$C_p(I,J+1) = C_p(I,J) + \frac{DT}{DY}\left\{\left[\frac{E(I+1)}{DY} + \nu_s\right]\left[C_p(I+1,J) - C_p(I,J)\right]\right.$$

$$\left. - \frac{E(I)}{DY}\left[C_p(I,J) - C_p(I-1,J)\right]\right\} + p\,\frac{6DT}{\kappa^2}\,[U(I) + \kappa UA]C_{p-1}(I,J)$$

$$+ p(p-1)DT\ EA(I)\ C_{p-2}(I,J) \quad . \tag{3-57}$$

The difference equation corresponding to Eq. (3-45) is

$$W_p(J+1) = W_p(J) + DT\alpha\nu_s\ C_p(1,J) - DT\gamma W_p(J) \quad . \tag{3-58}$$

The boundary conditions corresponding to Eqs. (3-46) and (3-47) are:

$$I = N \ : \left[\frac{E(I+1)}{DY} + \nu_s\right][C_p(I+1,J) - C_p(I,J)] = -\nu_s\ C_p(I,J)$$

and (3-59)

$$I = 1 \ : \ \frac{E(I)}{DY}\,[C_p(I,J) - C_p(I-1,J)] = -\nu_s(1-\alpha)C_p(I,J) - \gamma W_p(J)$$

(3-60)

The basic boundary conditions, Eqs. (3-59) and (3-60), are the same as in Sayre's (1968) program. Only the initial conditions and the values of α and γ in Eq. (3-60) are changed so as to simulate the two different situations described in the following pages.

Case 1 - The initial condition is that all the tracers are concentrated at the origin in the bottom layer of flow with the layer thickness equal to $\Delta\eta$. After the process has started, no re-entrainment of the tracer particles into the flow is allowed. Once the particles are deposited, the bed surface behaves as an absorbing barrier, so each tracer particle is absorbed by the bed after completing a step. This case simulates the condition that each tracer particle is ready to take a step and be absorbed by the bed after completing that step. The main purpose of this program is to find the distributions and mean values of step length for a given flow condition, $\Delta\eta$ value, and different fall velocities of sand which correspond to different sand particle sizes.

The initial conditions are

$$\left.\begin{aligned} C_p(I,1) &= \frac{1}{\Delta\eta} && I=1,\ p=0 \\ C_p(I,1) &= 0 && I\neq 1,\ p=0 \\ W_p(1) &= 0 && p=0 \\ C_p(I,1) &= 0 && p>0 \\ W_p(1) &= 0 && p>0 \end{aligned}\right\}. \qquad (3\text{-}61)$$

For the case of no entrainment from the bed and the bed surface behaving as an absorbing barrier, we should have $\gamma = 0$ and $\alpha = 1$.

The boundary condition, Eq. (3-59), remains the same, but Eq. (3-60) becomes

$$I = 1 \quad : \quad \frac{E(I)}{DY} [C_p(I,J) - C_p(I-1,J)] = 0 \qquad (3\text{-}62)$$

An important dimensionless fall velocity parameter, β, defined as $\nu_s/\kappa U_\tau$, is used in this computer program. The shear velocity, $U_\tau = \sqrt{gy_n S_e}$, is obtained from the actual flow condition with the known normal depth, y_n, and the water surface slope S_e. The κ value is determined from the slope of a dimensionless plot of log y/y_n vs U/U_τ obtained from velocity distribution measurements. Different β values were tried in order to simulate sediment particles of different fall velocities. The grid size chosen for this case was DT = 0.00001 and DY = 0.1. The data corresponding to the flow condition in Run 1C, which was a ripple case using the coarse tracer particles, were used in this program, with κ = 0.287, β = 1.20 and U/U_τ = 9.6.

Case 2 - All the tracer particles are initially in the bed at the origin, but entrainment into the bottom layer of the flow is permitted. Once a tracer particle is entrained into the bottom layer, it takes a step after which it is absorbed by the bed where it remains until it is re-entrained and takes another step. The main purpose of this program is to find out if the general one-dimensional stochastic model can be obtained as a special case of the dispersion problem for suspended sediment.

When there is no deposition, Eq. (3-40) reduces to

$$\frac{dW}{d\tau} = -\gamma W \tag{3-63}$$

which defines the dimensionless entrainment-rate coefficient γ. If the probability of entrainment is the same for all particles, and is independent of the length of time that a particular particle has remained at rest, then the solution of Eq. (3-63) is

$$\frac{W(\tau)}{W(0)} = e^{-\gamma\tau} \quad .$$

The probability that the particle will be entrained after a duration of resting time τ, is equal to the probability that the time which the particle remains at rest is equal or less than τ

$$\int_0^{\tau} f_T(\tau')d\tau' = 1-e^{-\gamma\tau} \quad .$$

The probability density function $f_T(\tau')$ can be obtained by differentiating the above equation with respect to time, i.e.,

$$f_T(\tau) = \gamma e^{-\gamma\tau} \quad , \tag{3-64}$$

which is the same as the probability density function for rest period durations given in Eq. (3-12). The only difference between Eq. (3-12) and Eq. (3-64) is that Eq. (3-64) is expressed in a dimensionless unit while Eq. (3-12) is expressed in a dimensional unit. Thus, γ should be equal to k_2 in dimensionless unit. Or,

$$\gamma = \phi k_2$$

where ϕ is a conversion factor which converts dimensional time units to dimensionless time units. The conversion factor ϕ can be obtained from Eqs. (3-38) and (3-52) as

$$\phi = \frac{6y_n}{\kappa U_\tau} \quad . \tag{3-65}$$

The γ value for Case 2 should then be

$$\gamma = \frac{6y_n}{\kappa U_\tau} \; k_2 \quad . \tag{3-66}$$

The α, β, κ and $\overline{U}/U_\tau$ values should be the same in Case 2 as in Case 1. The initial conditions are changed to simulate the condition that all the tracer particles are concentrated at the origin in the sand bed at the beginning of the process so that

$$\left.\begin{aligned} C_p(I,1) &= 0 && p = 0 \\ W_p(1) &= 1 && p = 0 \\ C_p(I,1) &= 0 && p > 0 \\ W_p(1) &= 0 && p > 0 \end{aligned}\right\} . \tag{3-67}$$

With $\alpha = 1$ and γ defined as in Eq. (3-66), the upper boundary condition still remains the same as in Eq. (3-59), and the lower boundary condition becomes

$$\begin{aligned} I = 1 \; : \; & \frac{E(I)}{DY}[C_p(I,J) - C_p(I-1,J)] \\ &= -\frac{6y_n}{\kappa U_\tau} k_2 \; W_p(J) \quad . \end{aligned} \tag{3-68}$$

A grid size of DT=0.002 and DY=0.1 was chosen for this case. The flow conditions corresponding to Run 1C were also adopted in this case with κ=0.287, β=1.20, γ=0.0131 and $\overline{U}/U_\tau$=9.6.

In both Case 1 and Case 2, the total amount, the average velocity, the mean displacement, the variance, and the skew coefficient for both the C and W components were calculated. Different DT values were tried in order to determine the most economical DT value without losing the accuracy and the stability of the result. The definitions used in these programs and the programs themselves can be found in Appendix A. For a more detailed development, the reader should refer to Sayre (1968).

F. Comparison Between the General One-Dimensional Stochastic Model and Aris' Moment Equation

Aris' moment equations are a good analytical approach for solving longitudinal dispersion problems in turbulent open-channel flow. Without any further restriction on the dispersion equation, Aris' moment transformation simplifies the dispersion equation by reducing the number of variables in it. The physical meaning of Aris' moment equation is very easy to accept, because the dispersion equation was derived from the continuity equation. Since, basically, Aris' moment equation is a dispersion equation, it can be used to describe the process of dispersion. When α, β and γ are given for a certain flow condition, Aris' moment equation can also be used to predict the dispersion process. However, from the Aris moment equation itself, the α and γ values cannot be determined. The finite difference

equations and the computer program originally established by Sayre give numerical solutions which provide information about the actual dispersion process. In general, changing the grid size, i.e. $\Delta\tau$ and $\Delta\eta$ values, may affect the accuracy and stability of the computer results. If the grid size is small enough so that the problem of accuracy and stability is eliminated, the change of grid size should not have any effect on the computer results in most cases. However, this is not true for our problem because a change of $\Delta\eta$ means a change of the initial condition in Eq. (3-61). Therefore, different $\Delta\eta$ values will give different answers for the step length. The biggest problem in applying the Aris' moment equation for predicting the dispersion process in this study is how to choose the right combination of β and $\Delta\eta$ to give the proper distribution of step lengths.

The method of deriving the general one-dimensional stochastic model in this chapter is better than that presented by Hubbell and Sayre (1964). The general one-dimensional stochastic model was derived in this chapter without having to specify the probability density functions for the step lengths and rest periods. So this method of approach can be applied to any kind of distribution function of step lengths and rest periods.

Three different methods can be applied to find all the parameters in this general one-dimensional stochastic model. The first method is based on the dispersion experiments to find k_1, k_2 and r from the mean rate of displacement, mean rate of spreading and the skew

parameters of the longitudinal dispersion curves. Because the skew parameters are obtained from the third moment of the longitudinal dispersion curves, they are not apt to be very reliable. Thus, if one can assume a proper value of r, then k_1 and k_2 can be obtained from the mean rate of displacement and spreading of the longitudinal dispersion curves. As long as the parameters are obtained from dispersion data, this general one-dimensional stochastic model can be used only for the purpose of describing the dispersion process; it cannot be used to predict the dispersion process.

The second method of obtaining k_1, k_2 and r is based on the bed configuration data. With the records of the variation of bed elevation in space and time domains, the mean rest period should be predictable. From the bed configuration, the mean depth of movement of sediment can also be determined. The actual total discharge of sediment can either be determined by actual measurement or estimated by using a total discharge equation such as Einstein's (1950) equation. With the total discharge of sediment and the mean depth of movement known, the mean velocity of tracer particles can be found from Eq. (2-3), and the mean step length can be found from Eq. (3-34). Solving Eqs. (3-11), (3-13) together with the assumed r value, the values of k_1 and k_2 for the general one-dimensional stochastic model can be determined.

The third method is a combination of the first two methods. Determine the mean rest period from bed configuration data, and mean step length from mean rest period, total sediment discharge and bed configuration data; then, determine the mean rate of spreading of longitudinal dispersion curves. By solving Eqs. (3-11), (3-13) and Eq. (3-23) simultaneously, k_1, k_2 and r can be determined.

Both the Aris moment equations and the general one-dimensional stochastic model should be able to provide good descriptions about the mean rate of displacement and spreading, and the skewness of the dispersion process. Both models indica e that the rest periods are exponentially distributed. The general one-dimensional stochastic model can provide the actual dispersion curves at any dispersion time, and can be applied to any probability density function of step length and rest period, whereas the Aris moment equation method gives only the moments, and is restricted to particular step-length and rest-period distribution functions. With k_1, k_2 and r given, this general one-dimensional stochastic model provides a more complete description of the dispersion process of sand along an alluvial bed than the Aris moment equations. When the r value is properly assumed, and $\frac{r}{k_1}$ and $\frac{1}{k_2}$ can be obtained from bed configuration and total sediment discharge data, this general one-dimensional stochastic model may also be used to predict the dispersion process according to the measured or calculated total sediment discharge and bed configuration data.

G. Total Sediment Discharge Equation

If we combine Eqs. (2-3) and (3-22), the total discharge of sediment having a certain characteristic c is

$$(Q_s)_c = i_c(\gamma_s)_c (1-\lambda) \, Bd\left(\frac{k_2 r}{k_1}\right)_c . \qquad (3\text{-}69)$$

Then, the total sediment discharge for all the sizes is

$$Q_s = \sum_c i_c (\gamma_s)_c (1-\lambda) \, Bd \left(\frac{k_2 r}{k_1} \right)_c \qquad (3\text{-}70)$$

where the d value can be found either from core sample data or from bed form data.

Chapter IV

EXPERIMENTAL EQUIPMENT AND PROCEDURES

A. Flume

The flume used in the experiment was a recirculating flume 60 feet long, 2 feet wide and 2 1/2 feet deep. The side walls were made of 1/2-inch plexiglass, and the floor was made of 1/4-inch stainless steel plate. The discharge could be adjusted from 0 to 8 cfs, and the slope from horizontal to 10 percent. A schematic diagram of this flume is shown in Fig. 4-1.

Figure 4-1, showing the parts of the flume, is self-explanatory except for the instrument carriage and the manometer board for measuring the water surface slope. The motor-driven instrument carriage, as shown in Fig. 4-2a, carried the transducer for the stream monitor, the point gage and the scintillation detector. The speed of this carriage was controlled by the control box as shown in Fig. 4-2b. The support bolts for the rail were equally spaced at an interval of 1 foot along the flume. An event marking mechanism on the carriage, which was activated by a microswitch brushing against the support bolts, marked the position of the carriage on a recorder. The speed of the carriage was maintained at 4 feet per minute.

In order to check the water surface slope, a manometer board, similar to the one used by J. F. Kennedy (1961), was designed for this purpose. The manometer board consisted of 11 plastic tubes, each 4 feet long and with an inner diameter of 3/8 inch as shown in Fig. 4-3.

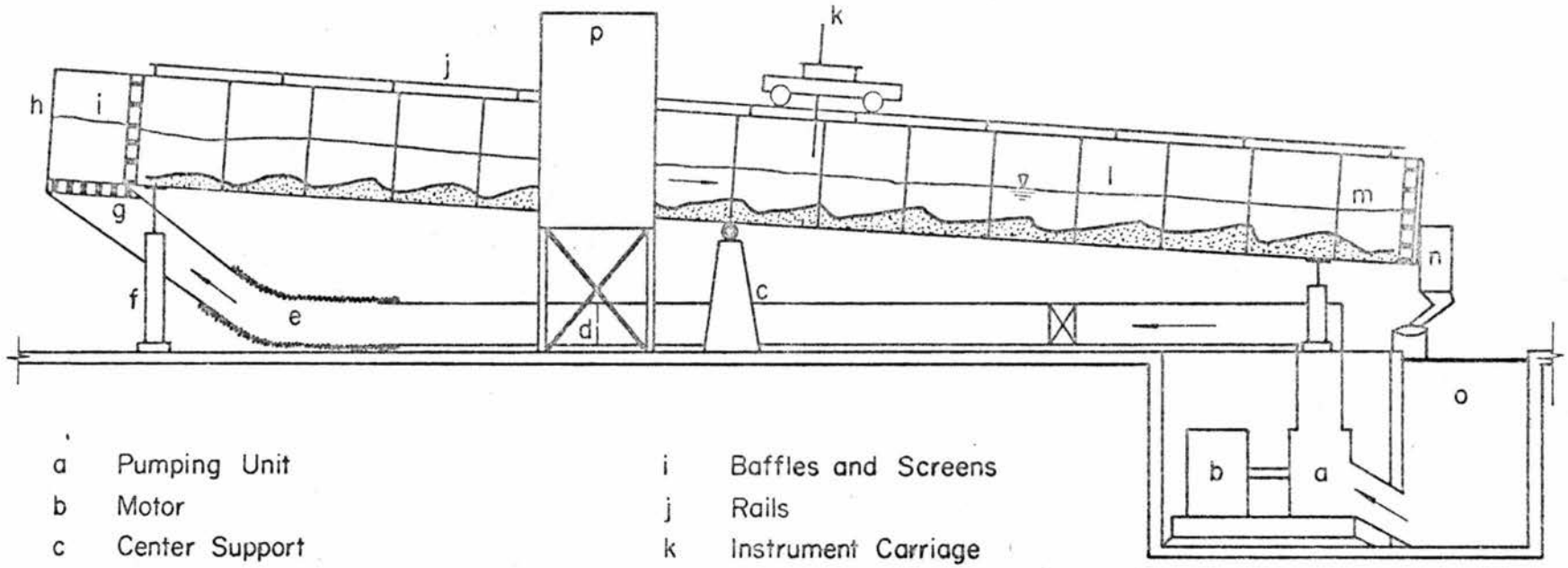

a	Pumping Unit	i	Baffles and Screens
b	Motor	j	Rails
c	Center Support	k	Instrument Carriage
d	Orifice	l	Flume
e	Flexible Connection	m	Tailgate
f	Jacks	n	Total Load Sampler
g	Manifold Diffuser	o	Tailbox
h	Headbox	p	Manometer Board

Figure 4-1. Schematic diagram of the 2-foot flume

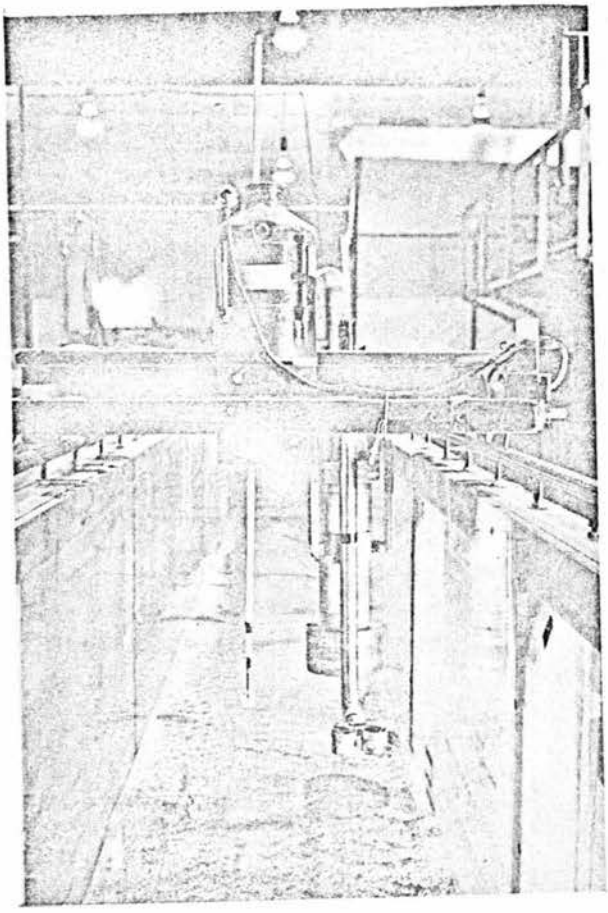

(a)
Instrument
carriage

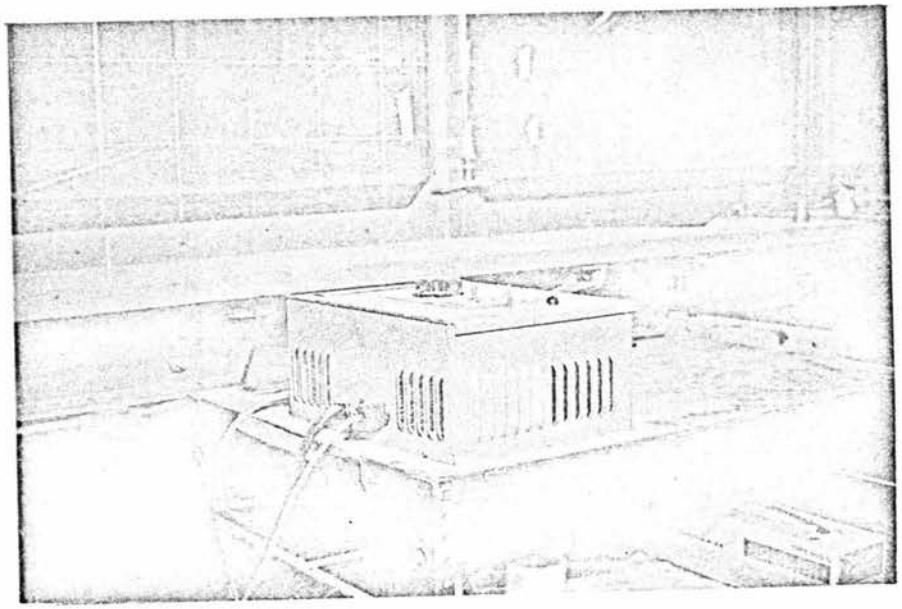

(b)
Control
box

Figure 4-2. Instrument carriage and its control box

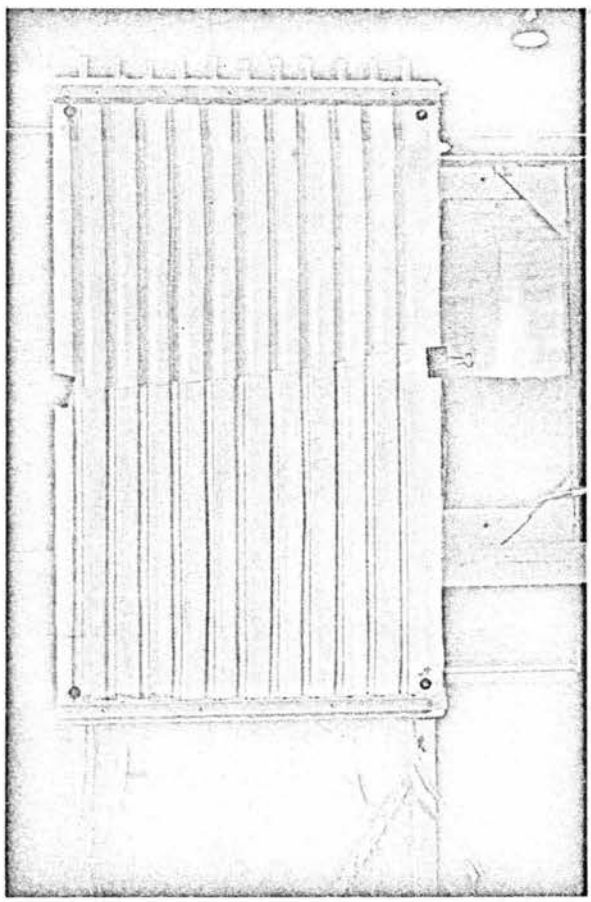

Figure 4-3. Manometer board.

B. The Method of Obtaining Equilibrium Condition

A complete equilibrium condition is obtained when the following parameters are constant or at least statistically constant with respect to time:

1. Discharge - The discharge of water could be determined by reading the manometer board connected to a side-contracted orifice meter. The discharge could be regulated by a valve.

2. Temperature - The average room temperature in the hydraulic laboratory was about 24° C. In order to keep a constant water temperature of 20° C, cold water was supplied to the tail box to bring the water temperature down to 20° C. The temperature was measured by an ordinary laboratory mercury thermometer near the entrance of the flume.

3. Water-Surface Slope - The slope of the flume was set to the right slope by using a surveying level and a rod. When equilibrium conditions are reached, the water-surface slope should be parallel to the bed slope. The slope of water could be adjusted by the tail gate. The water-surface slope was checked several times during each run by using the point gage on the carriage and also by the manometer board.

4. Bed Forms - When equilibrium conditions are reached, the average bed slope should be parallel to the water-surface slope and the same kind of bed forms (statistically speaking) should be observed along the flume as shown in Fig. 4-4a and Fig. 4-4b. The bed elevation was obtained by the point gage on the carriage. The actual bed form was obtained by the dual channel stream monitor, Automation

(a) ripple

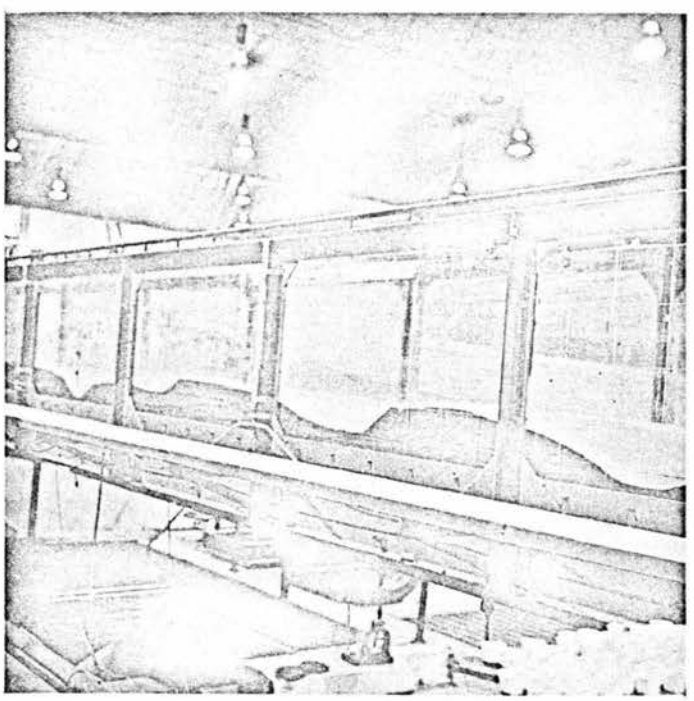

(b) dune

Figure 4-4. Ripple and dune bed configurations

Instruments, Model 1042, together with a transducer and a strip-chart recorder. With this combination of equipment and the event marker, which provided the position of the carriage, a bed surface profile could be obtained.

5. Depth of Flow - The depth of flow can be obtained from the difference of point gage reading on the carriage between the water surface and the corresponding bed surface. The average distance between the water surface and bed surface was the depth of flow. The depth of flow was measured several times during each run.

C. Sand and Tracer

The sand used in this experiment was plaster sand obtained from the Sterling Sand and Gravel Company, Fort Collins, Colorado. After sieving, a fairly uniform sand, ranging from 0.1 mm to 0.7 mm in diameter with a median diameter of 0.34 mm, was obtained. Figure 4-5 shows the sand size distribution. The shaded regions are the fine, medium and coarse sizes used as tracer particles in the experiment. The total amount of sand in the flume was about two tons.

The amount, size and activity of tracer particles used in each run are listed in Table 4-1. These tracer particles were obtained from the sand in the two-foot flume. After drying and weighing, they were sent to Hastings Radiochemical Works, Houston, Texas, for radioactive labeling. In the determination of the required amount of radioactivity, a uniformly distributed source was assumed. The amount of radioactivity required for each run was determined based on the assumption that after the tracer particles were very well distributed, the activity

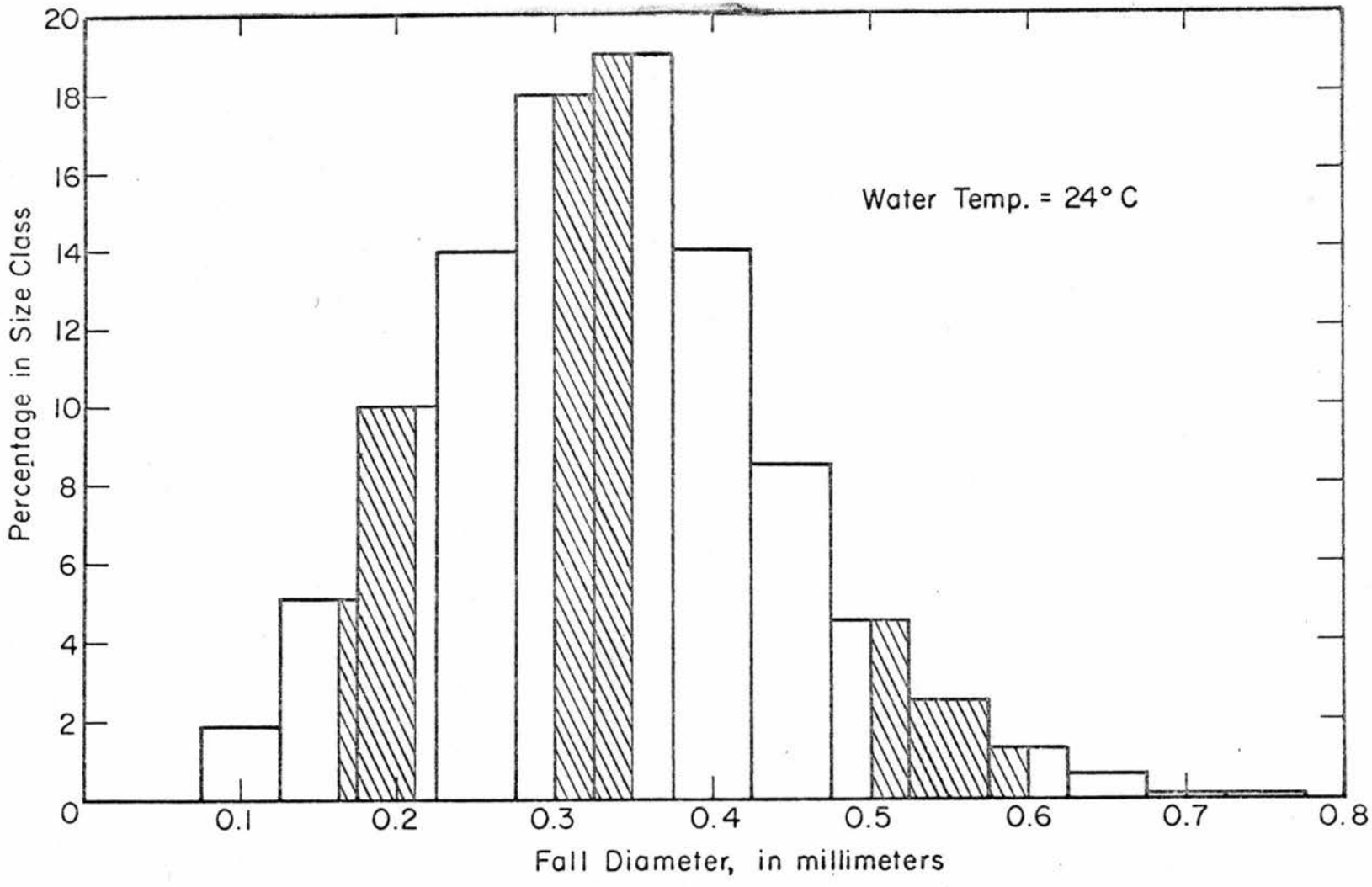

Figure 4-5. Size distribution of sand in the 2-foot flume

TABLE 4-1. EXPERIMENTAL VARIABLES AND PARAMETERS FOR THE 2-FOOT-WIDE FLUME

Run No.	1C	1M	1F	2M	2C	3M
Water surface slope x 10^2	0.088	0.088	0.088	0.212	0.204	0.37
Normal depth (ft)	0.499	0.518	0.522	0.521	0.555	0.517
Water discharge (cfs)	1.14	1.14	1.14	1.69	1.70	4.00
Velocity of water (ft/sec)	1.14	1.10	1.07	1.625	1.53	3.88
Water temperature (^oC)	20.0	20.0	20.0	20.0	20.3	20.0
Bed form	ripple	ripple	ripple	dune	dune	plane bed
Total sediment concentration (ppm)	88.00	60.21	82.21	871.55	614.84	4884.61
Total sediment discharge (lb/sec)	0.00626	0.00429	0.00585	0.0918	0.065	0.1218
Percentage of total load in the tracer size range	3.0	4.0	6.0	11.0	4.0	
Size of tracer (mm)	0.50-0.59	0.30-0.35	0.177-0.210	0.30-0.35	0.50-0.59	0.30-0.35
Calculated amount of tracer (gm)	10900	2350	450	2350	10900	500
Actual amount of tracer (gm)	2100	1600	600	1600	2100	300
Actual tracer activity (μc)	260	260	300	320	450	750
Initial station of tracer	15.0	15.0	15.0	10.0	11.5	12.0
Velocity of tracer (ft/hr)	0.848	0.585	1.131	4.7	4.1	
Rate of spreading of tracer (ft^2/hr)	2.68	1.724	6.48	20.2	16.6	
Period of experiment	1/21/67 15:12 -1/22/67 16:25	2/22/67 14:45 2/23/67 14:30	3/22/67 15:25 -3/23/67 10:10	4/12/67 09:35 -4/12/67 15:45	6/13/67 12:25 -6/13/67 19:09	7/11/67 12:30 -7/11/67 12:40

of the tracer at any point along the flume should be twice the background. The design criterion for the amount of tracer particle used in each run was to get a statistically significant number of tracer particles in each core sample segment. Assume that the variation in the number of tracer particles in each core sample segment (1/4 inch to 1/2 inch thick) follows the Poisson distribution, so the coefficient of variation $C_v = \frac{\sigma}{\bar{N}} = \frac{1}{\sqrt{\bar{N}}}$ where $\bar{N}$ is the average number of tracer particles per sample segment. If we set $\bar{N} = 100$, then $C_v = 10\%$. Based on the above criterion, the total amount of tracer particles required can be estimated. The lower limit, where the tracer particles will penetrate into the bed, was assumed to be the lower limit of the deepest sand trough existing in the flume. Following this reasoning, an example for the medium sized tracer particles is given as follows. For a sample of 3/4 inch diameter and 1/4 inch thick and tracers of 0.33 mm diameter with a specific gravity of 2.65,

$$\text{weight per particle} = \frac{\pi}{6} (0.033)^3 \times 2.65 = 50 \times 10^{-6} \text{ gm}$$

$$\text{weight per sample} = \frac{\pi}{4} \left(\frac{3}{4}\right)^2 \left(\frac{1}{4}\right) (2.54)^3 \times \frac{100}{62.4} = 2.90 \text{ gm} .$$

If we assume the thickness of movement of the sand is 0.25 foot and the dry bulk density of sand is 100 lb/ft^3, then the weight of sediment in movement = $60 \times 2 \times 0.25 \times 100 \times 454 = 1.36 \times 10^6$ gm. The total number of tracer particles = $\frac{100 \times 1.36 \times 10^6}{2.90} = 4.7 \times 10^7$, and the total weight of tracer particles = $4.7 \times 10^7 \times 50 \times 10^{-6} = 2{,}350$ gm. One condition that must be satisfied in using tracer particles in a dispersion experiment is that the amount of tracer introduced in the

channel is small enough so that the composition of the bed material near the source will not be changed too greatly. So the above calculation only served as a guide. Actually the amount of tracer particles used in each run is different from the calculated value and is listed in Table 4-1.

D. Introduction of the Tracer Particles

The flume was run until the right equilibrium condition was obtained. By inserting a board slowly at the tail gate and turning down the water discharge simultaneously, the bed configurations could be kept after the water was drained out. The methods of introducing the tracer particles were different for the ripple, dune and plane bed conditions.

For the ripple case, a trench was dug at the initial station across the flume. The depth of this trench equaled one standard deviation of the vertical variation of the bed configuration below the mean bed level. The width of the trench depended on the amount of tracer particles used. After the tracer particles were evenly distributed along the trench, they were covered by ordinary sand from the flume. The buried tracer particles were then covered by cloth anchored by sheet piling to protect them from being washed out before the right flow conditions were re-established. By removing the board at the tail gate slowly and increasing the discharge of water to the right discharge simultaneously, the right flow condition could be easily re-established. After the equilibrium condition was re-established, the cloth cover was removed, and the flow was allowed to scour out the buried tracer particles.

For the dune and plane bed cases, a steel plate was put under the tracer particles as shown in Fig. 4-6. Instead of allowing the tracer particles to be released slowly by the natural scouring action of the flow, they were released by lifting the steel plate to give an approximately instantaneous in-put into the flow. The main reason for this kind of artificial in-put is that it took too long for all the tracer particles to be scoured by the flow itself; while some particles were spread all along the flume, others remained buried at the source. The only difference of introducing the tracer particles between the dune condition and the plane bed condition was that the cloth covers were not used for plane bed conditions since only a thin layer of sediment was moving during the plane bed runs.

E. Determination of the Concentration Distribution Curves

The instruments used in obtaining the longitudinal concentration distribution curves were a scintillation detector (Nuclear-Chicago Corporation Model DS5), an analytical count ratemeter (Nuclear-Chicago Corporation Model 1620B), a radiation analyzer (Nuclear-Chicago Corporation Model 1810) together with a voltage regulator and a strip-chart recorder as shown in Fig. 4-2a and Fig. 4-7. A water-tight casing was put on the scintillation detector, which was carried by the instrument carriage on the flume. In order to improve the spatial resolution of the detection system, a collimator, consisting of two half annular lead shields that were one inch thick and three and one half inches high, was put on the bottom of the detector with a spacing of 3/4 inch

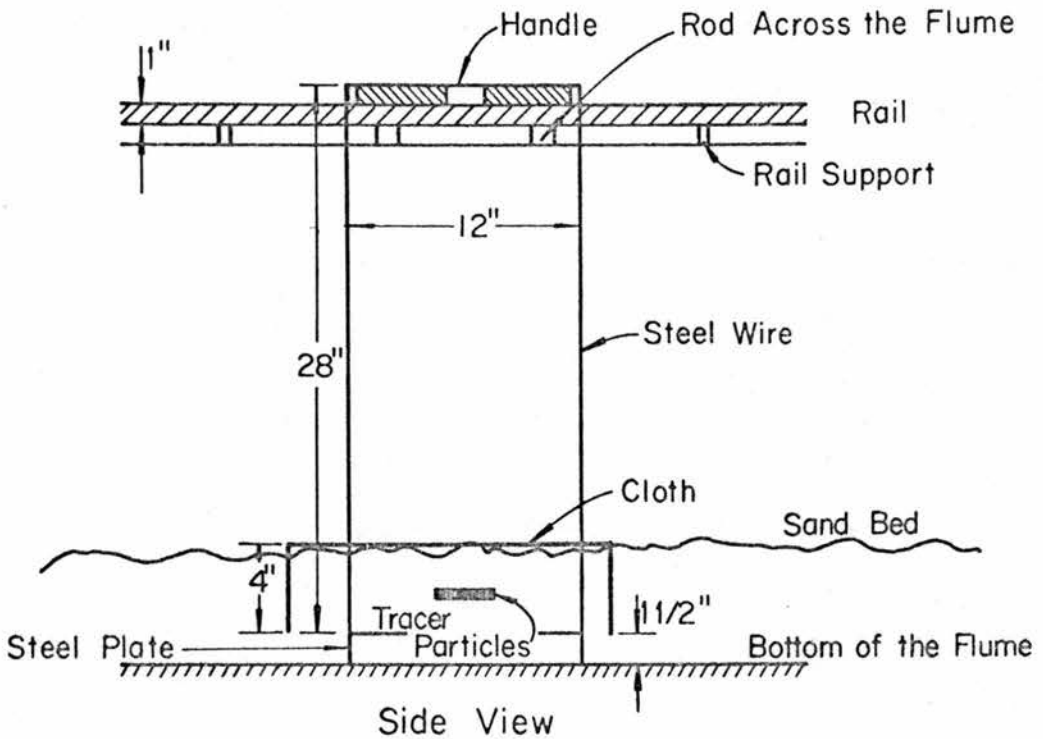

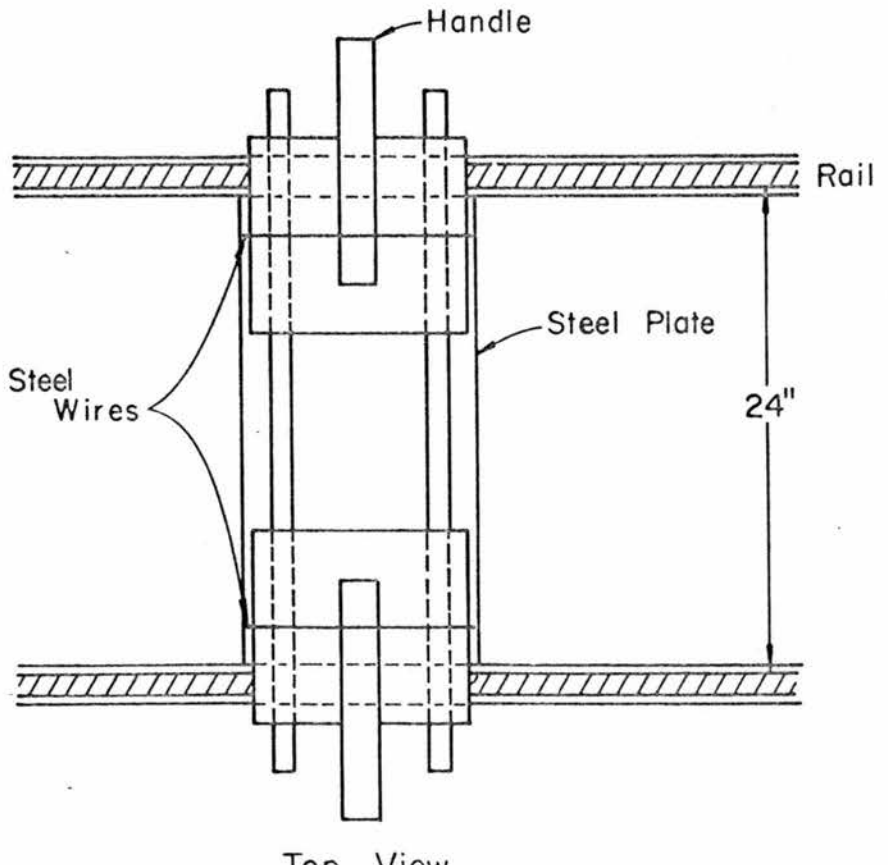

Figure 4-6. Schematic diagram of the tracer releaser used in dune and plane bed runs

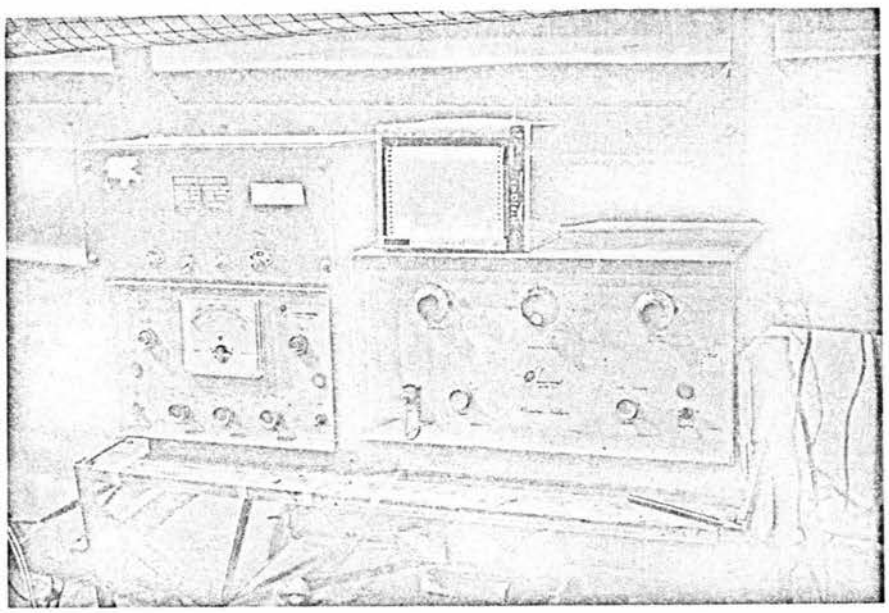

Figure 4-7. Some of the instruments used in determining the longitudinal concentration distribution of tracer particles

in between the two half annular lead shields. Fig. C-1 in Appendix C shows an example of how effective this collimator can improve the spatial resolution of the detector system when all the tracer particles are concentrated at the initial station as an approximate line source. This detector was connected with the radiation analyzer, and the radiation analyzer was connected to the analytical count ratemeter and strip-chart recorder. The voltage regulator was used to provide a constant power supply. The integral setting for the radiation analyzer was used. This set of instruments was calibrated before each run by using a 10 μc cesium-137 source as a standard. After the tracer particles were released, six to eight passes were made in each run. The detector was located at 1/2 foot to the left side of the center line of the flume, then at 1/2 foot to the right side of the center line for each pass. With the event-marker, a longitudinal radioactivity distribution curve with the stations was plotted on the strip-chart recorder.

F. Determination of the Tracer Distribution in the Bed by Using Core Sampler

In order to determine the vertical distribution of tracer particles in the bed, a core sampler was used. It is a 19-inch long, 3/4 inch, I.D. plastic tube as shown in Fig. 4-8. The section stop on the piston rod can provide a precise control for the thickness of the core sample segments. Core samples were taken only after

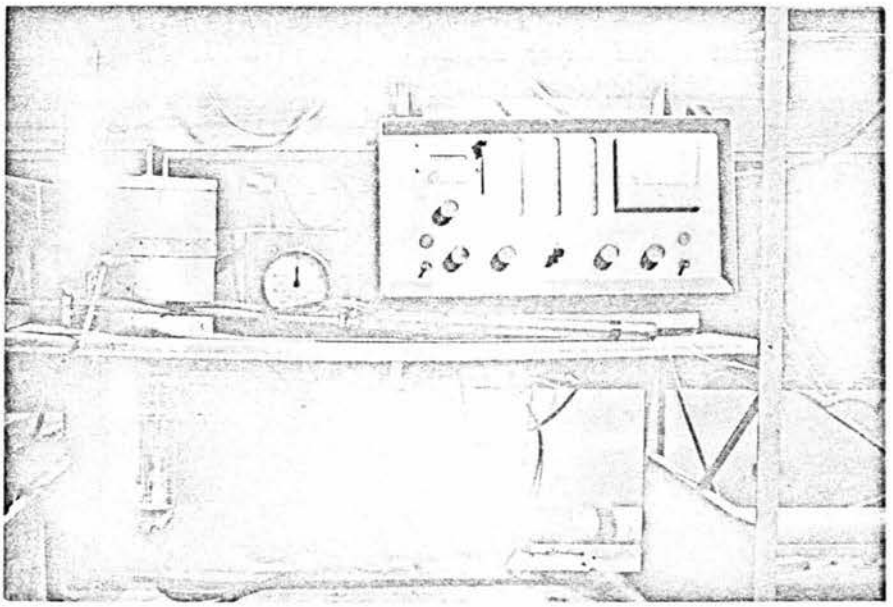

Figure 4-8. Instruments for determining the vertical concentration distribution of tracer particles in the sand bed

the tracer particles were spread out along several feet of the flume. The locations from which the core samples were taken were determined by inspecting the longitudinal concentration distribution data on the strip-chart, so that representative points were chosen. A pair of core samples at 1/2 foot on both sides from the center line of the flume were taken for each core sample location along the flume. The depth of core sample corresponded to the maximum trough of the sand bed during the experiment. After the core samples were taken, they were cut into slices of 1/4 inch to 1/2 inch and placed in paper cups. Then, the activity in each cup was counted by a scintillation detector together with a decade scaler and a timer as shown in Fig. 4-8.

G. Determination of the Total Load by Total Sediment Transport Sampler

The total sediment transport sampler was a width-depth integrating sampler which sampled a 1/2 inch wide section of the pipe and could be moved back and forth across the end of the flume as shown in Fig. 4-9. The outlet of this sampler is a triangular trough which conveyed the water-sediment mixture to a circular tank. A point gage was mounted on the circular tank to measure the volume of water-sediment mixture. The sediment in the circular tank was then removed, dried and weighed. About ten samples were taken in each run and the average total sediment discharge was obtained.

H. Special Methods Used for Plane Bed Condition

For the plane bed case, since the bed is a flat plane, no bed configuration information was necessary. Because the tracer parti-

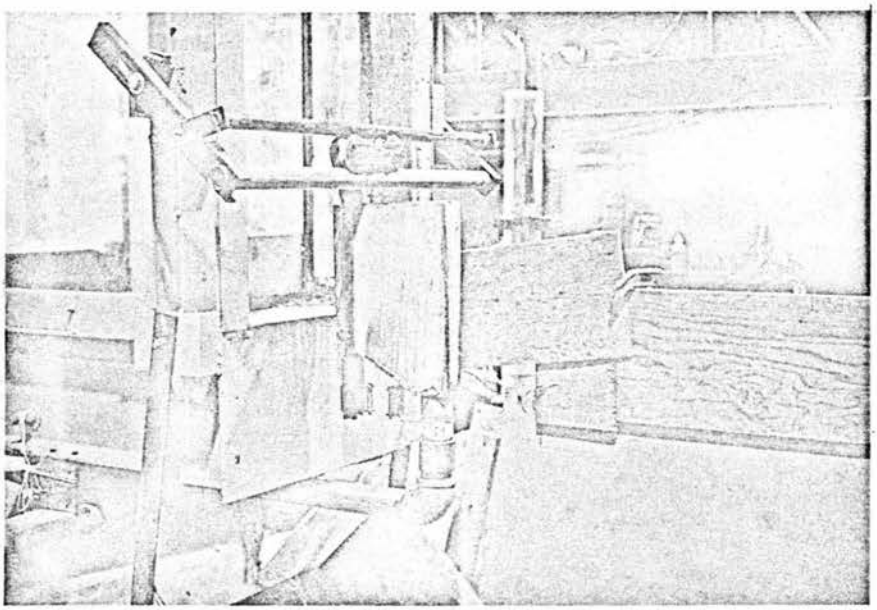

Figure 4-9. Total sediment transport sampler

moved much faster in this case than in ripple or dune conditions, where the movement of tracer particles is relatively slow as compared with the speed of the carriage, the method of obtaining longitudinal concentration distribution data used for the ripple and dune cases was not valid. Two scintillation detectors were used for the plane bed condition. These were located at stations 35 and 55, respectively, to observe the tracer particles passing by the detectors. A portable scintillation detector was located at the entrance to see when the tracer particles would appear again through recirculation. Once the tracer particles reappeared through recirculation, the experiment was completed.

I. Preliminary Experiments for the Determination of the Step Length and Rest Period of a Single Particle

These experiments were done during the summer of 1966. A 20 cm wide, 20 cm deep and 10 m long recirculating plastic flume was used for these experiments. White plastic particles with d_{50} = 2.2 mm and specific gravity 1.1 served as bed material. Black plastic particles with the same properties as the white plastic particles were used as tracers. The experiments were done under the following conditions:

water discharge = 0.1065 cfs to 0.1547 cfs

water-surface slope = 0.0006

water temperature = 24° C

average water depth = 0.25 ft to 0.41 ft

average height of dune = 0.08 ft to 0.13 ft

average length of dune = 2.2 ft to 3.5 ft.

Since the white plastic particles were transparent, the black tracing particles could be seen even if they were buried. The step lengths of each tracer particle were actually measured by using a measuring tape, and the rest periods were measured by using a stop watch. The purpose of these experiments was to determine the probability distribution functions for step lengths and rest periods.

Chapter V

ANALYSIS AND DISCUSSION OF RESULTS

A. Distribution of Step Lengths and Rest Periods of a Single Plastic Tracer Particle

The distribution of step lengths of a single plastic tracer particle obtained in a 20-cm-wide plastic flume for two different flow conditions is shown in Fig. 5-1. With the mean and variance obtained from the actual step length data, k_1 and r can be found by solving Eq. (3-11) together with

$$\sigma_s^2 = \frac{r_s}{k_{1s}^2} \tag{5-1}$$

where σ_s^2 is the variance of the step length distribution which follows the gamma distribution function equation (3-10), the subscript s denoting step length. The curves in Fig. 5-1 are the theoretical gamma distribution function as described by equation (3-10). We can see that the distribution of step lengths of this particle is adequately represented by the gamma distribution function. The scattering of the actual data about the theoretical curve is due to the fact that less than 100 step lengths were measured in each flow condition, which is not sufficient to give a smooth curve.

The rest periods of the same particle for the same two flow conditions were also measured. The results are plotted on exponential

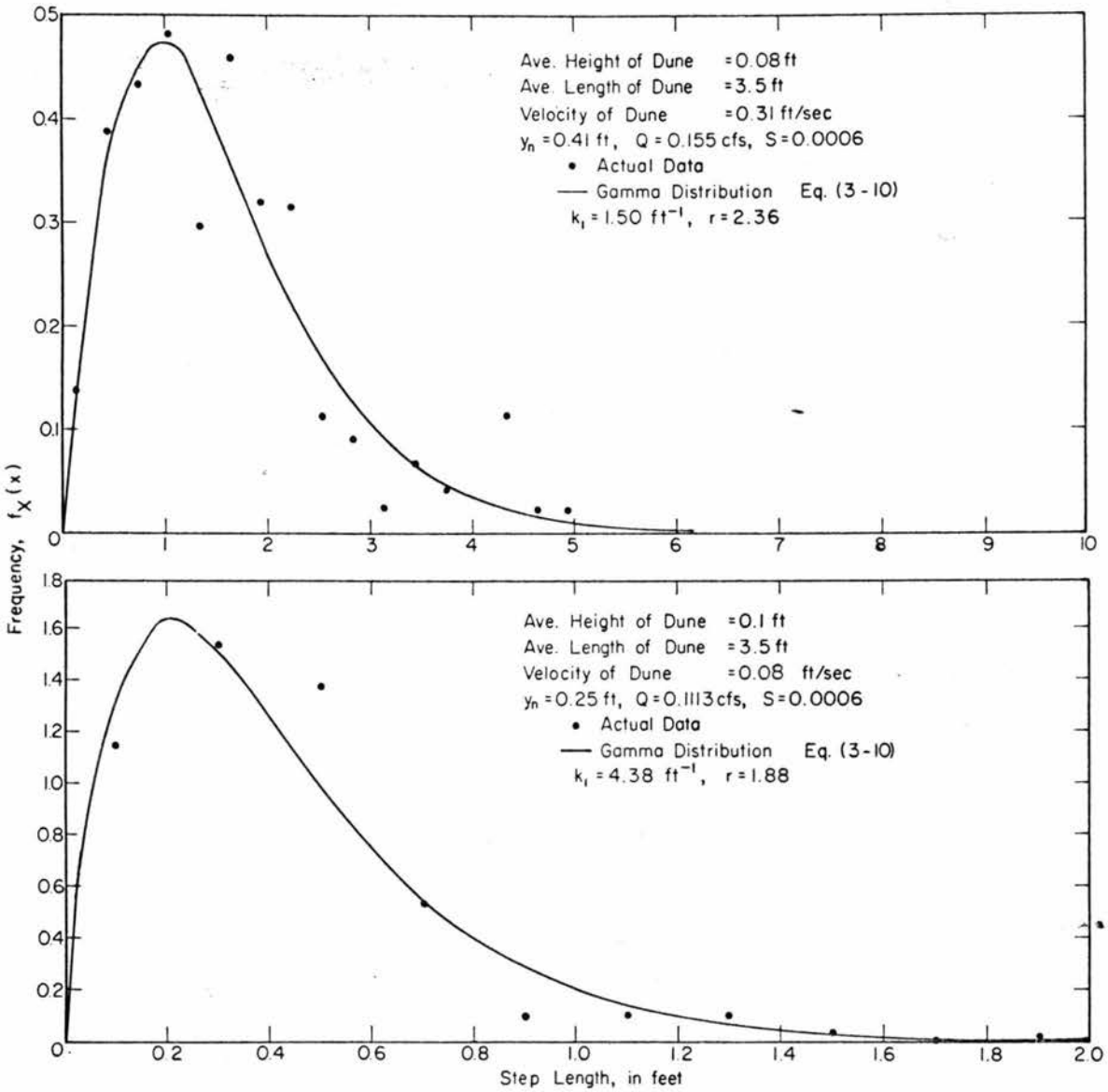

Figure 5-1. Distribution of step lengths of a single plastic tracer particle

probability paper. The actual mean rest periods were substituted into Eq. (3-13) to get the k_2 values. The straight lines in Fig. 5-2 follow the integral of Eq. (3-12) for exponentially distributed rest periods. From Fig. 5-2 we can see that the rest periods follow the exponential probability distribution function quite closely. These conclusions about the distribution of step lengths and rest periods for light-weight plastic particles may or may not be applied to the distribution of step lengths and rest periods of sand particles.

B. Longitudinal Concentration Distribution

In order to get a general idea of how the dispersion process goes, a set of longitudinal concentration distribution curves would be helpful in showing how the process develops over a period of time. However, the same kinds of curves are also needed for later comparison with the stochastic model and the core sample results. For the sake of avoiding duplication, presentation of these data will be postponed until Figs. 5-14, 4-15 and Appendix C, where the comparison of the experimental longitudinal dispersion curves with the stochastic model and the core sample results is discussed.

According to Eq. (3-22), the mean rate of movement of tracer particles should be a constant for a certain flow condition and particle size. If the mean distance traveled by tracer particles is plotted as a function of dispersion time, the result should be a straight line passing through the origin. This relationship can be seen from Fig. 5-3 for the ripple conditions, and from Fig. 5-4 for

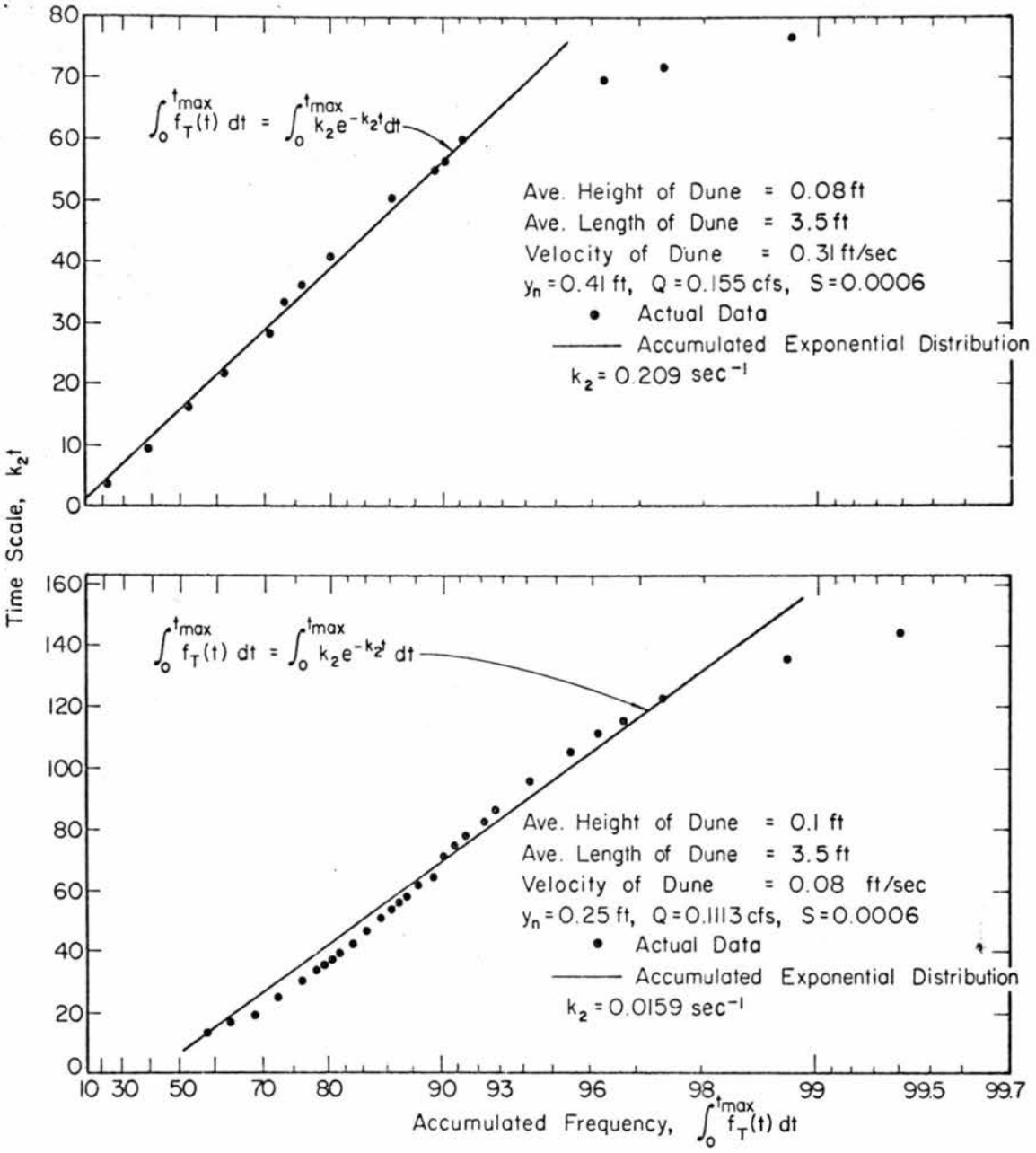

Figure 5-2. Distribution of rest periods of a single plastic tracer particle

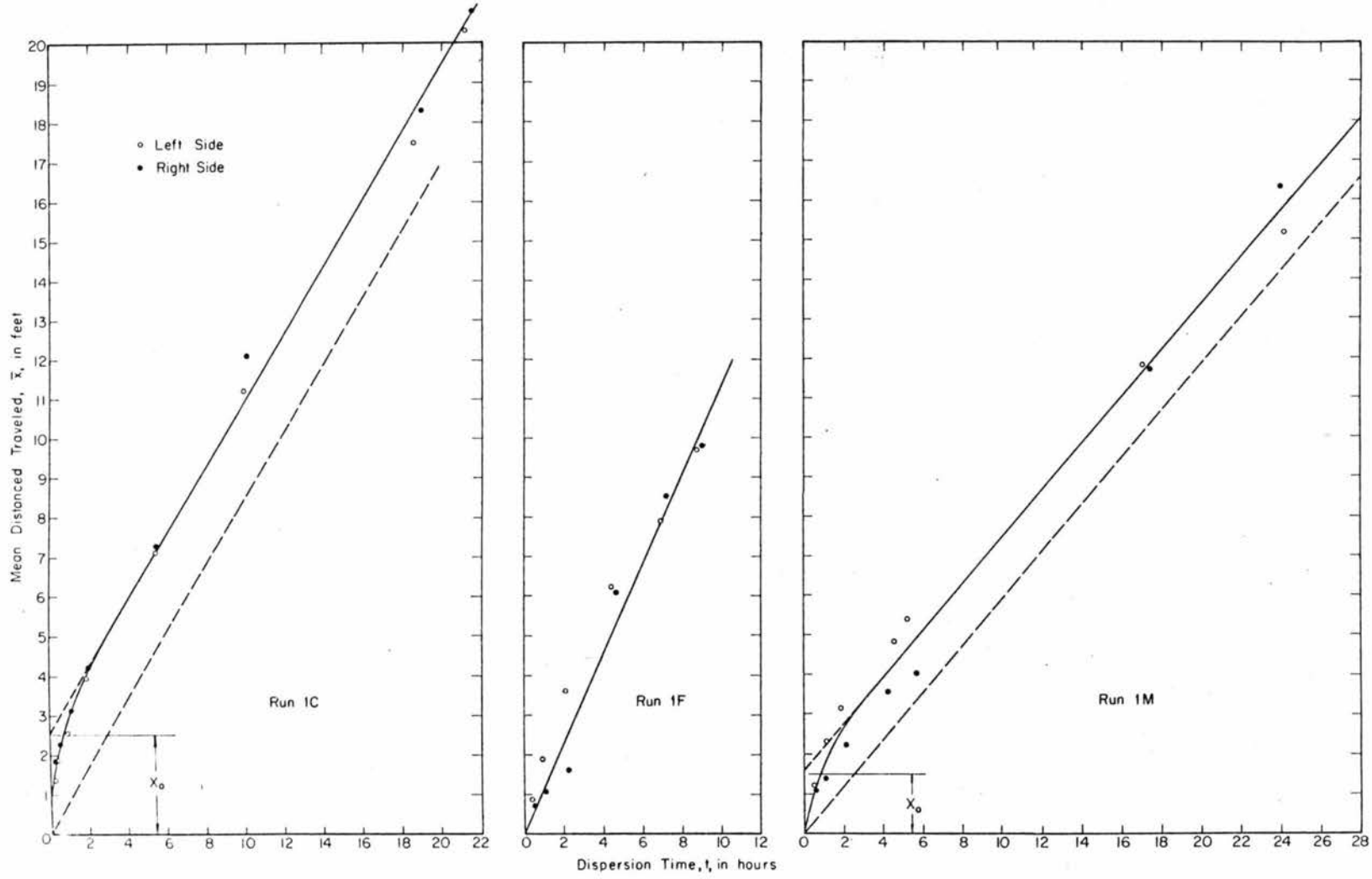

Figure 5-3. Location of mean as a function of dispersion time for ripple conditions

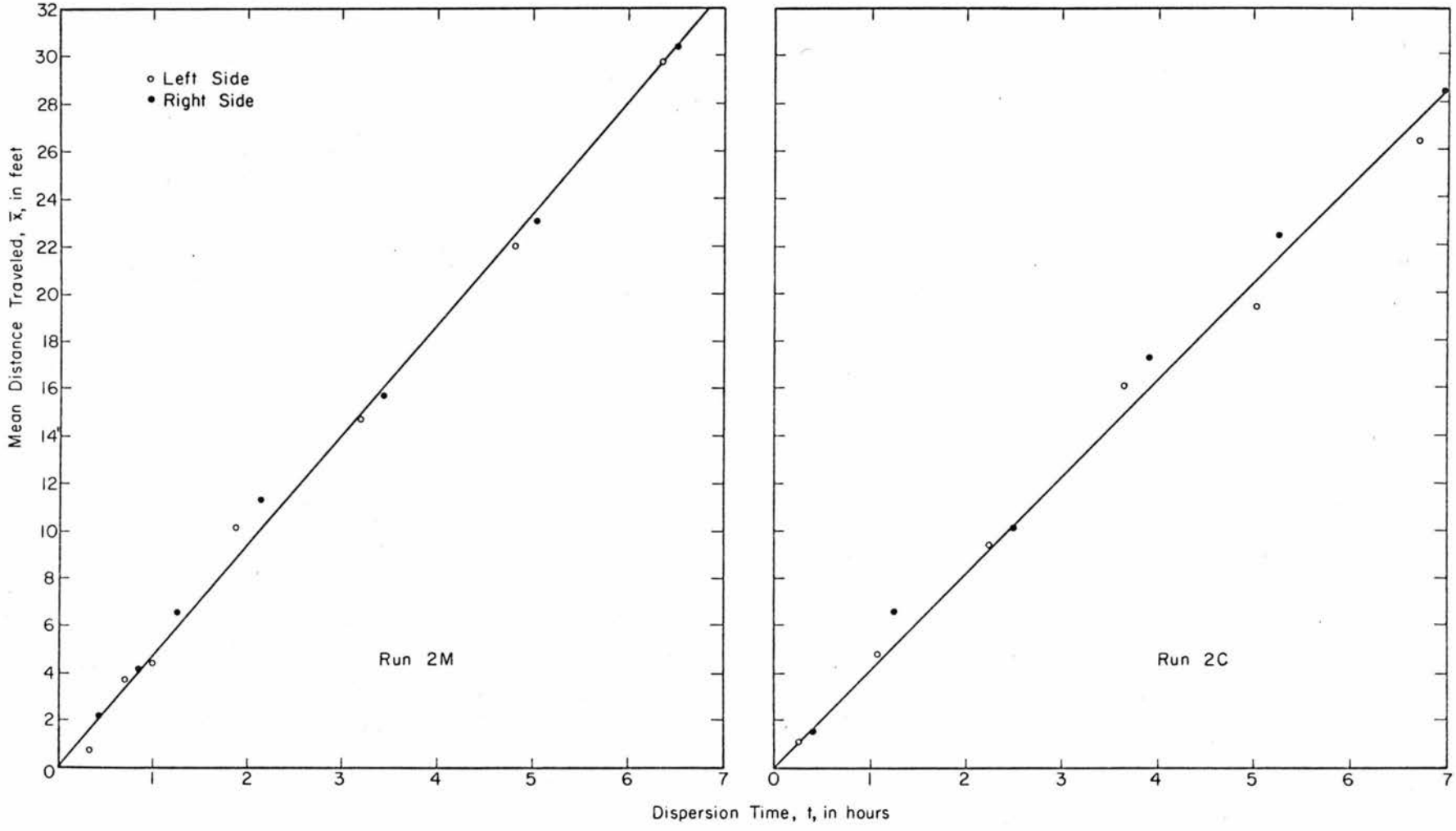

Figure 5-4. Location of mean as a function of dispersion time for dune conditions

the dune conditions. In each case the data were obtained 1/2 foot either side of the center line of the flume. The reason for the curved portion near the origin in some of the relationships is that the tracer particles were not mixed uniformly over the entire depth of layer of moving particles at the beginning of the experiment. For the same flow condition and bed configuration, finer particles should move faster than coarser particles. This is true for both the ripple and the dune cases with the exception being Run 1C, which has a higher mean rate of movement of tracer particles than Run 1M. This can be explained by the fact that the flow condition for Run 1C was such that the measured total sediment discharge for Run 1C was higher than that for Run 1M. Since both the water velocity and the total discharge of sediment are higher for dune conditions than for ripple conditions, the mean rate of movement of tracer particles is also higher. The technique of raising the tracer particles toward the surface of the bed by means of a steel plate at the beginning of the experiment is apparently very effective as can be seen from the results for Run 2M and Run 2C where the $\bar{x}$ vs t relationships are straight lines going through the origins.

According to Eq. (3-23) the relationship between the variance of the longitudinal distribution and the dispersion time is also linear. Figure 5-5 and Fig. 5-6 show the relationships between the variance, σ_x^2, and the dispersion time, t, for ripple and dune conditions, respectively. Similar effects on the results due to the

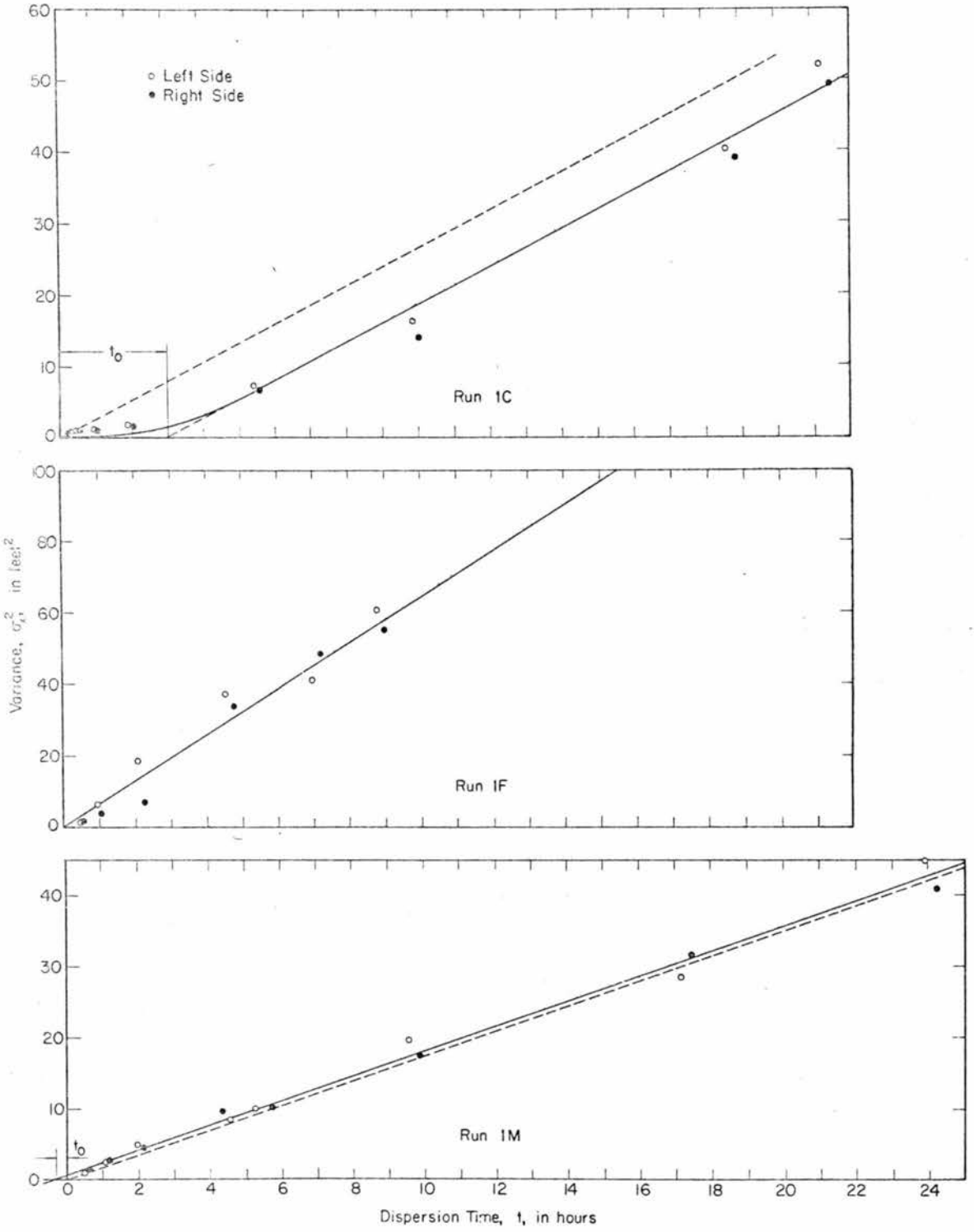

Figure 5-5. Variance as a function of dispersion time for ripple conditions

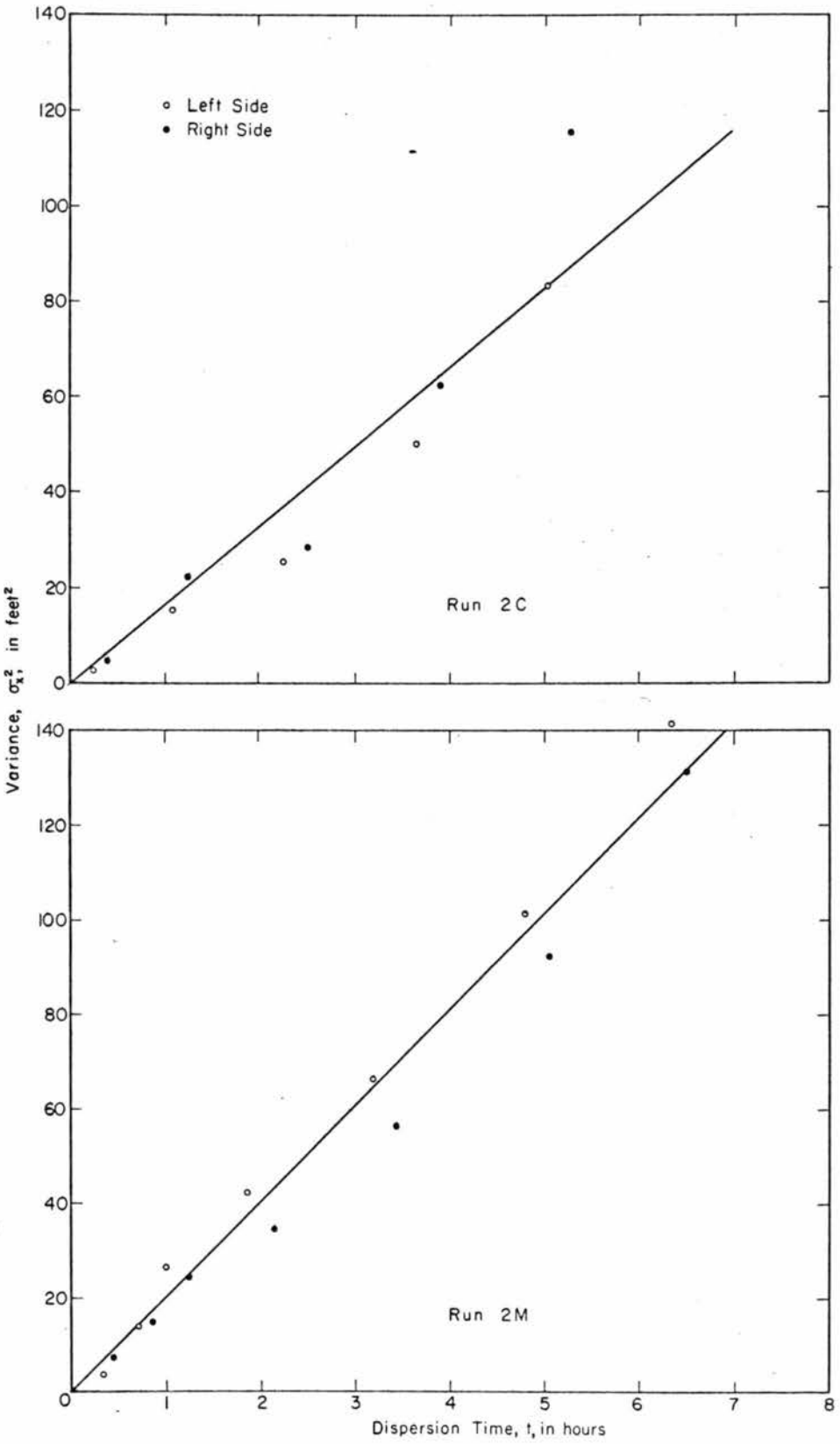

Figure 5-6. Variance as a function of dispersion time for dune conditions

method of releasing the tracer, the size of tracer particles, the bed form and flow condition can be found from Fig. 5-5 and Fig. 5-6 as discussed for Fig. 5-3 and Fig. 5-4.

For Hubbell and Sayre's stochastic model, Eq. (2-2), only two parameters are needed. When r = 1, Eq. (3-22) becomes

$$\frac{d\bar{x}}{dt} = \frac{k_2}{k_1} \quad . \tag{5-2}$$

After taking the derivative of σ_x^2 with respect to t and substituting Eq. (5-2) and r = 1 into Eq. (3-23), the rate of change of variance is

$$\frac{d\sigma_x^2}{dt} = \frac{2k_2}{k_1^2} = \frac{2\ d\bar{x}/dt}{k_1} \quad . \tag{5-3}$$

The two parameters, k_1 and k_2, can be obtained by solving Eq. (5-2) and Eq. (5-3) simultaneously with the $d\bar{x}/dt$ and $d\sigma_x^2/dt$ values obtained from the experimental results. In cases where there is curvature near the origin in Fig. 5-3 and Fig. 5-5, a correction is necessary. This correction can be done by drawing a dashed straight line through the origin parallel to the experimental results at larger dispersion time. The correction factors x_o and t_o are the distance difference and time difference between the solid and dashed straight lines, respectively. The corrected distance and time coordinate system should be $t' = t - t_o$ and $\bar{x}' = \bar{x} - x_o$, respectively. In the new coordinate system the dashed straight lines pass through the origin. The direction of the time correction based on the mean is,

in some cases, contrary to that based on variance. This means at the beginning stage the tracer is traveling faster but spreading slower. This may be caused by releasing the tracer particles within a short time period which is not the natural condition of movement. The slopes in Fig. 5-3 through Fig. 5-6 and the values of k_1 and k_2 for the Hubbell-Sayre model that were obtained in the different runs are listed in Table 5-1.

For the general one-dimensional stochastic model, three parameters k_1, k_2 and r, are needed. It would seem that these three parameters could be obtained by simultaneously solving Eq. (3-22) together with the derivative of Eq. (3-23) with respect to t

$$\frac{d\sigma_x^2}{dt} = \frac{k_2 r}{k_1^2} \quad (r+1) \tag{5-4}$$

TABLE 5-1. PARAMETERS USED IN HUBBELL AND SAYRE'S ONE-DIMENSIONAL STOCHASTIC MODEL

Parameter / Run No.	$\frac{d\bar{x}}{dt}$ (ft/hr)	$\frac{d\sigma_x^2}{dt}$ (ft^2/hr)	k_1 (ft^{-1})	k_2 (hr^{-1})
Run 1C	0.848	2.68	0.633	0.537
Run 1M	0.585	1.724	0.679	0.397
Run 1F	1.131	6.48	0.349	0.392
Run 2M	4.7	20.2	0.465	2.18
Run 2C	4.1	16.6	0.494	2.025

and the skew parameter, $S\sqrt{t}$, from Eq. (3-24), i.e.,

$$S\sqrt{t} = \frac{r+2}{\sqrt{k_2 r(r+1)}} \quad . \tag{5-5}$$

If the rate of change of mean displacement is equal to a constant ψ_1 and the rate of change of variance equals another constant ψ_2 , then the skew parameter, $S\sqrt{t}$, should be

$$S\sqrt{t} = \frac{r+2}{r+1} \frac{\psi_2}{\psi_1} = \frac{r+2}{r+1} \frac{1}{\psi_3} \quad . \tag{5-6}$$

Figure 5-7 shows the relation between ψ_3 $S\sqrt{t}$ and r. The variation of ψ_3 $S\sqrt{t}$ is limited between 1.0 and 2.0. The actual experimental relationships between the skew parameter, $S\sqrt{t}$, and the dispersion time, t, are shown in Fig. 5-8 and Fig. 5-9. All the curves drawn through the data were made to approach constants as required by Eq. (5-6). These constant values are shown by the heavy lines at large dispersion time. The result for Run 1C is not shown here because the results scatter too much. However, because the skew parameter is based on the third moment of the longitudinal concentration distribution data, a little difference near the tail of the concentration distribution curve will make a big difference in the result of the skew parameter. The negative skew parameters are probably caused by pockets of tracer particles which were buried near the initial station and released much later. The parameters of the general one-dimensional stochastic model obtained by this method for Run 1F are k_1 = 0.434 1/ft, k_2 = 0.33 1/hr and r = 1.49.

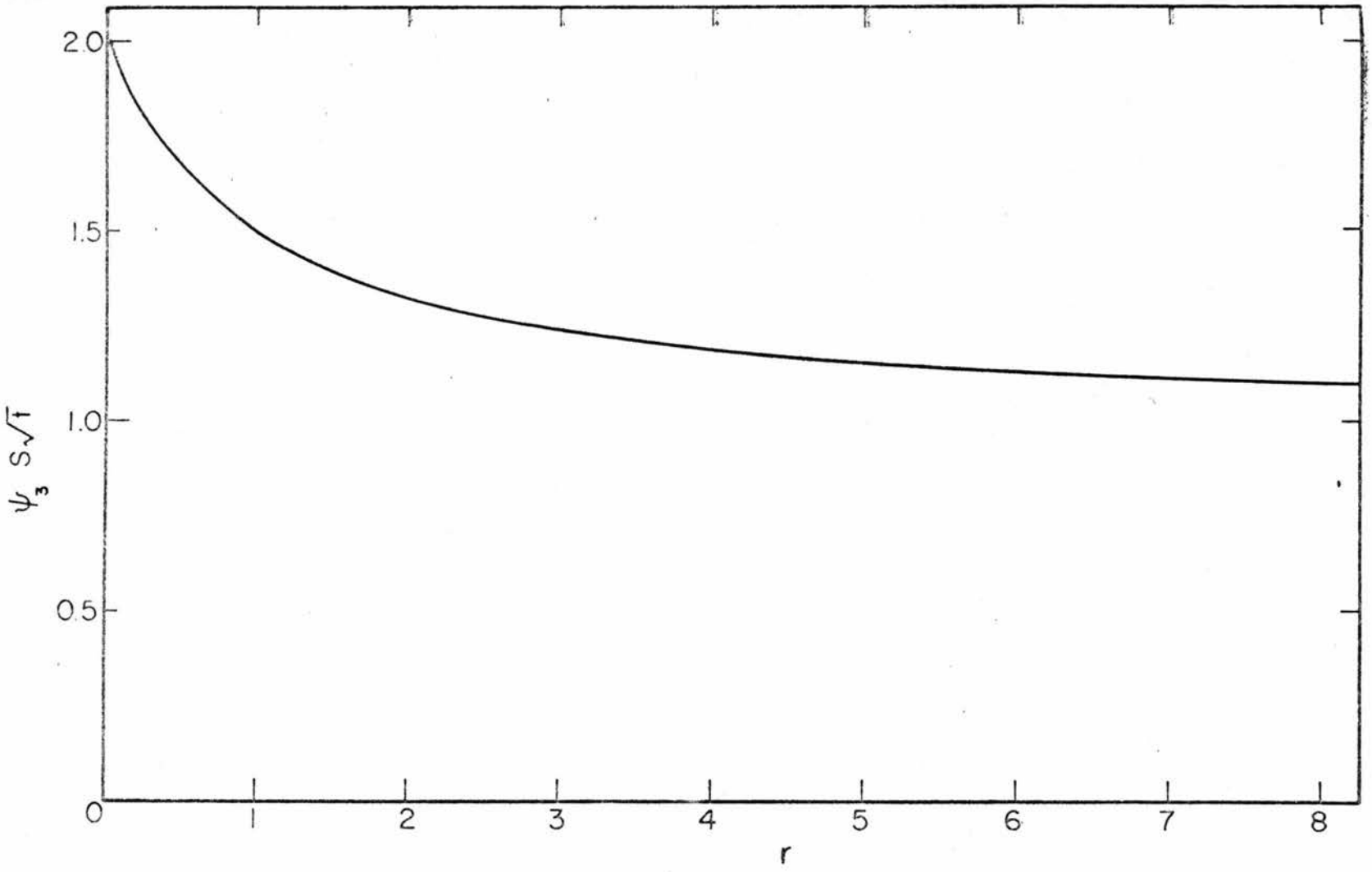

Figure 5-7. The relationship between ψ_3 S$\sqrt{t}$ and r .

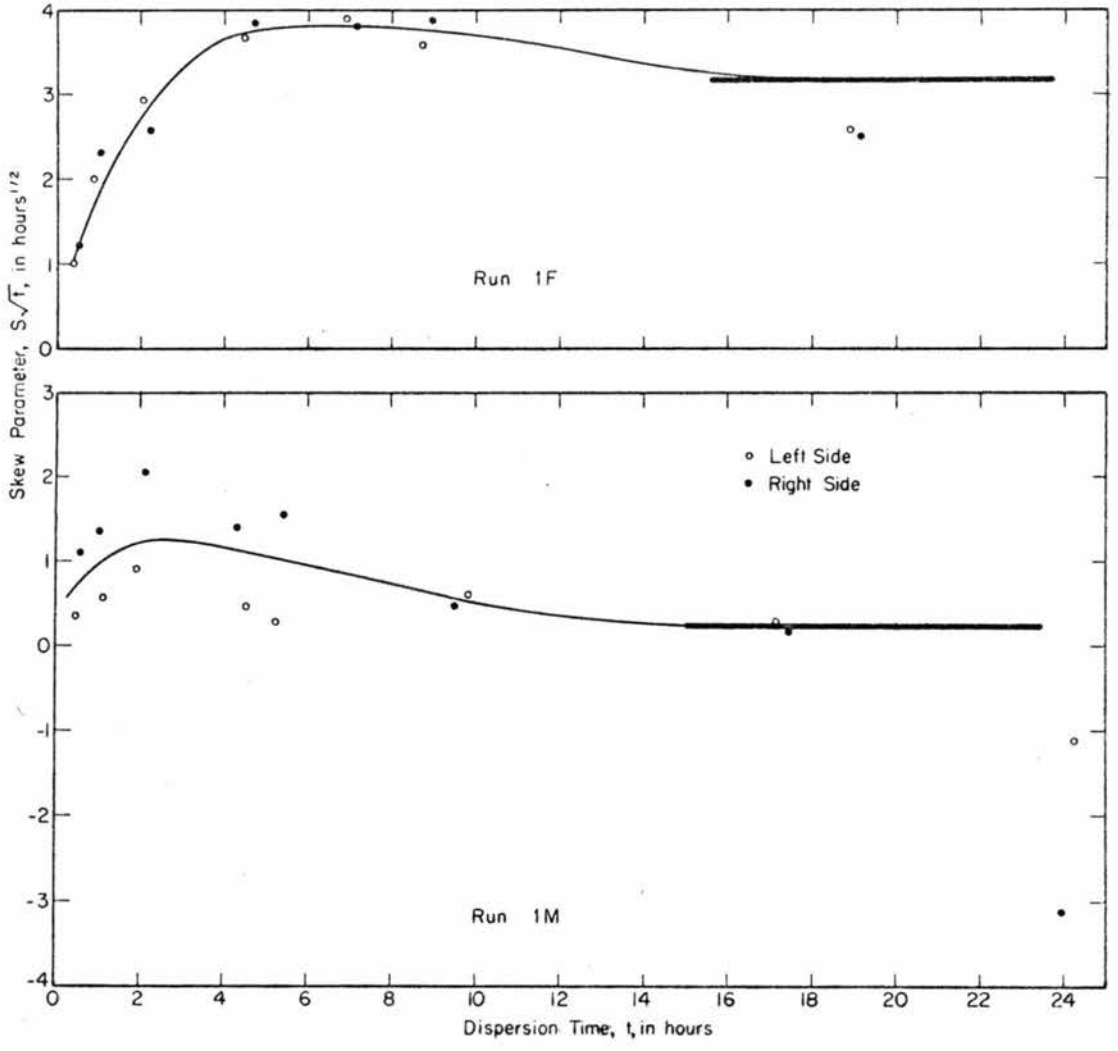

Figure 5-8. Skew parameter as a function of dispersion time for ripple conditions

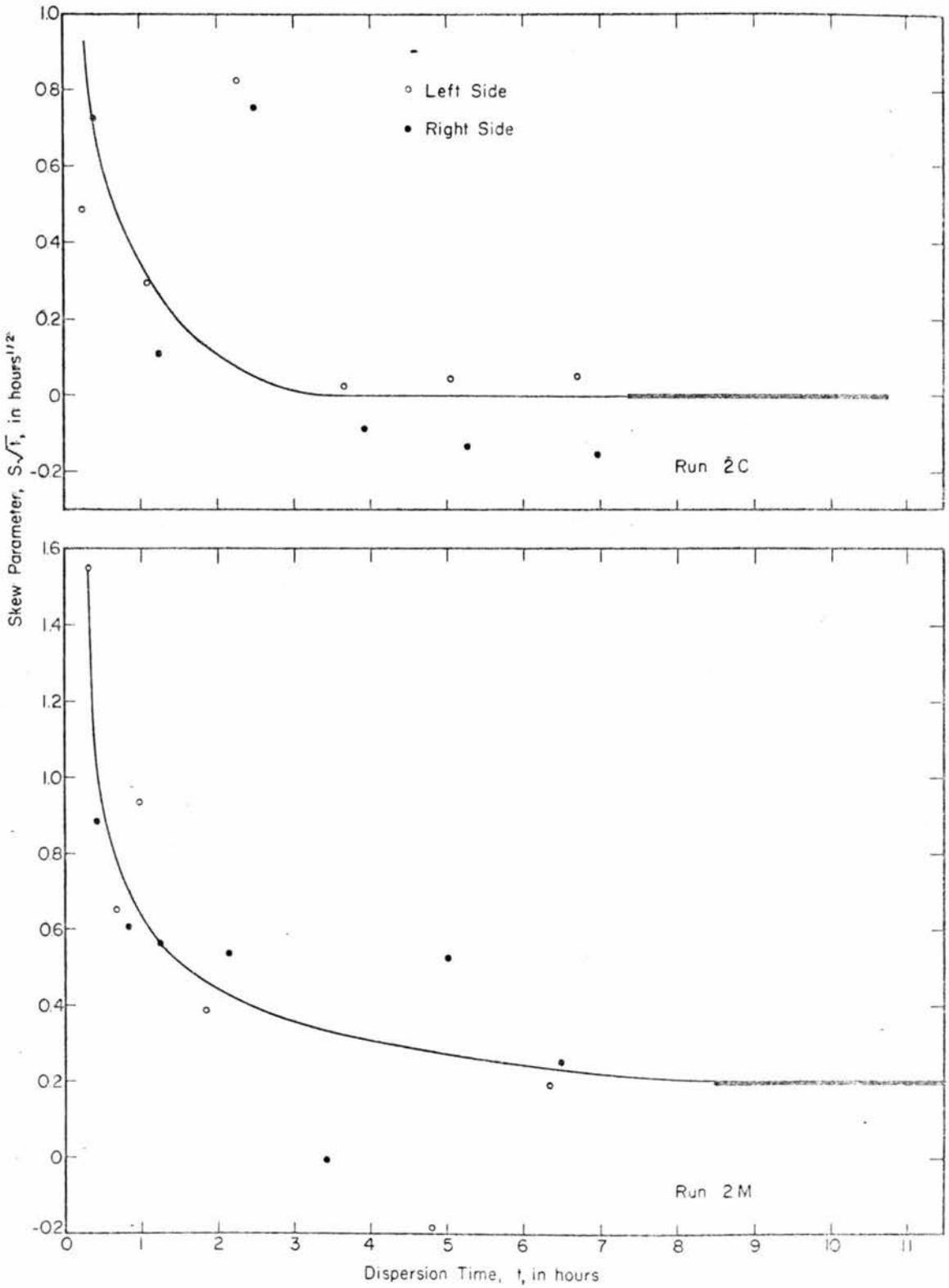

Figure 5-9. Skew parameter as a function of dispersion time for dune conditions

The r values for some other runs turned out to be negative, which is impossible for a gamma distribution function. These results may be caused by the fact that the flume is too short for this kind of dispersion study so that data were taken before the dispersion process became fully developed. In Fig. 5-7 the change of skew parameter value is small compared with the change of r values, especially at large r values. As a consequence of this result, a particular set of $f_t(x)$ curves can apparently be closely approximated by using many different combinations of k_1, k_2 and r values. So this method, although it is one way of getting the parameters for the general one-dimensional stochastic model, may not be the best way.

Following the initial release of the tracer particles, a certain length of time, which may be called an initial mixing period, is required for establishing an overall vertical distribution pattern in the bed that depends on the bed configuration. In general, at the beginning of the dispersion process, these tracer particles will penetrate deeper and deeper into the alluvial bed. The depth of penetration of tracer particles is eventually limited by the deepest troughs of the ripples or dunes. The radioactivity measured by a scintillation detector from a tracer particle depends not only on the strength of the activity of that particle, but also on the medium and the distance between the particle and the detector. As a result of these phenomena and the possibility of loss of some of the radioactive label, the total activity recorded along the flume or the area under the longitudinal concentration curve decreases and approaches a constant as the dispersion time increases as shown in Fig. 5-10 and Fig. 5-11.

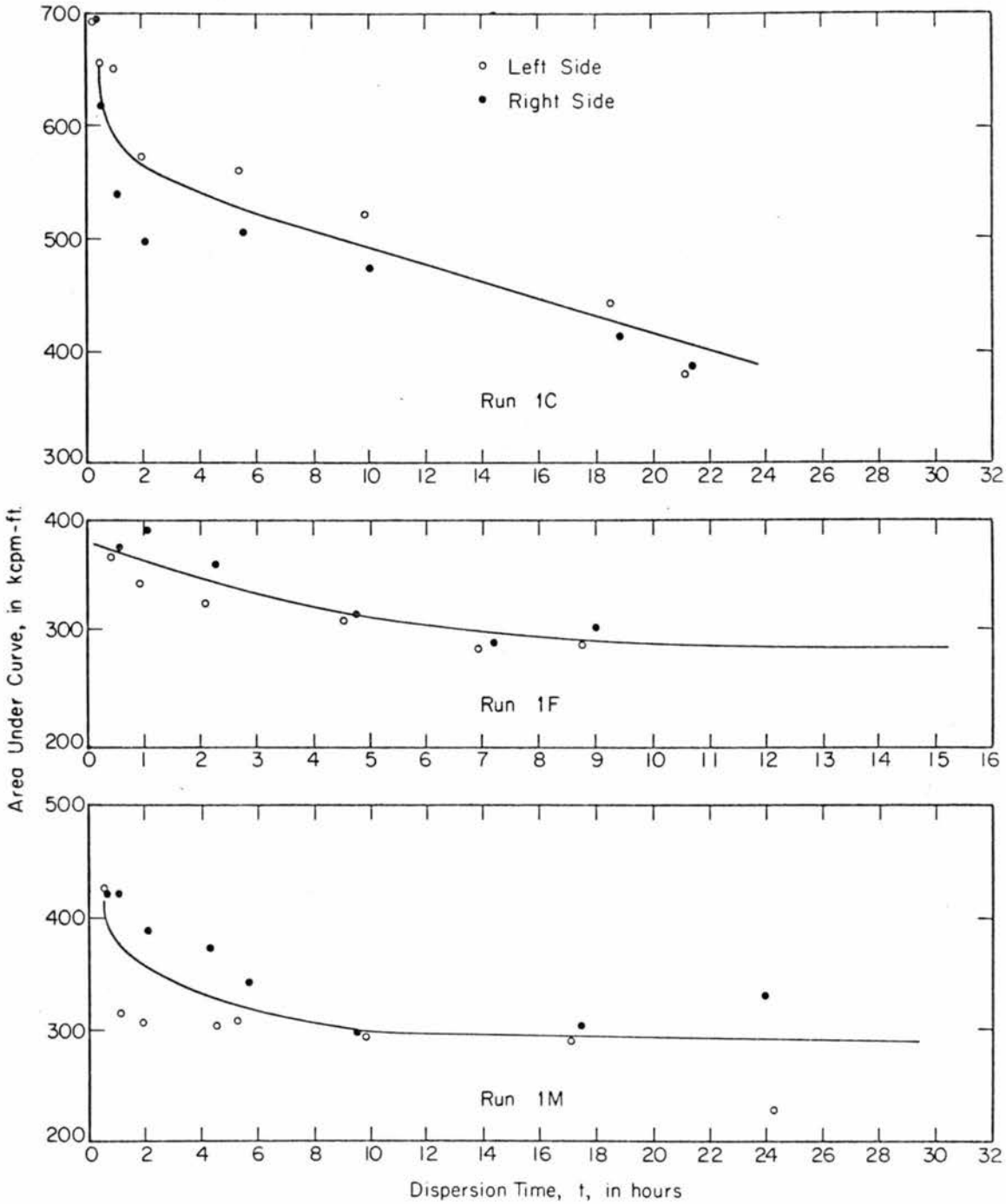

Figure 5-10. Area under the experimental longitudinal concentration distribution curve as a function of dispersion time for ripple conditions

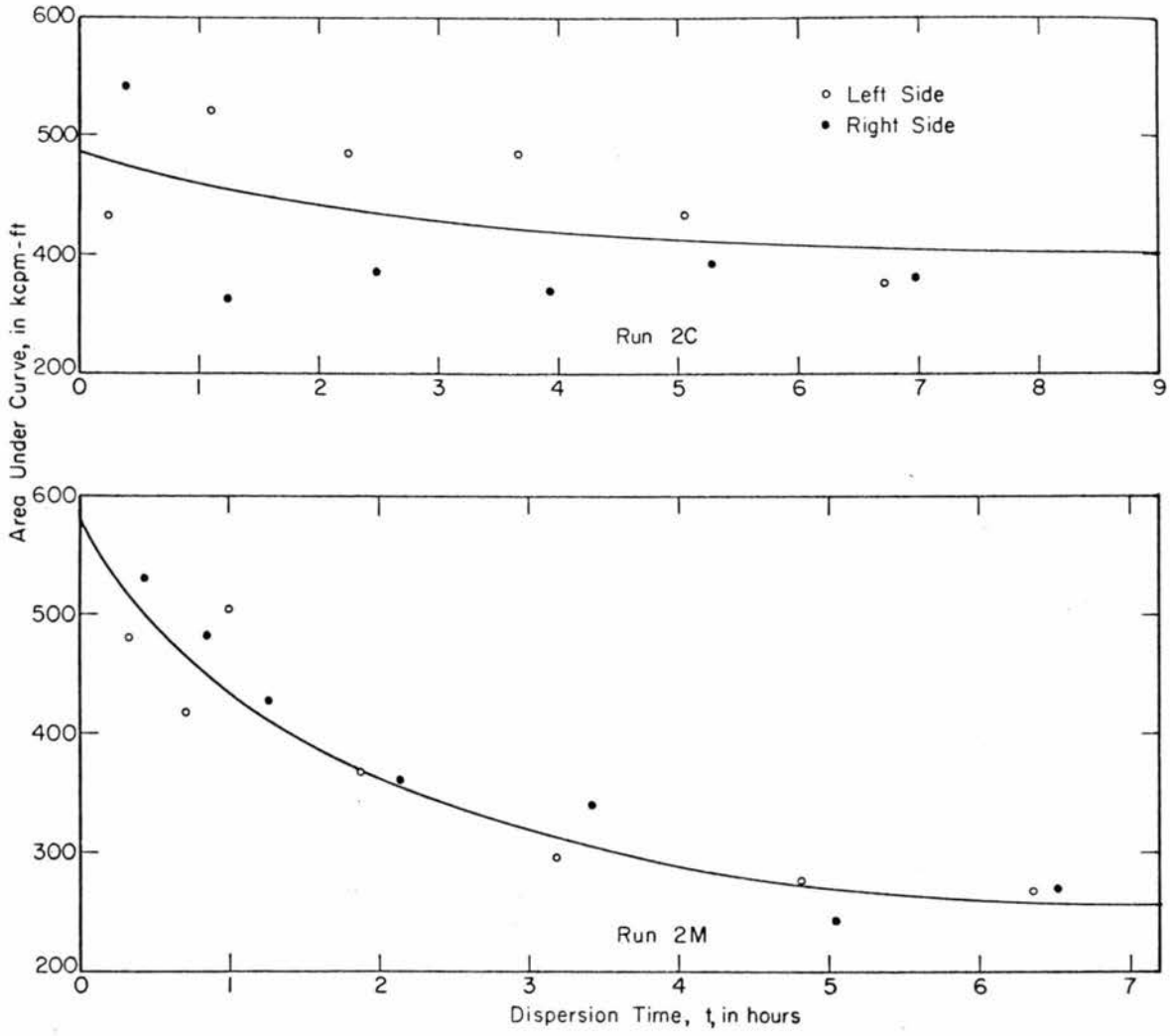

Figure 5-11. Area under the experimental longitudinal concentration distribution curve as a function of dispersion time for dune conditions

A computer program in Appendix B serves the purpose of calculating the function $f_t(x)$ in Eq. (3-19) for all possible combinations of the parameters in that equation. Different numbers of steps, i.e. N values, were tried in the computer program. The results indicate the rate that $f_t(x)$ approaches its theoretical value, i.e. when $N=\infty$, decreases with increasing N values. In our experiments, when N is greater than 100, it adds no practical contribution to the values of $f_t(x)$. Figure 5-12 gives an example of the computer result which shows the variation of $f_t(x)$ as a function of dispersion time. According to Eq. (3-24) the skew coefficient decreases when the dispersion time increases. So, at large dispersion time, $f_t(x)$ tends to become more symmetrical as shown in Fig. 5-12. From Eq. (3-10) and Eq. (3-12), the distribution of step lengths is related to r, but the distribution of rest periods is independent from r. So, the effect of r on $f_t(x)$ is completely due to the effect of r on the distribution of step lengths. Comparing Eq. (5-6) with Eq. (5-9) in the next section, the change of skewness in the step-length distribution function is more sensitive to a change in r than is the change of skewness of $f_t(x)$. From Eq. (3-24), when k_1 and k_2 are held constants at a particular dispersion time, the skew coefficient decreases with increasing r values, and $f_t(x)$ should approach symmetry with increasing r values as shown in Fig. 5-13. When the mean step length and mean rest period are held constant at a particular dispersion time, the effect of different r values on the shape of $f_t(x)$ can be seen from Fig. 5-14. It is clearly shown in Fig. 5-14, that when the mean step length and mean rest

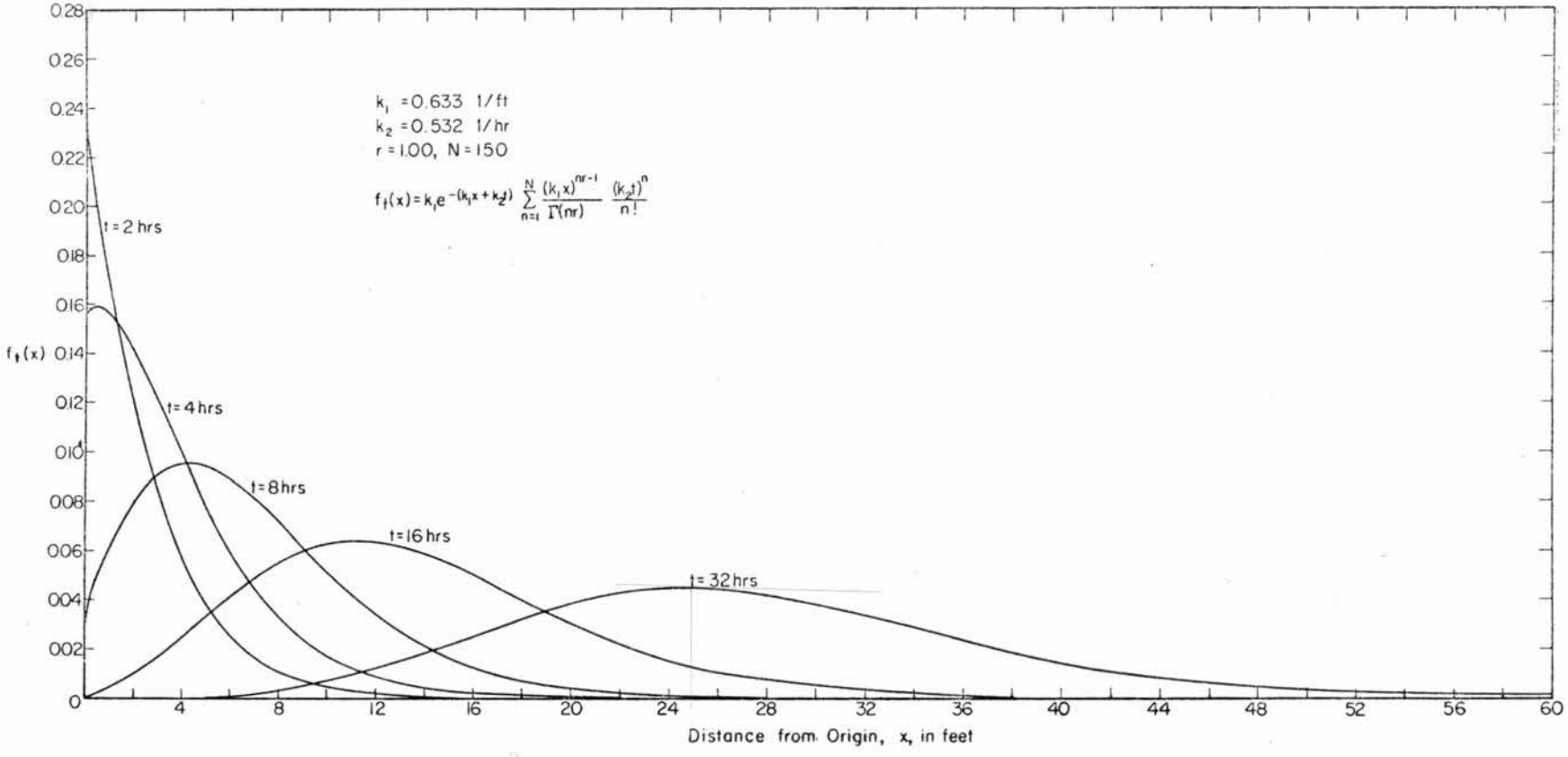

Figure 5-12. Variation of $f_t(x)$ for a particular set of k_1, k_2 and r values as a function of dispersion time

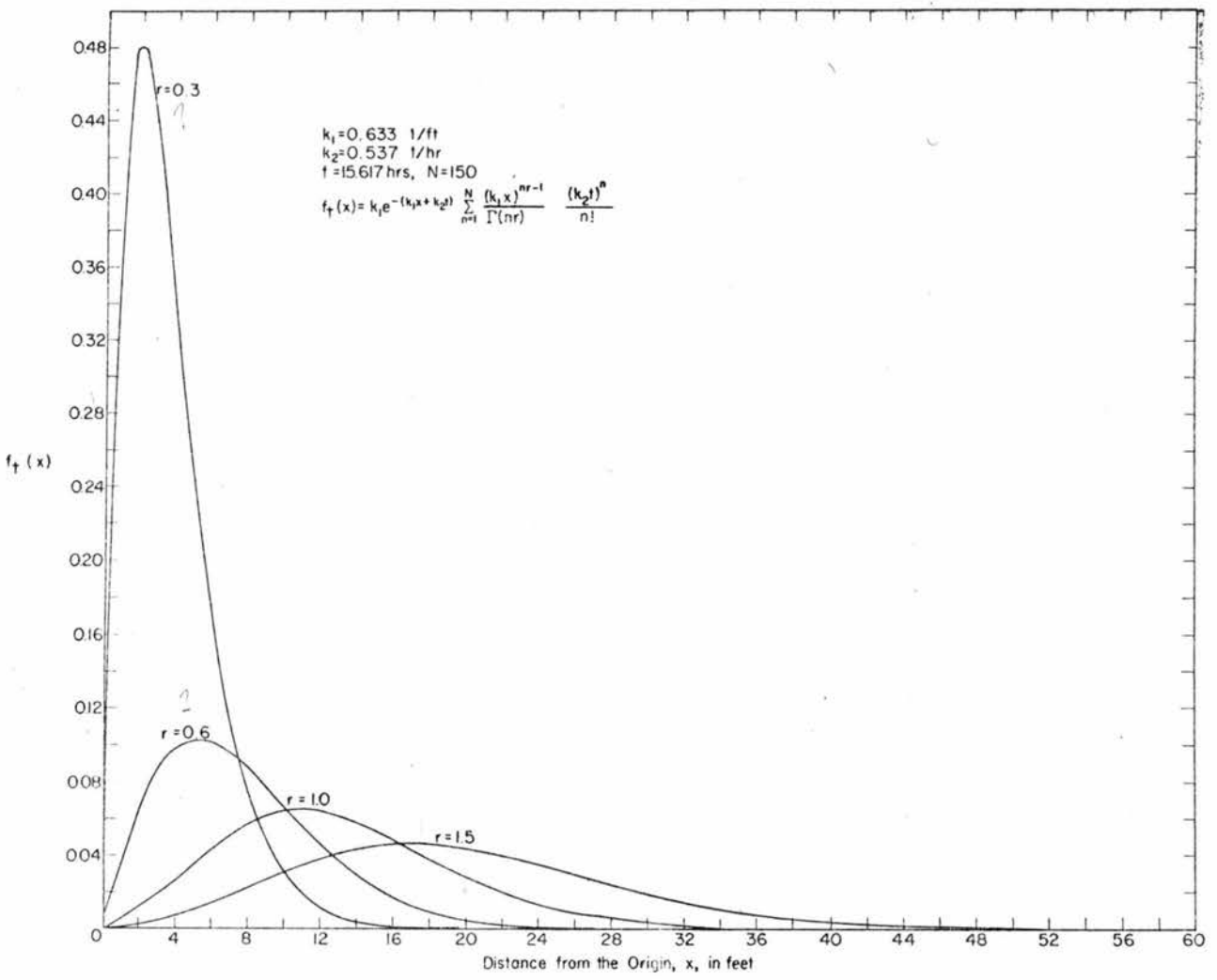

Figure 5-13. Variation of $f_t(x)$ for a particular set of k_1, k_2 and t values as a function of r

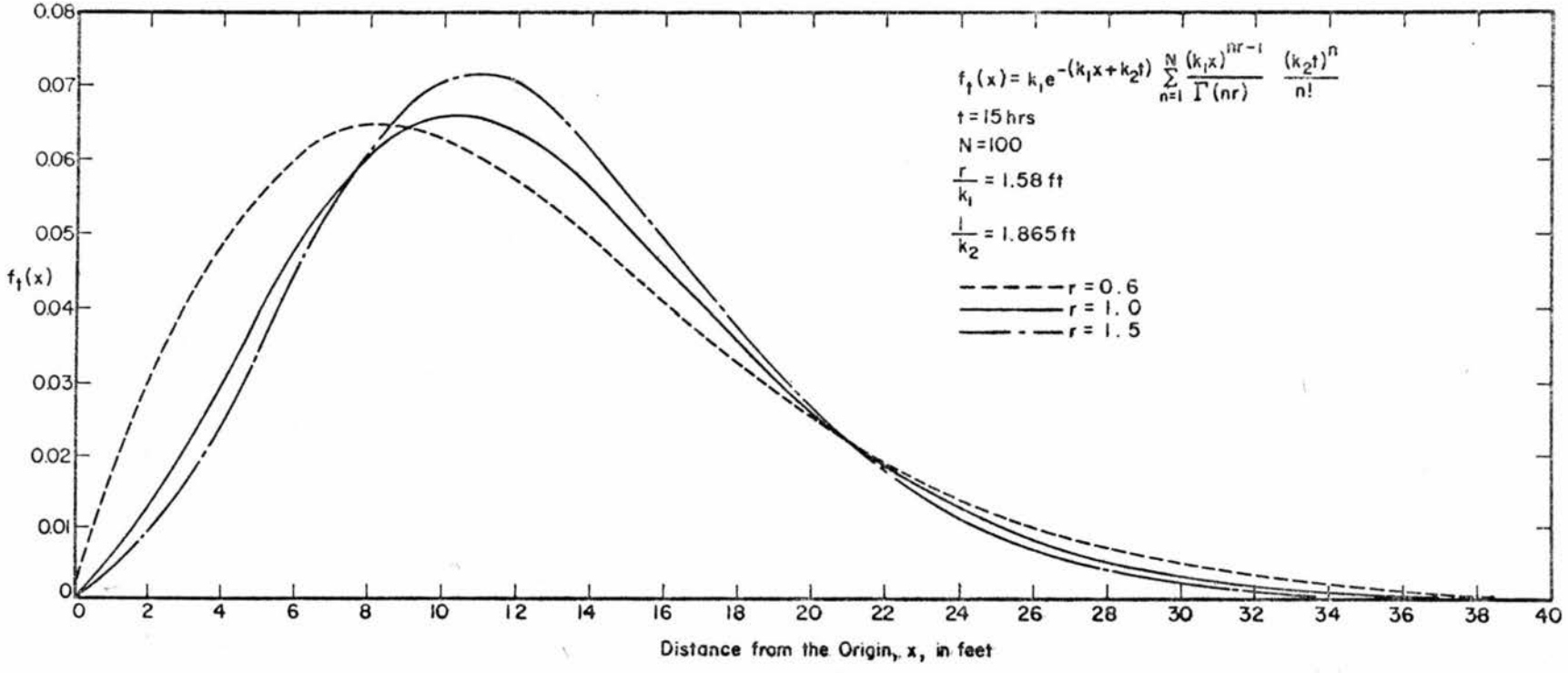

Figure 5-14. Variation of $f_t(x)$ for a particular set of dispersion times, mean step lengths and mean rest periods as a function of r

period are held constant, the skewness of the $f_t(x)$ curves decreases with increasing r values. This tendency agrees with the characteristics of the gamma distributed step length function; when the mean is kept constant, the skewness of gamma distribution function decreases with increasing r values.

Due to the irregularity of the bed configuration, the irregularity of the experimental longitudinal concentration curves is not surprising. Figure 5-15a shows the comparison of the experimental longitudinal dispersion curve with Hubbell-Sayre's stochastic model and the general one-dimensional stochastic model. The irregularity of the experimental curves was caused by pockets of tracer particles which were buried in deep troughs and released later. The area under the theoretical curves will not equal 1 unless k_2t is infinite in Eq. (3-20). However, the area approaches 1 very rapidly at small k_2t values. When $k_2t = 5$, the areas under the theoretical curves for both models are 0.99. The slight area difference between Hubbell-Sayre's model and the general one-dimensional model in Fig. 5-15a is caused by using different k_2 values in each model. The comparison indicates that the dispersion process can be described by the general one-dimensional stochastic model at least as well as by Hubbell and Sayre's stochastic model.

This is more easily seen in Fig. 5-16, a comparison of the mean, variance, and skew coefficient between these two models. In Fig. 5-16 the rate of change of mean and variance for both models is

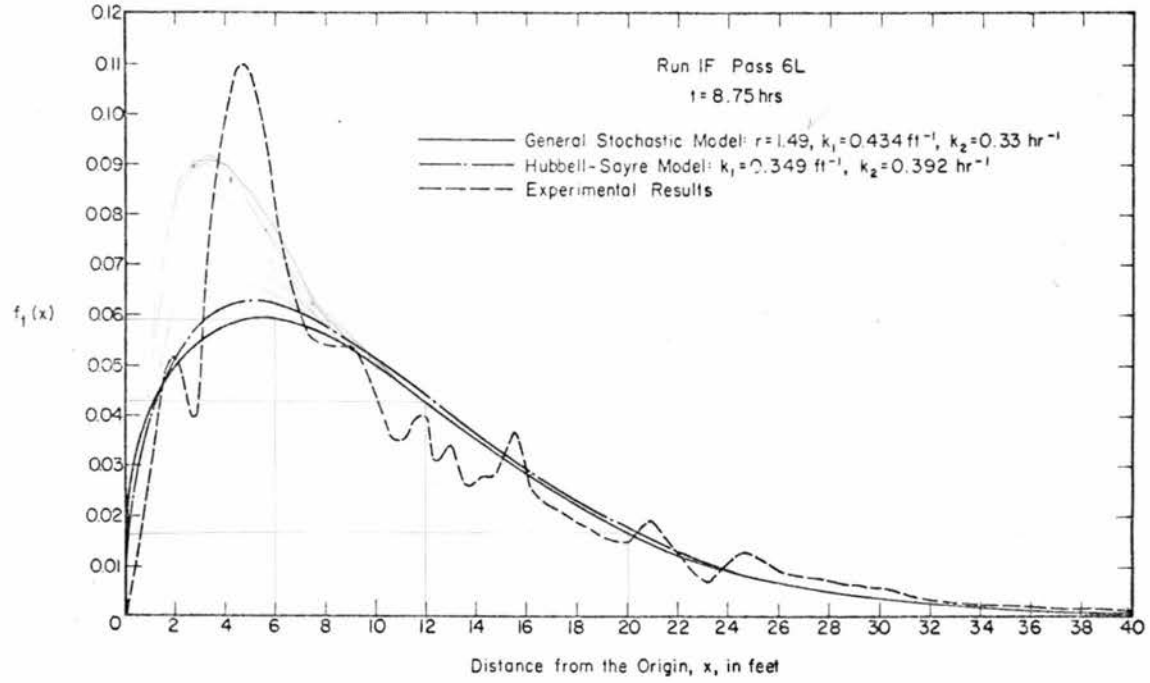

Figure 5-15a. Comparison of the experimental longitudinal concentration distribution curve with Hubbell-Sayre stochastic model and the general one-dimensional stochastic model for Run 1F Pass 7L

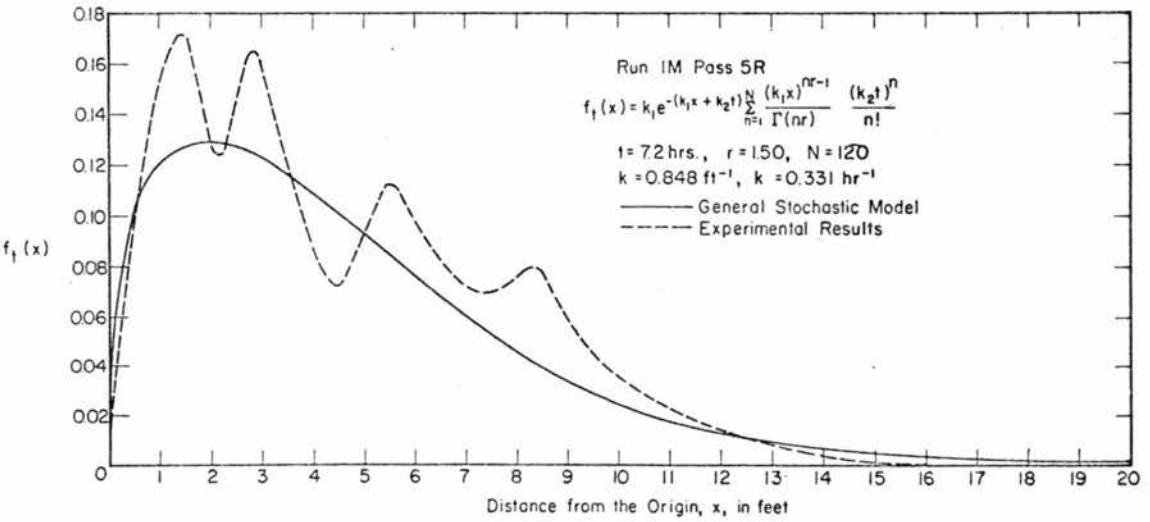

Figure 5-15b. Comparison of the experimental longitudinal concentration distribution curve with the general one-dimensional stochastic model with assumed r value for Run 1M Pass 5R

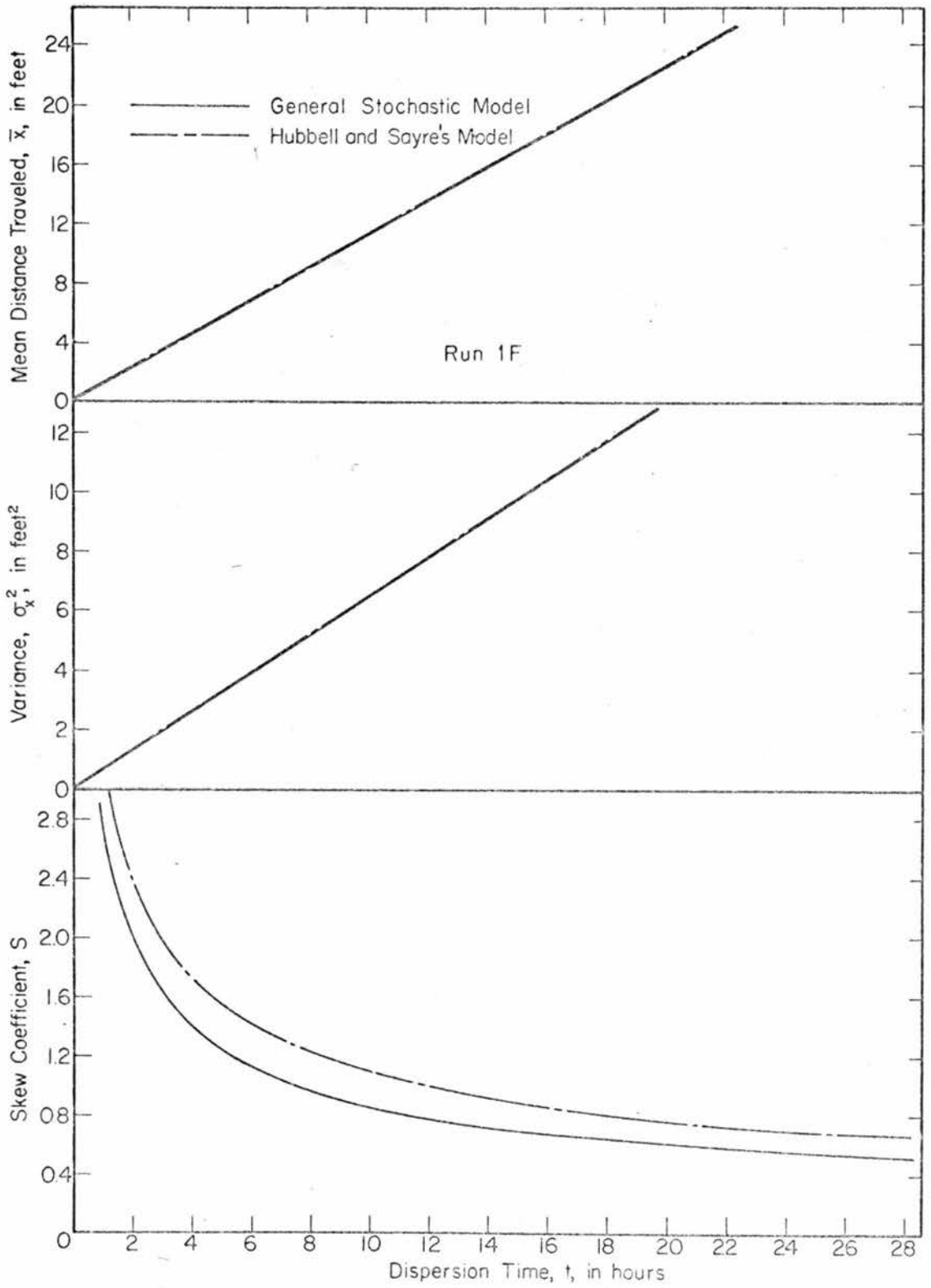

Figure 5-16. Comparison of the mean, variance and skew coefficient as functions of dispersion time between Hubbell-Sayre stochastic model and the general one-dimensional stochastic model for Run 1F

the same and the difference of rate of change of skew coefficient is not significant enough to change the pattern $f_t(x)$ very much. This demonstrates the impracticality of attempting to define all three parameters from longitudinal dispersion data alone.

Fig. 5-15b demonstrates the possibility and the applicability of assuming an r value for the general one-dimensional stochastic model to describe the actual dispersion process. After the r value is assumed, k_1 and k_2 can be obtained from the mean rates of displacement and spreading of the tracer particles without going into the problem of skewness. The agreement between experimental result and the general one-dimensional stochastic model increases the possibility and confidence that if the mean step length and rest period can be found from bed configuration data and total sediment discharge, all the parameters used in the general one-dimensional stochastic model can be obtained by solving Eqs. (3-11) and (3-13) together with the assumed r value without having to perform a dispersion experiment. Thus, this general one-dimesional stochastic model not only can be used to describe the process of dispersion, but also may be used to predict the dispersion process. The area difference between the experimental result and the general one-dimensional stochastic model as shown in Fig. 5-15b, is due to the same reason as explained for Fig. 5-15a.

C. Computer Results of Solving Aris' Moment Equation

The computer program of solving Aris' moment equation was designed to simulate the flow condition of Run 1C. However, the values of the von Karman turbulence coefficient, κ, were computed from velocity distribution data from Run 5 for 0.33 mm sand in the same two foot wide flume as given in the U.S. Geological Survey Professional Paper 462-I, which has the same flow condition as Run 1C. Figure 5-17 shows for the conditions specified in Case 1, the relation between the dimensionless mean displacement of the deposited sediment from the source and the dimensionless dispersion time for different β values. The asymptotic values represent dimensionless mean step lengths $\overline{\xi}_{w_s}$. The β value is proportional to the fall velocity of sand particles. For the same flow condition, higher β values should be associated with shorter step lengths as shown in Fig. 5-18. The computer results for Case 1 can be seen in Table 5-2.

TABLE 5-2. COMPUTER RESULTS FOR CASE 1 GIVING PREDICTED STEP LENGTH CHARACTERISTICS FOR RUN 1C

β	$\overline{\xi}_{w_s}$	$\sigma^2_{w_s}$	S_{w_s}	$r_{w_s} = \frac{\overline{\xi}^2_{w_s}}{\sigma^2_{w_s}}$	$S'_{w_s} = \frac{2}{\sqrt{r_{w_s}}}$
1.0	4.62	119.0	4.64	0.179	4.73
1.2	3.139	60.69	5.196	0.1625	4.97
2.0	1.09	7.84	6.49	0.1513	5.14
3.0	0.51	1.55	7.21	0.168	4.88
4.0	0.31	0.507	7.37	0.1898	4.59
5.0	0.21	0.222	7.40	0.1988	4.48

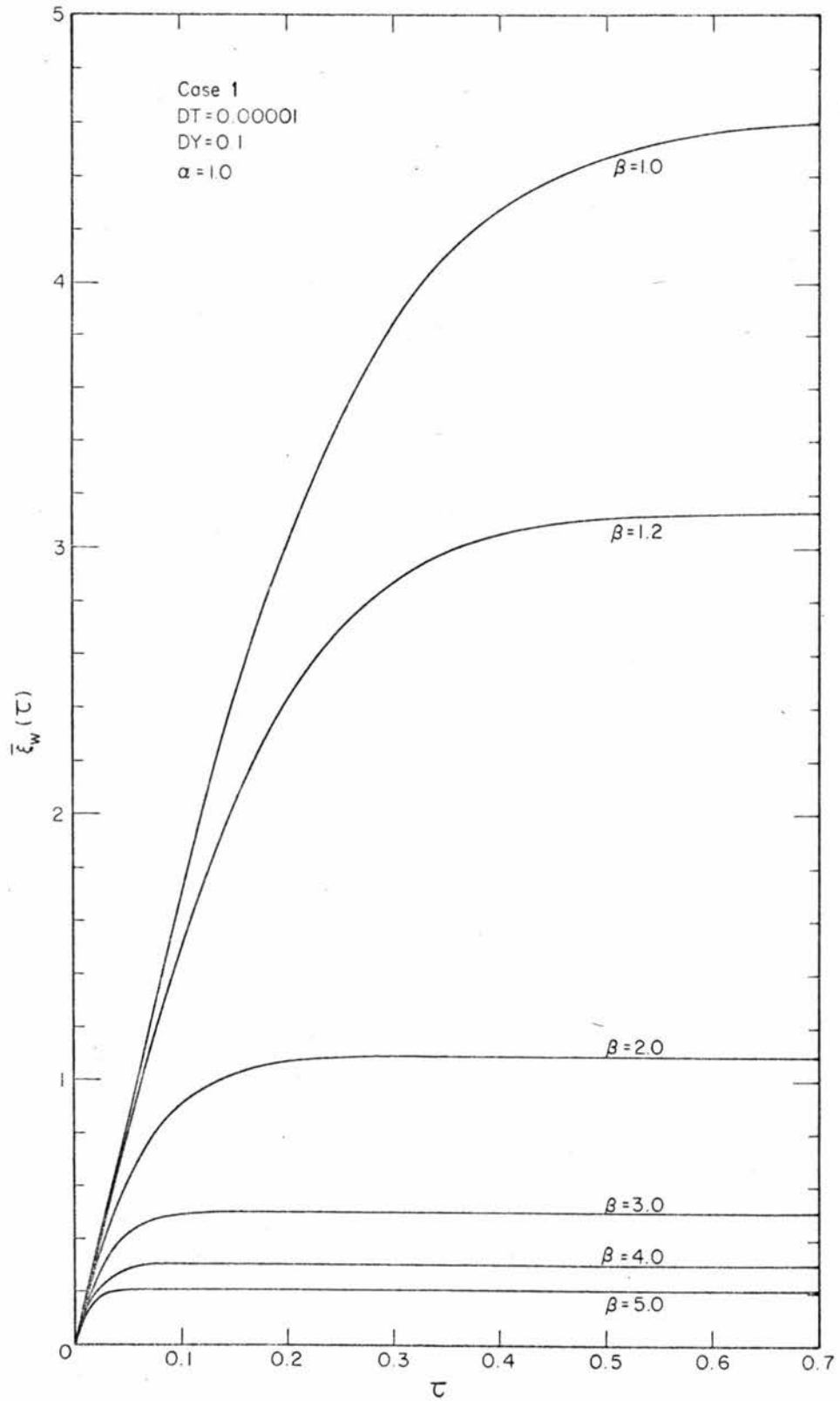

Figure 5-17. Dimensionless mean displacement of the deposited sediment from the source as a function of dimensionless dispersion time for different β values with $\gamma = 0.0$, $\overline{U}/U_\tau = 9.6$ and $\kappa = 0.29$

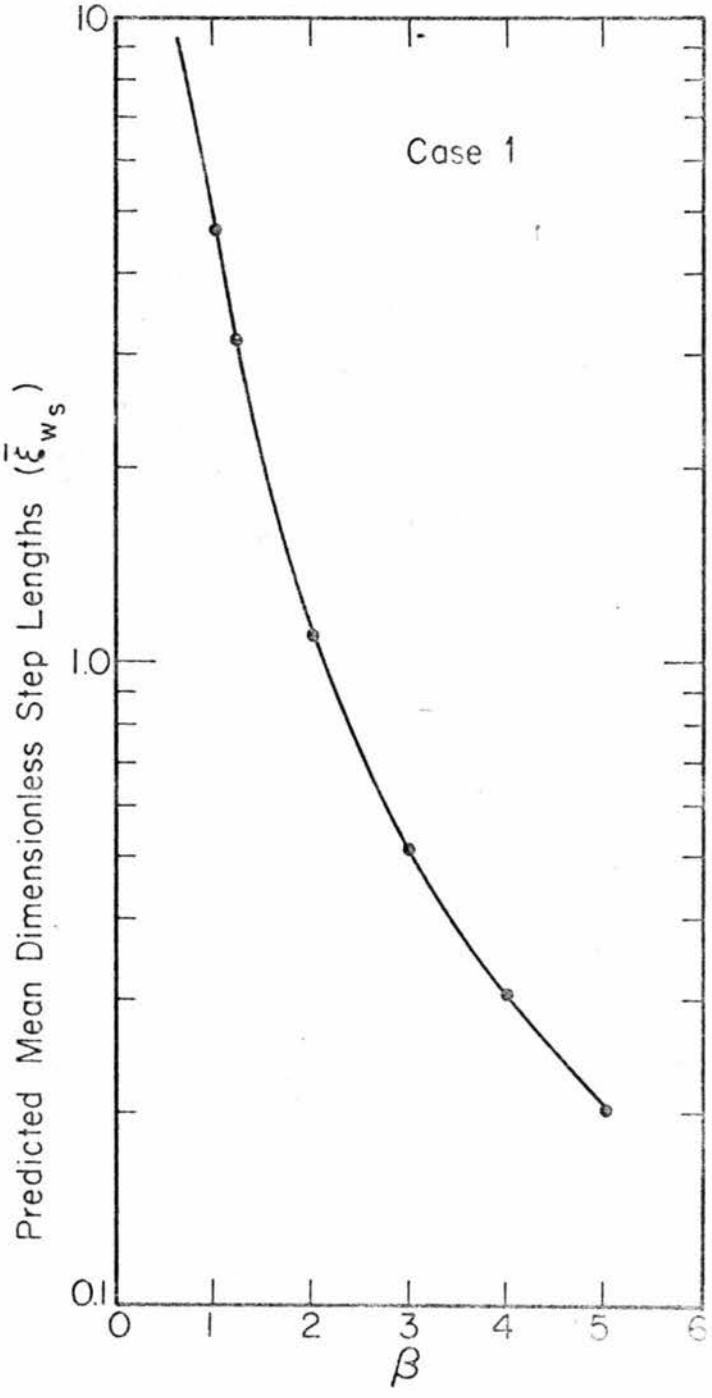

Figure 5-18. Dimensionless mean step lengths predicted by Case 1 as a function of β

For a gamma distributed step length, Eq. (3-10), the dimensionless forms of the mean step length, the variance and the skew coefficient are

$$\overline{\xi}_{w_s} = \frac{r_{w_s}}{k_{1w}} \tag{5-7}$$

$$\sigma^2_{w_s} = \frac{r_{w_s}}{k^2_{1w}} \tag{5-8}$$

and

$$S'_{w_s} = \frac{2}{\sqrt{r_{w_s}}} \tag{5-9}$$

where the subscript w denotes the deposited sand and s denotes the step length. Case 2 follows Case 1 to make the mean step length and mean rest period correspond to the experimental results of Run 1C. Using the computer results of Case 1, as shown in Table 5-2, the proper r_w and k_{1w} values can be found by solving Eqs. (5-7) and (5-8). Equation (5-9) serves the purpose of a double check. The calculated r_w and k_{1w} values are 0.1625 and 0.05175, respectively. Based on these r_w and k_{1w} values, and Eqs. (5-7), (5-8) and (5-9), we have $\overline{\xi}_w = 3.139$, $\sigma^2_w = 60.69$ and $S_w = 4.97$ which agree well with those values listed in Table 5-2. This strongly suggests that the step lengths predicted by Case 1 are gamma distributed with $r_w < 1$.

The input for Case 2 is based on the flow conditions, which are the same as Case 1, and γ corresponding to Run 1C. Since $1/\gamma$ equals the mean rest period in dimensionless units, $k_{2w} = \gamma = 0.0131$. From the general one-dimensional stochastic model, and using the results obtained from Case 1, we have

$$\frac{d\bar{\xi}_w}{d\tau} = \frac{k_{2w} r_w}{k_{1w}} = 0.0413$$

and

$$\frac{d\sigma_w^2}{d\tau} = \frac{k_{2w}\, r_w\, (r_w+1)}{k_{1w}^2} = 0.928$$

which agree with the slopes in Fig. 5-19 obtained from the numerical solution of the Aris moment equations for Case 2. From Eq. (3-24) the skew coefficient for the deposited sediment is

$$S_w = \frac{r_w+2}{\sqrt{(r_w+1)\, r_w k_{2w}\, \tau}} = 43.5(\tau)^{-1/2} \quad . \qquad (5\text{-}10)$$

Figure 5-20 shows the comparison between Eq. (5-10) and the results from the computer program Case 2; the agreement is very good.

Now it can be confirmed that both the general one-dimensional stochastic model and the Aris' moment equations lead to the same solution of the dispersion problem under the condition of Case 2. For a given value of β, the characteristics of the step length distribution function predicted by the Aris' moment method depends also on

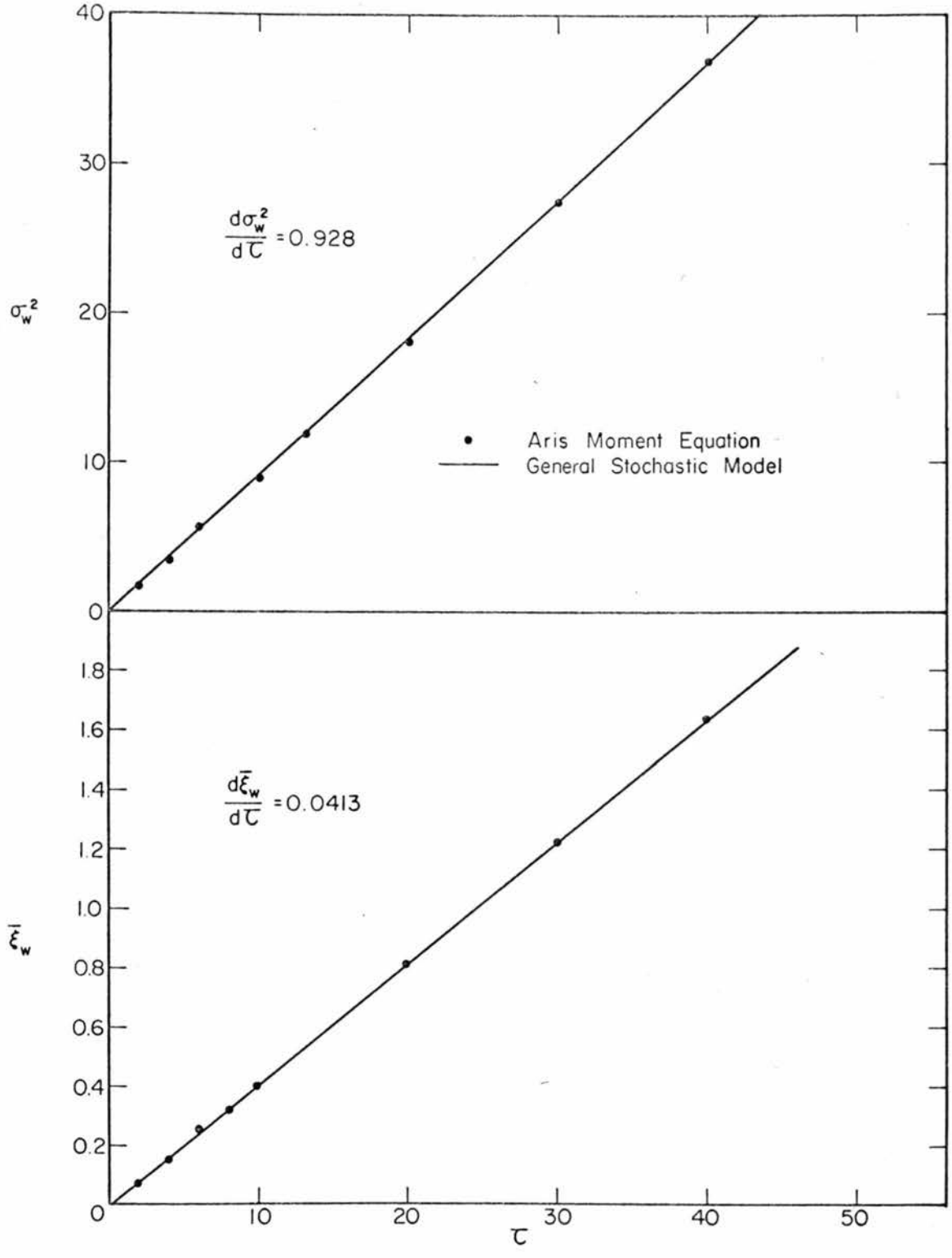

Figure 5-19. Comparison of the dimensionless mean and variance as functions of dimensionless time between computer program Case 2 and the general one-dimensional stochastic model

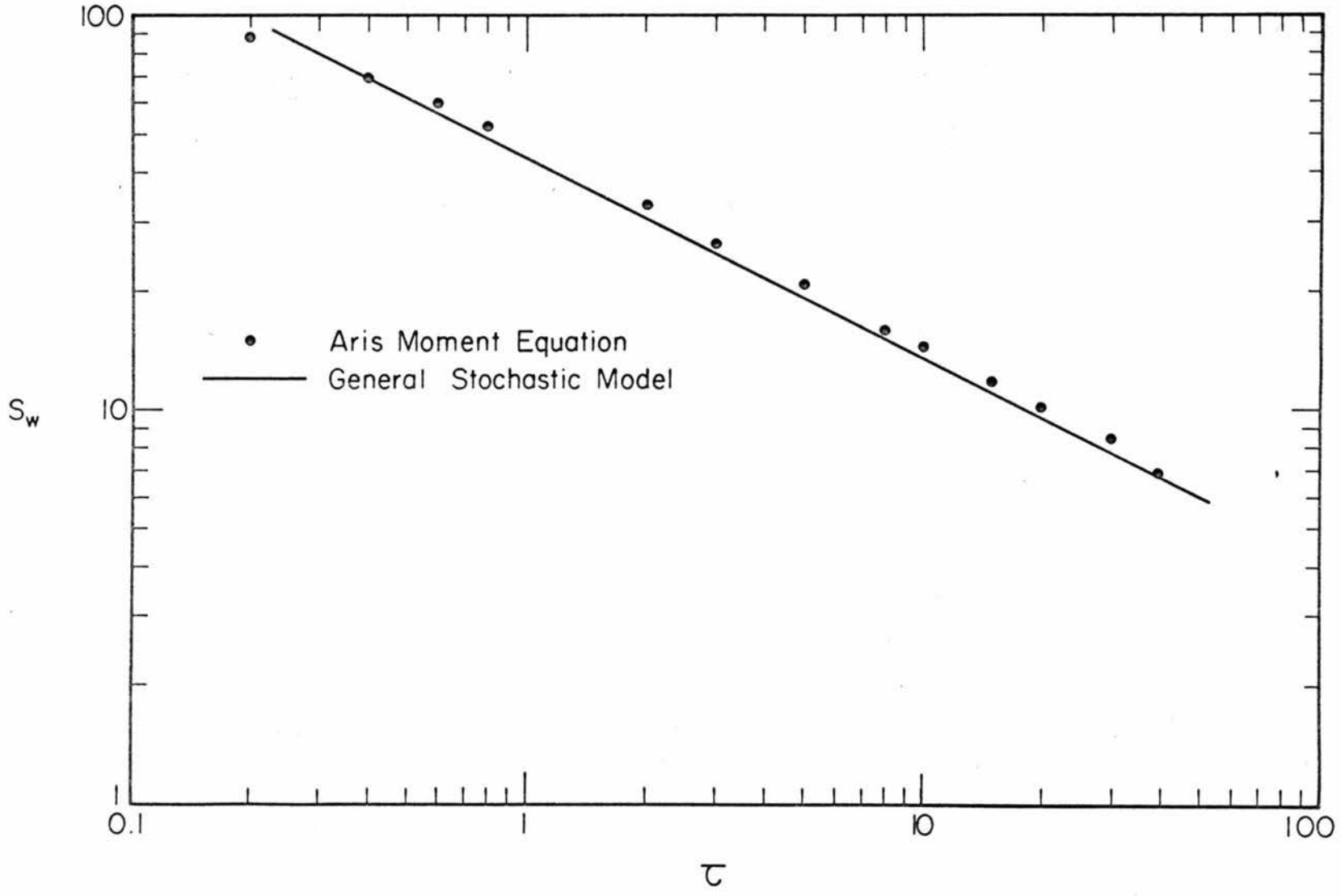

Figure 5-20. Comparison of the skew coefficient as a function of dimensionless time between computer program Case 2 and the general one-dimensional stochastic model

the selection of the thickness of the bottom layer of flow $\Delta\eta$. Therefore, without some meaningful physical criteria to govern the selection of $\Delta\eta$, this method cannot be used to predict the characteristics of $f_\chi(x)$ quantitatively. However, it may still be useful for predicting qualitatively the nature of relationship between the characteristics of $f_\chi(x)$ and β and $\overline{U}/U_\tau$, for example.

D. Vertical Concentration Distribution of Tracer Particles in an Alluvial Bed

The vertical concentration distribution of tracer particles in the bed was obtained by using a core sampler. The data in Appendix C give some examples of the vertical distribution in the bed at different stations. The water surface was taken as the origin for all the vertical concentration distribution graphs. The depth axes of these vertical concentration distribution graphs are located directly under the stations at which they were taken. The relatively good agreement between the longitudinal concentration distributions determined by the scintillation detector and the plotted points, which represent the total amount of radioactivity in the core, indicate that variation in vertical distribution of tracer particles along the flume does not cause any serious distortion in longitudinal distribution curves obtained by the use of a scintillation detector above the water surface. The time lags between these two sets of data are due to the fact that the core sample data were taken after taking the longitudinal concentration distribution data. The time

lags between the left and right side scintillation detector data are due to the same cause. No significant tendency concerning the vertical distribution of tracer particles in the alluvial bed is apparent in our present data.

The average depth of penetration of tracer particles in the bed can also be found in Appendix C. The average depth of penetration increases slightly with the dispersion distance as a general tendency. This general tendency is not true near the end of the flume, however, because a wooden sill at the average bed level was located at the end of the flume to help maintain the correct slope of the sand bed. As a result of this, instead of increasing, the average depth of penetration of tracer particles tends to decrease somewhat near the end of the flume.

E. Bed Configuration Analysis

Figure 5-21 gives typical examples of the actual bed configurations for the ripple and dune bed conditions. Since the dunes are much larger than the ripples, and the flume is only 60 feet long, from a statistical point of view not enough information about the variation of bed configuration can be obtained for the dune condition. Even for ripple conditions, the data are barely enough to demonstrate the tendency of some statistical properties.

Since the movement of sand is closely related to the bed forms and how they move, it is reasonable to assume that the distribution

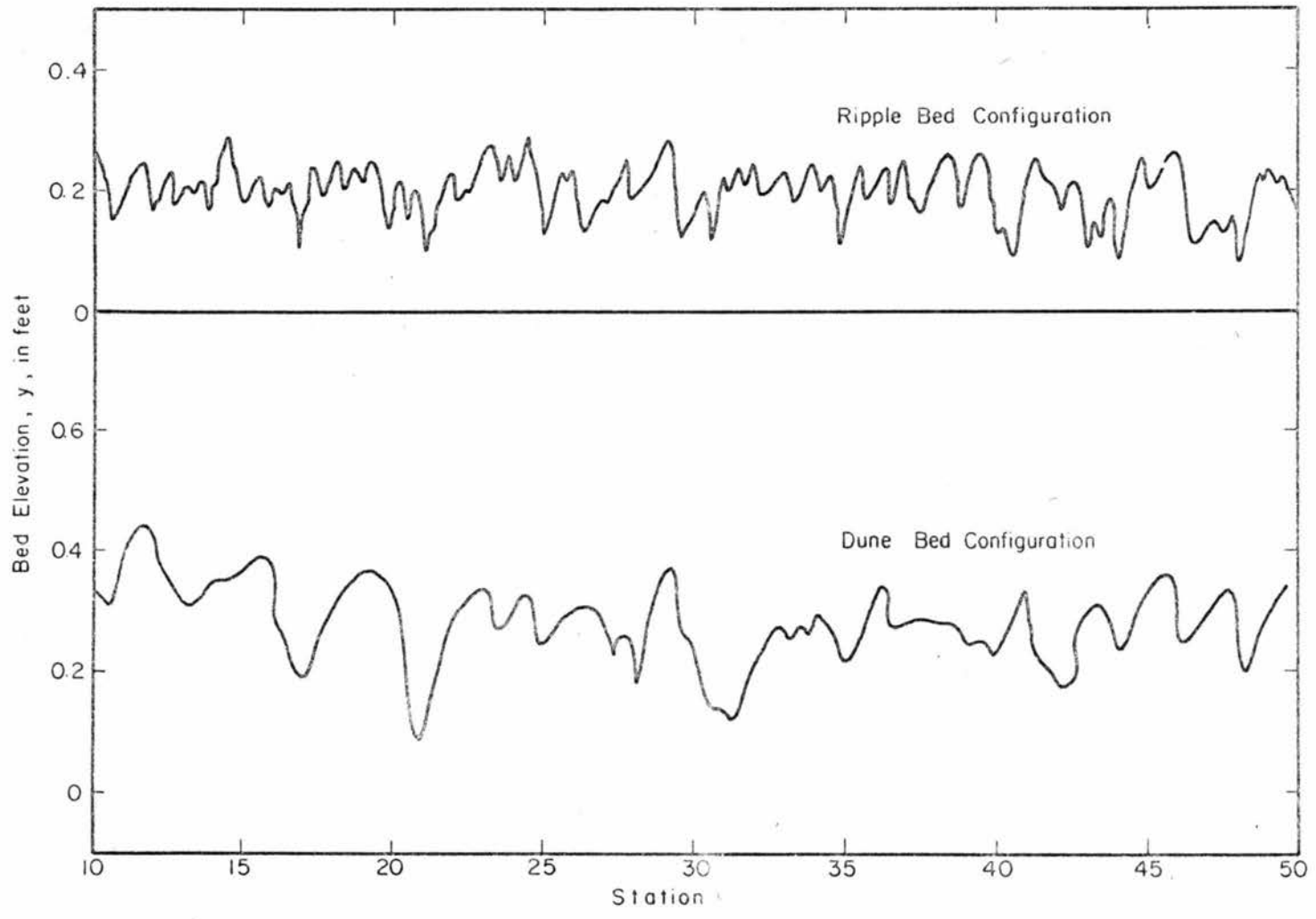

Figure 5-21. Typical bed configurations for ripple and dune bed conditions

function of step length is related to the distribution function of the zero crossings of the bed configuration. Figure 5-22 shows the distribution of zero crossings of the bed forms for Run 1M and Run 1F. These data show that the distribution of zero crossings can be adequately represented by the gamma distribution function. The scattering of the data about the theoretical gamma distribution function is mainly due to insufficient length of record. Nordin's (1968) computer program was used to calculate the distribution of zero crossings of the bed configuration.

Two analyses of the frequency distribution of the bed elevation were performed for both ripple and dune beds. The stationary data were taken by a transducer located at station 30. Figure 5-23 gives an example of frequency distirbution data obtained by a stationary transducer for Run 1M. The subscript Y_T used for the relative frequency in Fig. 5-23 denotes reference to the variation in the time domain of the bed elevation with respect to a stationary reference point. Another set of data was taken from a transducer on the carriage which moved along the flume. Figure 5-24 gives an example of the frequency distribution based on the variation of bed elevation along the flume for Run 1M also. A computer program in Appendix D was developed for calculating this distribution of bed elevation. Both Fig. 5-23 and Fig. 5-24 show that the distribution of bed elevation follows the normal distribution closely. Also, in Fig. 5-24 there is no significant difference between the results

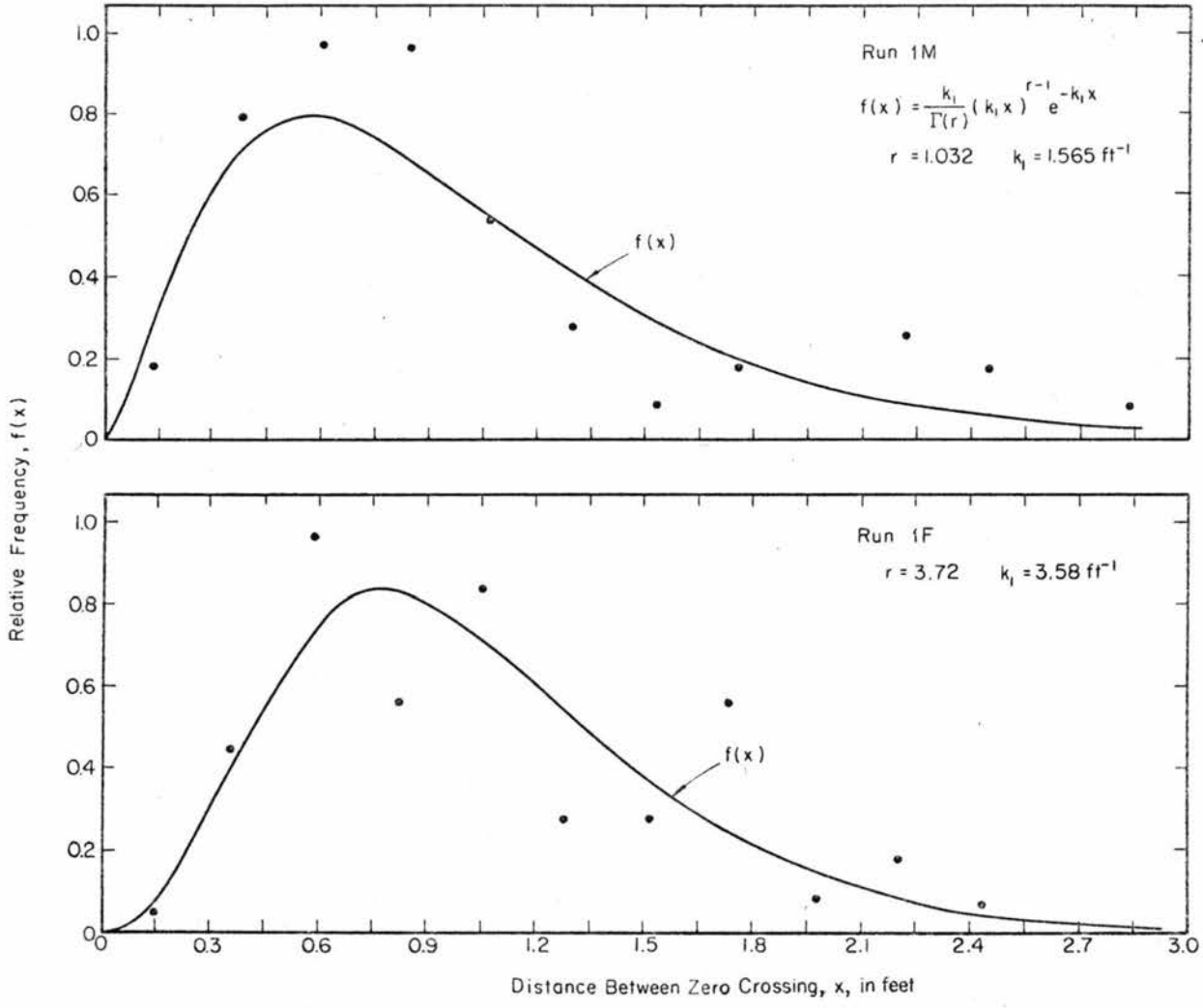

Figure 5-22. Distribution of zero crossings of the bed configurations for Run 1M and Run 1F

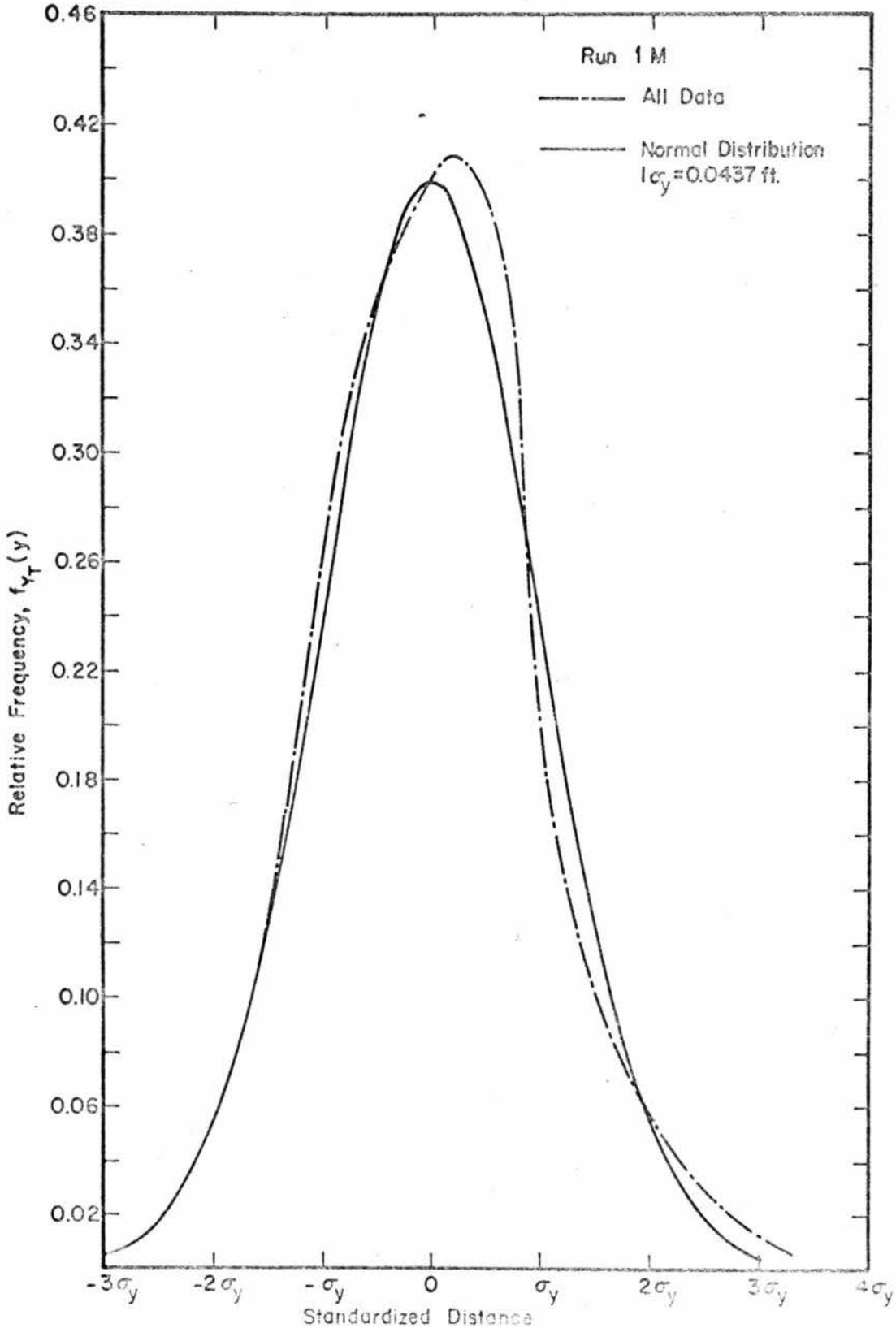

Figure 5-23. Statistical distribution of the variation of bed elevation with time for Run 1M

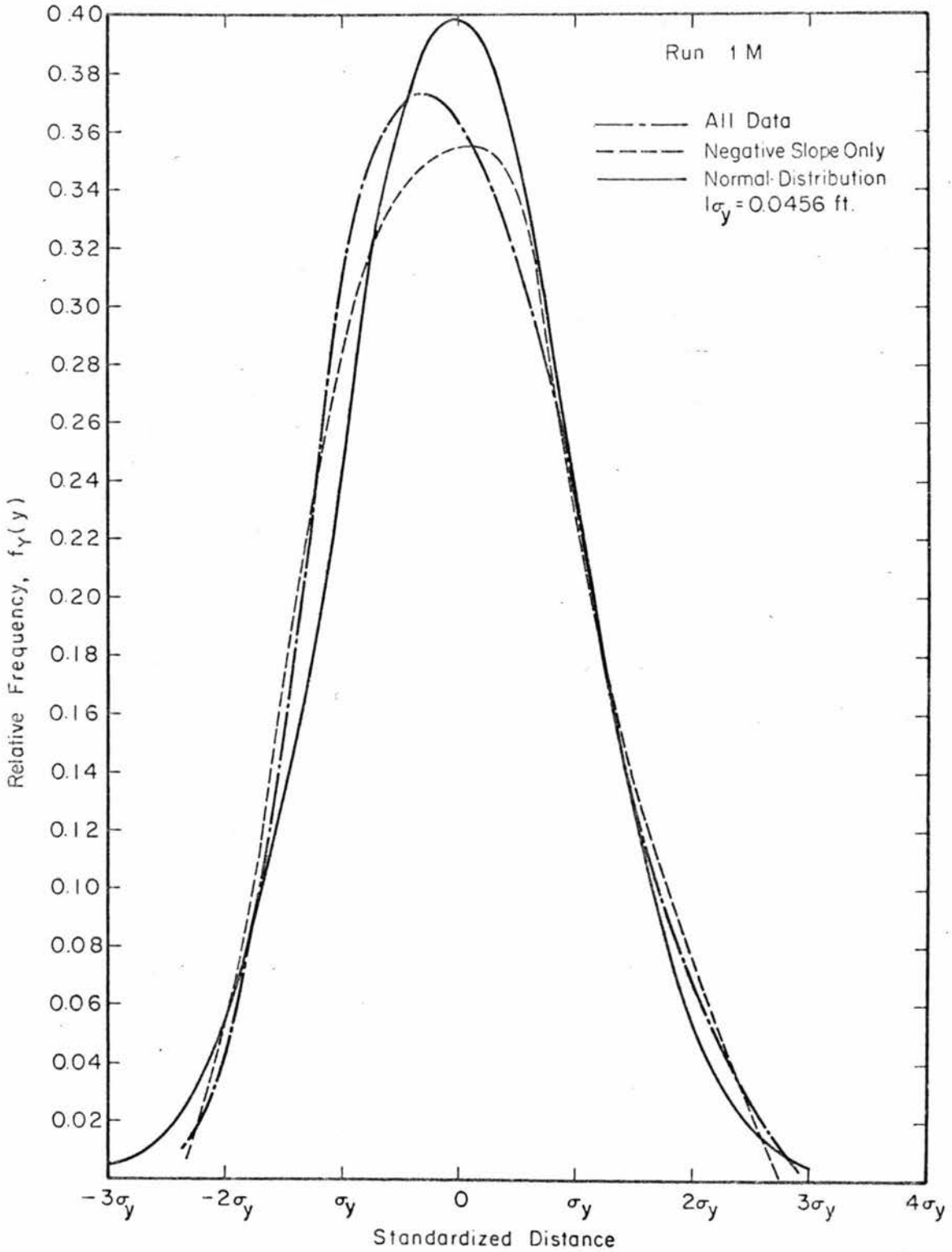

Figure 5-24. Statistical distribution of the variation of bed elevation along the flume for Run 1M

obtained by considering both the positive and negative slope, and those obtained by considering only the negative slope. Therefore, it is assumed that it is equally likely that sand particles will be deposited anywhere on the downstream faces of bed forms but not on the upstream faces, the distribution in Fig. 5-24 is equivalent to $f_Y(y)$, the probability density function for the elevation at which a sand particle is deposited. There is no significant difference between $F_{Y_T}(y)$ and $F_Y(y)$ when Fig. 5-23 and Fig. 5-24 are compared, which means the distribution of bed elevation may follow an ergodic process, i.e., the statistics over a long time interval for any one system are the same as the statistics over the ensemble of systems at any one instant of time.

In order to evaluate the mean rest period from the distribution of bed elevation by using Eq. (3-30), we must have data on the distribution of bed elevation over a sufficiently long time period. Our records available at present are not long enough to adequately evaluate $f_{T|Y}(t|y)$ and $F_Y(y)$. From Fig. 5-23 and Fig. 5-24, the variation of bed elevation follows normal distributions closely; thus, Eq. (3-30) may be used to calculate the mean rest period. From the bed elevation data in the time domain, the T_o value in Eq. (3-30) is equal to 19.8 minutes for Run 1M. With T_o equal to 19.8 minutes and $f_Y(y)$ from the normal distribution curve in Fig. 5-24, the mean rest period can be obtained by integrating Eq. (3-30) numerically from minus three standard deviation to plus three standard deviation of the variation of bed elevation. This calculated mean rest period is about 1 hour. The

mean rest period for Run 1M obtained from the Hubbell-Sayre stochastic model is about 2.5 hours, which is larger than the result obtained from the bed configuration data. But, the readers should be aware that the mean rest period obtained from the bed configuration data represents the mean rest periods for all sand particles in the flume and is independent from the tracer size; while the mean rest period obtained from the dispersion experiment is dependent on the tracer size. The fact that the dispersion experiments represent the overall results along the flume, while T_o is only emphasized at a particular point in the flume, may also cause some differences between the mean rest period obtained from these two methods. Another reason for this difference between the two methods is that the time record for the bed configuration is not long enough; thus, the T_o value may not be the true T_o value for a much longer record. Thus, the evaluation of the mean rest period, E(T), needs much longer records of the variation of bed elevation with respect to time and space.

F. Total Sediment Discharge

The average total sediment discharge for each run is shown in Table 4-1. The comparison between Eq. (3-70) and the actual measurement of some other known total sediment discharge equation is outside the scope of this study. The data are available for those readers who are interested in making this comparison.

G. Results Obtained from Plane Bed Conditions

Due to the short length of the flume and the high velocity of moving sand, it took only about 15 seconds for the tracer particles

to pass through the whole experimental reach. Under such conditions, the response characteristics of the instruments is a very important factor to the results, and the results obtained under this condition are not considered to be reliable. Therefore, no further analysis of this data was made.

Chapter VI

SUMMARY AND CONCLUSIONS

The general objective of this investigation was to study the transport and dispersion of sand particles along the bed of an alluvial channel. The specific objectives were to (1) review and compare some existing mathematical models for describing the transport and dispersion process, (2) use some numerical and/or stochastic approaches to describe and predict the dispersion process, (3) obtain some additional experimental information on the effect of flow conditions and particle size on the transport and dispersion process.

In order to achieve these objectives, the following investigations were undertaken. (1) A general one-dimensional stochastic model describing the longitudinal dispersion of sand particles was derived and its properties were investigated. (2) Existing equations for the transport and deposition of suspended sediment particles together with appropriate initial and boundary conditions were adapted to the case of sand particles transported along the bed of the channel. These equations were transformed by the Aris moment method and solved numerically. (3) The results obtained from the Aris moment method and the general one-dimensional stochastic model were compared for comparable conditions. (4) A series of laboratory flume experiments with radioactive tracer particles was conducted. In these experiments the movement and

longitudinal dispersion of tracer particles along the flume, and the penetration of tracer particles into the bed were investigated. Experiments were conducted with coarse, medium and fine tracer particles for two flow conditions that were characterized respectively by ripple and dune bed configurations. (5) Experiments were conducted with lightweight plastic particles to find the distribution functions of step lengths and rest periods of a single plastic particle. (6) Statistical anlaysis of bed configuration was made to find the mean rest period of tracer particles along an alluvial bed.

These investigations led to the following conclusions:

1. Based on the preliminary study with a single lightweight plastic particle, the step lengths very closely follow a gamma distribution with parameter r approximately equal to 2; the rest periods follow an exponential distribution very closely. This conclusion disagrees in part with the assumption which Hubbell and Sayre (1964) made in their one-dimensional stochastic model, in which they assumed that both the step lengths and rest periods of a single particle are exponentially distributed. It is not known yet to what extent this conclusion applies also to sand particles, but readers should be aware that the exponential distribution function is a special case of the gamma distribution function with $r = 1$.

2. The method of approach in deriving the general one-dimensional stochastic model can be applied to any distribution function of step length and rest period. Three parameters are needed

in the general one-dimensional stochastic model, namely, k_1, k_2, and r. The rest period is determined by k_2 and the step length is determined by k_1 and r.

3. According to this general one-dimensional stochastic model, the mean displacement and the variance of the longitudinal distribution of tracer particles increase linearly with dispersion time, and the skew coefficient approaches zero at large dispersion time. This means that the longitudinal concentration distribution of tracer particles described by this model approaches symmetry at large dispersion time.

4. Due to the irregularity of bed configuration, the irregularity of the experimental longitudinal concentration distribution of tracer particles along the flume should be expected. In spite of this irregularity, the mean rate of displacement and spreading (variance) of the tracer particles still approach different constants under different flow conditions at large dispersion times. These linear relationships exist even near the initial stage for those runs in which the tracer particles were initially well mixed with the sand in the flume. According to the general one-dimensional stochastic model, when the mean rate of displacement and spreading of the tracer particles are kept constant, the skew parameter should also be a constant. Because the skew parameter was obtained from the third moment of the longitudinal concentration distribution data, it is less reliable than the mean and variance obtained from the first and second

moment of the same data. The limitation in length of the experimental flume increases this irregularity and unreliability of the skew parameter. The experimental skew parameters scatter considerably.

5. In order to determine k_1, k_2 and r in the general one-dimensional stochastic model from the experimental results, three relations, obtained from the data, are needed, which can be solved simultaneously. The mean rates of movement and spreading of the longitudinal concentration distribution of tracer particles provide two satisfactory relationships. However, due to the scatter, the skew parameter does not provide a sufficiently reliable third relationship. For given values of mean rate of displacement and spreading of tracer particles, the pattern of $f_t(x)$ can almost as well be described by using different combinations of k_1, k_2 and r values. The change of r values has little influence on the skewness of $f_t(x)$, especially when $r > 2$.

6. If r is assumed, an alternative method of finding k_1 and k_2 is used in this study. Since the change of r values has little influence on the skewness of $f_t(x)$, an r value can be assumed for a given flow condition. With the assumed r value, k_1 and k_2 can be found from the mean rate of displacement and spreading of longitudinal concentration distribution data of tracer particles. Fairly good agreement has been obtained between the experimental result and the stochastic model by using this method.

7. Theoretical investigation of the bed configuration is made to find the mean rest period and mean step length of tracer particles.

The mean rest period $1/k_2$ can be determined from the bed configuration. The mean step length r/k_1 can be determined from the mean rest period, total sediment discharge, and bed configuration data. When the r value is properly assumed, all the three parameters in the general one-dimensional stochastic model can be determined without doing dispersion experiments. However, the presently available data are not sufficient to adequately evaluate this method.

8. Since a higher flow velocity and higher total sediment discharge existed in the dune condition than in the ripple condition, the mean rate of displacement and spreading of tracer particles are also higher for the dune condition than for the ripple condition.

9. The size of tracer particles should have some influence on the rate of displacement and spreading of tracer particles. The finer the tracer particles are, the faster they should travel and spread. The experimental results indicated no significant difference between the behavior of the medium and coarse tracer particles, but the fine tracer particles traveled and spread much faster than the medium and coarse tracer particles. This may be caused by the fact that the fine tracer particles were temporarily suspended during part of their movement.

10. The distribution of step lengths may be closely related to the distribution of zero crossings of the bed forms. The distribution of zero crossings for the ripple condition of this study follows the gamma distribution closely with parameter r approximately equal to 3.

11. The distributions of bed elevation in both the time and space domains follow the normal distributions closely, and there is no significant difference between the results obtained by considering both the positive and negative slopes of the bed configuration and the negative slope only. Therefore, if it is assumed that it is equally likely that sand particles will be deposited anywhere on the downstream face of the bed forms (negative slope), then the above distribution is equivalent to the probability density function for the elevation at which a sand particle is deposited. The agreement between the distributions of the bed elevation in the time and space domains suggests that the distribution of bed elevation may follow an ergodic process.

12. As the dispersion process goes on, the tracer particles have a general tendency to penetrate deeper and deeper into the sand bed until they are distributed to the level of the deepest sand troughs, which impose a lower limit. The vertical concentration distribution of tracer particles in the sand bed, obtained by core sampling, is very irregular, with no clear indication as to what kind of distribution function it follows. The agreement between longitudinal concentration distributions obtained by the scintillation detector and core sample methods indicates that the variation in vertical distribution of tracer particles along the flume does not cause any serious distortion in the longitudinal concentration distribution as determined by a scintillation detector located above the water surface.

13. The computer program originally developed by Sayre (1968) to solve the Aris moment equations numerically is a valuable tool to obtain a solution that can describe and predict the behavior of sand particles in open channel flow, if the parameters in the program corresponding to actual conditions can be determined. When applied to particles that are creeping along the bed, however, the numerical solution depends to some extent on the grid size, i.e., $\Delta\eta$ value. The $\Delta\eta$ value which corresponds best to a particular actual situation cannot be predicted, so this method cannot be used to predict the step length quantitatively. However, it is a good method for describing the dispersion process and relating some of its attributes to basic hydraulic parameters and sediment properties.

14. The numerical solution of the Aris moment equations for the initial condition that all the tracers are concentrated at the origin in the bottom layer of flow with the layer thickness equal to $\Delta\eta$, and the boundary condition that each tracer particle is absorbed by the bed after completing a step, indicates that the step lengths are gamma distributed with $r < 1$. The value of r obtained from this case depends to some extent on the value of $\Delta\eta$ selected.

15. The agreement between the general one-dimensional stochastic model and the numerical solution of the Aris moment equations for initial and boundary conditions corresponding to those in the stochastic model is excellent. They apparently lead to the same solution under the same conditions. The general one-dimensional

stochastic model can serve to predict the dispersion process as well as to describe it, if the mean rest period can be found from the bed configuration data; if mean step length can be found from the mean rest period, total sediment discharge and bed configuration data; and if the r value can be properly assumed. If only the discharge of water, the water surface slope, the channel dimensions and bed material properties are given, the general one-dimensional stochastic model will not be able either to describe or to predict the dispersion process. However, the Aris moment equations can give some qualitative description of the dispersion process with this limited information.

16. When all the necessary information is given for both the general one-dimensional stochastic model and the dispersion model by solving Aris' moment equations, the stochastic model gives a more realistic picture of the movement of sand particles along a sand bed. Also, the stochastic model can provide longitudinal concentration distribution curves at any dispersion time, a function which the dispersion model is unable to perform.

Chapter VII

SUGGESTIONS FOR FURTHER RESEARCH

1. In any further similar longitudinal dispersion experiment, a flume at least 100 feet long should be used.

2. From this dispersion study, the behavior of each individual tracer particle is not clear. No direct measurement of the step lengths and rest periods of a single tracer particle is possible from a dispersion study. In order to have a better understanding of the behavior of each sand particle along an alluvial bed, an experiment in which only a single tracer particle or a few identifiable tracer particles are followed should be carried out. A strongly radioactive tracer particle which has the same properties as the sand in the alluvial bed may be the best choice for this kind of study.

3. A longer flume should be used for this single tracer particle study, so that longer bed configuration records can be obtained. These bed configuration data are helpful in relating step lengths and rest periods to other variables and serving as a double check.

4. Such a single tracer particle experiment should be carried out for different flow conditions and different sizes of tracer particles to find the relationships between the flow conditions, the size of tracer particles, and the parameters used in the general one-dimensional stochastic model.

5. The results of the single tracer particle experiment should be compared with the result of the dispersion study for the same conditions to see if they agree.

6. The method of using the skew parameter and the mean rate of displacement and spreading, obtained from the longitudinal concentration distribution curve, to find three parameters in the general one-dimensional stochastic model is not the best way. More study should be done to find a better parameter with good physical meaning to the dispersion process to replace the skew parameter.

7. After this general one-dimensional stochastic model has been tested, the two-dimensional stochastic model developed by Sayre and Conover (1967) should also be tested.

8. The Aris' moment equations should be generalized to the three-dimensional case, so that it can be applied to the point source dispersion study.

9. More studies about the velocity distribution of flow, fall velocity of sediment particles, the exchange of sand particles between the bed and the flow, and the mechanics of entrainment should be undertaken, especially in an alluvial channel, so the parameters used in the Aris' moment equations can be better determined.

10. The total sediment discharge should be analyzed, so the total sediment discharge equation, Eq. (3-69) can be tested.

BIBLIOGRAPHY

BIBLIOGRAPHY

Aris, R., On the dispersion of a solution in a fluid flowing through a tube, Proc. Royal Soc. of London, Vol. 235A, 1956, pp. 67-77.

Brush, L. M., Jr., Exploratory study of sediment diffusion, Journ. Geophysical Research, Vol. 67, No. 4, 1962, pp. 1427-1435

Crickmore, M. J., and G. H. Lean, The measurement of sand transport by means of radioactive tracers, Proc. of Royal Soc. of London, Series A, Vol. 266, 1962, pp. 402-421.

De Vries, M., Applications of luminophores in sand transport studies, Delft, 1966, 86 p.

De Vries, M., Discussion of "Sand transport studies with radioactive tracers;" Proc. of ASCE, No. HY1, 1965, pp. 173-185.

Dobbins, W. E., Effect of turbulence on sedimentation, ASCE Transaction Paper No. 2218, 1944, pp. 629-651.

Einstein, H. A., Der Geschiebetrieb als Wahrscheinlichkeitsproblem, Verlag Aascher, Zurich, 1937, 110 p.

Einstein, H. A., The bed-load function for sediment transportation in open channel flows, U.S. Dept. of Agriculture Technical Bulletin, No. 1026, Sept. 1950.

Fischer, H. B., Longitudinal dispersion in laboratory and natural stream, Ph.D. Dissertation, California Institute of Technology, Pasadena, California, 1966, 250 p.

Guy, H. P., D. B. Simons, and E. V. Richardson, Summary of Alluvial channel data from flume experiments, 1956-61, USGS Professional Paper No. 462-I, 1966.

Hubbell, D. W., and W. W. Sayre, Sand transport studies with radioactive tracers, Proc. of ASCE, Vol. 90, No. HY3, 1964, pp. 39-68.

Hubbell, D. W., and W. W. Sayre, Closure of the discussion of sand transport studies with radioactive tracers, Proc. of ASCE, Vol. 91, No. HY5, 1965, pp. 139-149.

Kennedy, J. F., Stationary waves and antidunes in alluvial channels, Ph.D. Dissertation, California Institute of Technology, Pasadena, California, 1961, pp. 40-44.

Lane, E. W., and A. A. Kalinske, The relation of suspended to bed material in rivers, Hydrology Vol. 20, 1939, pp. 637-641.

Nordin, C. F., Statistical properties of dune profiles, Ph.D. Dissertation, Colorado State University, Fort Collins, Colorado, 1968, 137 p.

Parzen, E., Stochastic Process, Holden-Day Inc., San Francisco, Calif., 1962, pp. 17.

Sayre, W. W., Dispersion of mass in open-channel flow, Colorado State University Hydraulics Paper No. 3, Fort Collins, Colorado, 1968, 73 p.

Sayre, W. W., and W. J. Conover, General two-dimensional stochastic model for the transport and dispersion of bed-material sediment particles, Proc. of 12th Congress of IAHR, Fort Collins, Colorado, Sept. 1967.

Simons, D. B., and E. V. Richardson, Resistance to flow in alluvial channels, Journal of the Hydraulics Division, Proc. of ASCE, Vol. 86, No. HY5, 1960, pp. 73-99.

Tchen, C. M., Mean value and correlation problems connected with the motion of small particles suspended in a turbulent fluid, Publ. 51 of Lab for Aero and Hydraulics, Technical University, Delft, 1947.

Todorovič, P., A stochastic process of monotonous sample function, Matematnykn bechnk 4(19), C_B 2, 1967, pp. 149-158.

APPENDIX A

COMPUTER PROGRAM AND SUPPLEMENTARY INFORMATION OF ARIS MOMENT EQUATIONS

SELECTED VARIABLE NAMES USED IN PROGRAM
FOR SOLVING ARIS MOMENT EQUATION

Variable Name	Term Represented
DT	$\Delta\tau$
DY	$\Delta\eta$
K1	$1/\Delta\eta$
K2	No. of $\Delta\tau$ steps in program
K3	No. of $\Delta\tau$ steps between print outs
E(I)	$\psi(\eta)$
U(I)	equation 3-55
EA(I)	equation 3-56
T	κ
B	β
A	α
G	γ
UA	$\overline{U}/U_*$
CO(I,J)	$C_o(\eta,\tau)$
C1(I,J)	$C_1(\eta,\tau)$
C2(I,J)	$C_2(\eta,\tau)$
C3(I,J)	$C_3(\eta,\tau)$
WO(J)	$W_o(\tau)$
W1(J)	$W_1(\tau)$
W2(J)	$W_2(\tau)$
W3(J)	$W_3(\tau)$

Variable Name	Term Represented
SCO	$m_0(\tau) \sum_{I=1}^{K1} C_o(I,J)DY$
SUCO	$\frac{6}{\kappa^2} \sum_{I=1}^{K1} C_0 I,J)U(I)\Delta\eta$
EC1(I)	$\overline{\xi}_S(\eta,\tau)$
SC1	$\sum_{I=1}^{K1} C_1(I,J)\Delta\eta$
VAR(I)	$\sigma_S^2(\eta,\tau)$
SC2	$\sum_{I=1}^{K1} C_2(I,J)\Delta\eta$
S(I)	$S_S(\tau)$
SC3	$\sum_{I=1}^{K1} C_3(I,J)\Delta\eta$
US	$\overline{\mu}_s(\tau)$
ESC1	$\overline{\xi}_S(\tau)$
AVAR	$\sigma_S^2(\tau)$
SK	$S_S(\tau)$
EW	$\overline{\xi}_W(\tau)$
VARW	$\sigma_W^2(\tau)$

Variable Name	Term Represented
SKW	$S_W(\tau)$
UST	$\overline{\mu}_T(\tau)$
COT	$m_0(\tau)+W_0(\tau)$
C1T	$\overline{\xi}_T(\tau)$
VART	$\sigma_T^2(\tau)$
SKT	$S_T(\tau)$

Velocity and Diffusion Coefficients in Program for Solving Aris' Moment Equations, Logarithmic Velocity Distribution, DY = 0.1

I	U(I)	E(I)	E(A)
1	-2.30258	0.00000	0.28000
2	-0.91629	0.54000	0.76000
3	-0.39303	0.96000	1.12000
4	-0.05325	1.26000	1.36000
5	0.19941	1.44000	1.48000
6	0.40077	1.50000	1.48000
7	0.56829	1.44000	1.36000
8	0.71157	1.26000	1.12000
9	0.83688	0.96000	0.76000
10	0.94823	0.54000	0.28000
11		0.00000	
Sum	0.00000		10.00000

CASE 1

```
*FORTRAN
      PROGRAM SAYRE
      DIMENSION E(51),U(50),EA(50),CO(50,2),C1(50,2),C2(50,2),EC1(50),
     1 VAR(50),D2(50),D3(50),D4(50),D5(50),C3(50,2),S(50),D6(50),
     2 WO(2),W1(2),W2(2),W3(2)
   10 FORMAT (F8.6,F5.2,I3,1X,2I9)
      READ (5,10) DT,DY,K1,K2,K3
   20 FORMAT (3F6.3,F8.5,F7.3)
   25 FORMAT (1H0,5H  T =,F6.3,5H, B =,F6.3,5H, A =,F6.3,5H, G =,F8.5,
     1 6H, UA =,F7.3//)
      K4=K1+1
      K5=K1-1
   30 FORMAT(F8.5,3X,F8.5,3X,F8.5)
      READ (5,30) (E(I),U(I),EA(I),I=1,K1)
   35 FORMAT(F8.5)
      READ (5,35) E(K4)
      D1=DT/DY
   36 READ (5,20) T,B,A,G,UA
      IF (T-9.999) 37,170,170
   37 WRITE (6,25) T,B,A,G,UA
      D7= D1*6.*B*(1.-A)
      D8 = DT*A*6.*B
      D9=0.0
      G1 = D1*G
      G2 = DT*G
      DO 40 I=1,K1
      D2(I)=E(I+1)/DY+6.*B
      D3(I)=E(I)/DY
      D4(I)=6.*DT*(U(I)+T*UA)/T**2
      D5(I)=2.*DT*EA(I)
      D6(I)=D4(I)/DT
      C1(I,1)=0.0
      C2(I,1)=0.0
   40 C3(I,1)=0.0
      CO(1,1)=10.0
      DO 45 I=2,K1
   45 CO(I,1)=0.0
      WO=0.0
      W1(1) = 0.0
      W2(1) = 0.0
      W3(1) = 0.0
      L=1
      DO 160 J=1,K2
      I=1
      CO(I,2)=CO(I,1)+D1*(D2(I)*(CO(I+1,1)-CO(I,1)))+D7*CO(I,1)
     1 + G1*WO(1)
      DO 50 I=2,K5
   50 CO(I,2)=CO(I,1)+D1*(D2(I)*(CO(I+1,1)-CO(I,1))-D3(I)*(CO(I,1)-
     1 CO(I-1,1)))
      I=K1
      CO(I,2)=CO(I,1)-D1*(D3(I)*(CO(I,1)-CO(I-1,1))+6.*B*CO(I,1))
      WO(2) = WO(1) + D8*CO(1,1) - G2*WO(1)
      I=1
      C1(I,2)=C1(I,1)+D1*(D2(I)*(C1(I+1,1)-C1(I,1)))+D4(I)*CO(I,1)
     1 +D7*C1(I,1) + G1*W1(1)
      DO 60 I=2,K5
```

```
 80 C1(I,2)=C1(I,1)+D1*(D2(I)*(C1(I+1,1)-C1(I,1))-D3(I)*(C1(I,1)-
   1 C1(I-1,1)))+D4(I)*CO(I,1)
    I=K1
    C1(I,2)=C1(I,1)-D1*(D3(I)*(C1(I,1)-C1(I-1,1))+6.*B*C1(I,1))
   1 +D4(I)*CO(I,1)
    W1(2) = W1(1) + D8*C1(1,1) - D9*WO(1) - G2*W1(1)
    I=1
    C2(I,2)=C2(I,1)+D1*(D2(I)*(C2(I+1,1)-C2(I,1)))+2.*D4(I)*C1(I,1)
   1 +D5(I)*CO(I,1) + D7*C2(I,1) + G1*W2(1)
    DO 100 I=2,K5
100 C2(I,2)=C2(I,1)+D1*(D2(I)*(C2(I+1,1)-C2(I,1))-D3(I)*(C2(I,1)-
   1 C2(I-1,1)))+2.*D4(I)*C1(I,1)+D5(I)*CO(I,1)
    I=K1
    C2(I,2)=C2(I,1)-D1*(D3(I)*(C2(I,1)-C2(I-1,1))+6.*B*C2(I,1))
   1 +2.*D4(I)*C1(I,1)+D5(I)*CO(I,1)
    W2(2) = W2(1) + D8*C2(1,1) - 2.*D9*W1(1) - G2*W2(1)
    I=1
    C3(I,2)=C3(I,1)+D1*(D2(I)*(C3(I+1,1)-C3(I,1)))+3.*D4(I)*C2(I,1)
   1 +3.*D5(I)*C1(I,1) + D7*C3(I,1) + G1*W3(1)
    DO 105 I=2,K5
105 C3(I,2)=C3(I,1)+D1*(D2(I)*(C3(I+1,1)-C3(I,1))-D3(I)*(C3(I,1)-
   1 C3(I-1,1)))+3.*D4(I)*C2(I,1)+3.*D5(I)*C1(I,1)
    I=K1
    C3(I,2)=C3(I,1)-D1*(D3(I)*(C3(I,1)-C3(I-1,1))+6.*B*C3(I,1))
   1 +3.*D4(I)*C2(I,1)+3.*D5(I)*C1(I,1)
    W3(2) = W3(1) + D8*C3(1,1) - 3.*D9*W2(1) - G2*W3(1)
    IF (J-L-K3) 150,110,170
110 SCO=0.0
    SUCO=0.0
    SC1=0.0
    SC2=0.0
    SC3=0.0
    DO 120 I=1,K1
    SCO=SCO+CO(I,1)*DY
    SUCO=SUCO+D6(I)*CO(I,1)*DY
    IF (CO(I,1)) 115,116,115
115 EC1(I)=C1(I,1)/CO(I,1)
    VAR(I)=C2(I,1)/CO(I,1)-EC1(I)**2
    S(I)=((C3(I,1)-3.*EC1(I)*C2(I,1))/CO(I,1)+2.*EC1(I)**3)/
   1 VAR(I)**1.5
    GO TO 117
116 EC1(I)=0.0
    VAR(I)=0.0
    S(I)=0.0
117 SC1=SC1+C1(I,1)*DY
    SC2=SC2+C2(I,1)*DY
120 SC3=SC3+C3(I,1)*DY
    IF (SCO-0.00001) 36,36,121
121 US=SUCO/SCO
    ESC1=SC1/SCO
    AVAR=SC2/SCO-ESC1**2
    SK=((SC3-3.*ESC1*SC2)/SCO+2.*ESC1**3)/AVAR**1.5
    IF (WO(1)) 125,126,126
    UST=SCO*US
    VARW = W2(1)/WO(1) - EW**2
    SKW = ((W3(1)-3.*EW*W2(1))/WO(1)+2.*EW**3)/VARW**1.5
```

```
      COT = SCO + WO(1)
      UST = SCO*US - WO(1)*U.*UA/T
      C1T = (SC1 + W1(1))/COT
      C2T = (SC2 + W2(1))/COT
      VART = C2T - C1T**2
      C3T = (SC3 + W3(1))/COT
      SKT = (C3T - 3.*C1T*C2T + 2.*C1T**3)/ VART**1.5
  126 J1=J-1
  130 FORMAT(1H ,I3,3X,I3,3X,F8.5,3X,F9.4,3X,F10.4,3X,F9.4)
      WRITE (6,130) (J1,I,CO(I,1),EC1(I),VAR(I),S(I),I=1,10)
  140 FORMAT (1HO,I5,3X,F8.4,3X,F8.5,3X,F9.4,3X,F10.5,3X,F9.5/)
      WRITE (6,140) J1,US,SCO,ESC1,AVAR,SK
  144 FORMAT(1H ,I5,2X,F9.4,3X,F8.5,3X,F9.4,3X,F10.5,3X,F9.5///)
  145 FORMAT(1H ,I5,14X,F8.5,3X,F9.4,3X,F10.5,3X,F9.5//)
      IF (WO(1)) 146,147,146
  146 WRITE (6,145) J1,WO(1),EW,VARW,SKW
      WRITE (6,144) J1,UST,COT,C1T,VART,SKT
  147 L=J
  150 WO(1) = WO(2)
      W1(1) = W1(2)
      W2(1) = W2(2)
      W3(1) = W3(2)
      DO 160 I=1,K1
      CO(I,1)=CO(I,2)
      C1(I,1)=C1(I,2)
      C2(I,1)=C2(I,2)
  160 C3(I,1)=C3(I,2)
      GO TO 36
  170 STOP
      END
```

CASE 2

Essentially there is no difference between the computer program for case 1 and case 2, except the initial and boundary conditions. The difference between case 1 and case 2 are listed as follows.

Case 1	Case 2
D6(I)=D4(I)/DT	D6(I)=D4(I)/DT
C1(I,1)=0.0	CO(I,1)=0.0
C2(I,1)=0.0	C1(I,1)=0.0
40 C3(I,1)=0.0	C2(I,1)=0.0
CO(I,1)=10.0	40 C3(I,1)=0.0
DO 45 I=2, k1	WO(1)=1.0
45 CO(I,1)=0.0	W1(1)=0.0
WO=0.0	W2(1)=0.0
W1(1)=0.0	W3(1)=0.0
W2(1)=0.0	
W3(1)=0.0	

APPENDIX B

COMPUTER PROGRAM AND SUPPLEMENTARY INFORMATION FOR THE GENERAL ONE-DIMENSIONAL STOCHASTIC MODEL

SELECTED VARIABLE NAMES USED IN THE PROGRAM
FOR THE GENERAL ONE-DIMENSIONAL STOCHASTIC MODEL

Variable Name	Term Represented
F	$f_t(x)$
G	r
T	t
TABLE (J)	gamma function from mathematics table
X	x
XK1	k_1
XK2	k_2

```
*FORTRAN
      PROGRAM FUNXT
      DIMENSION X(100),TABLE(201),Q1(400),Q2(400),Q3(400),XK1X(100)
    3 READ (5,4) (TABLE(J),J=100,200)
    4 FORMAT (10F8.5)
    1 READ (5,2) T,XK1,XK2,G
      IF (T.EQ.222.22222) 80,6
    2 FORMAT (4F8.5)
    6 M1=1
   10 M2=M1+9
      READ (5,9) (X(M),M=M1,M2)
    9 FORMAT (10F8.5)
      DO 5 M=M1,M2
      IF ((X(M)-.00099)-.00010) 7,7,5
    7 KI=M-1
      GO TO 8
    5 CONTINUE
      M1=M2+1
      GO TO 10
    8 N=100
      WRITE (6,70) XK1,XK2,G,T
   70 FORMAT (4F10.5)
      DO 74 M=1,KI
      DO 45 I=1,N
      XI=I
      XIG=XI*G
      XK1X(M)=XK1*X(M)
      IF (XIG.EQ.1.0) GO TO 39
   25 CONTINUE
      IGX=XIG*100.0
      J=IGX
      IF (XIG-2.0) 31,31,40
   31 IF (XIG-1.0) 38,39,36
   36 Q1(I)=(XK1X(M)**(XIG-1.0))/TABLE(J)
      GO TO 45
   38 JD=(XIG+1.0)*100.0
      J=JD
      Q1(I)=(XK1X(M)**(XIG-1.0))/(TABLE(J)/XIG)
      GO TO 45
   39 Q1(1)=1.0
      GO TO 45
   40 P=XIG-1.0
      L=P-1
      DO 42 K=1,L
      B=K+1
   42 P=P*(XIG-B)
      C=L+1
      J=(XIG-C)*100.0
      GM=P*TABLE(J)
   44 Q1(I)=(XK1X(M)**(XIG-1.0))/GM
   45 CONTINUE
      XK2T=XK2*T
      Q2(1)=XK2T
```

```
      DO 48 I=2,N
      XI=I
   48 Q2(I)=Q2(I-1)*XK2T/XI
      DO 63 I=1,N
   63 Q3(I)=Q1(I)*Q2(I)
      SUM=0.0
   66 DO 67 I=1,N
   67 SUM=SUM+Q3(I)
   68 CONTINUE
      Q4=EXP(-XK1X(M)-XK2T)
      F=XK1*Q4*SUM
      WRITE (6,71) (X(M),F)
   71 FORMAT (2F15.5)
   74 CONTINUE
   75 GO TO 1
   80 STOP
      END
```

APPENDIX C

CORE SAMPLE RESULTS AND SOME COMPARISONS WITH RESULTS FROM LONGITUDINAL CONCENTRATION DISTRIBUTION EXPERIMENTS

LIST OF FIGURES IN APPENDIX C

Figure | Page

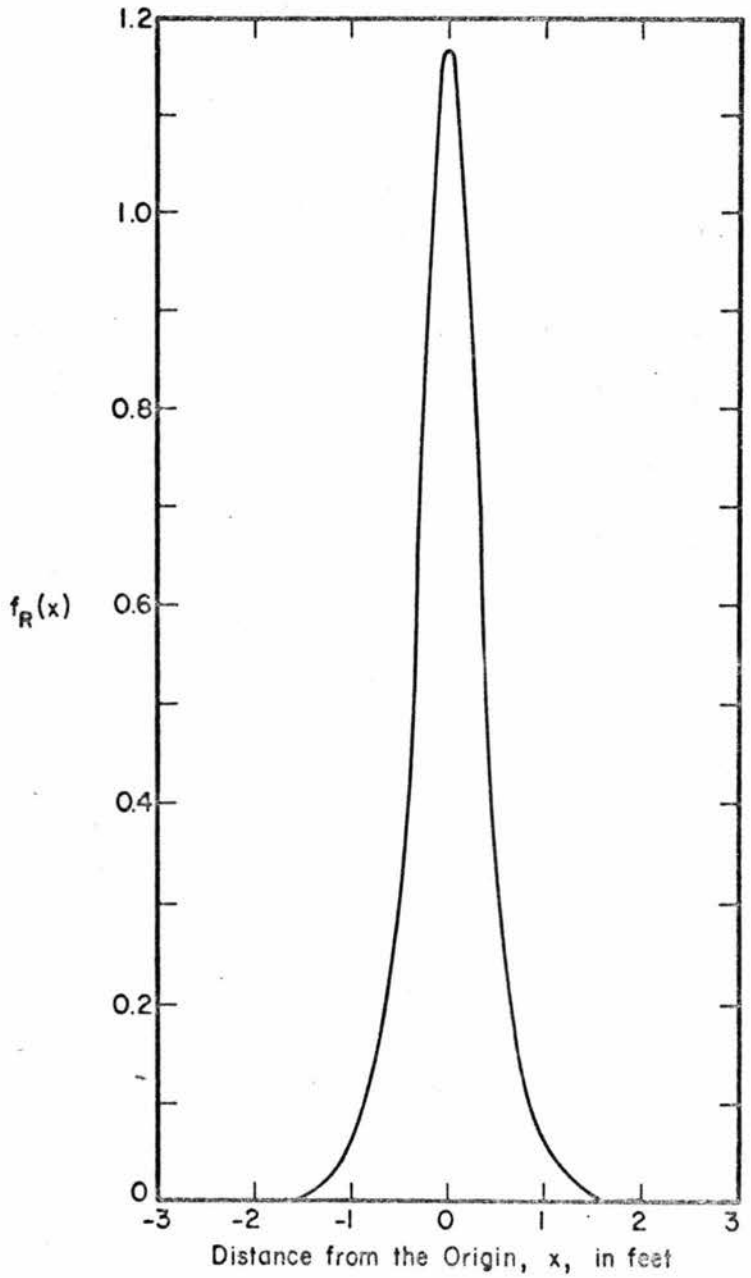

Figure C-1. Response of detection system to line source across flume.

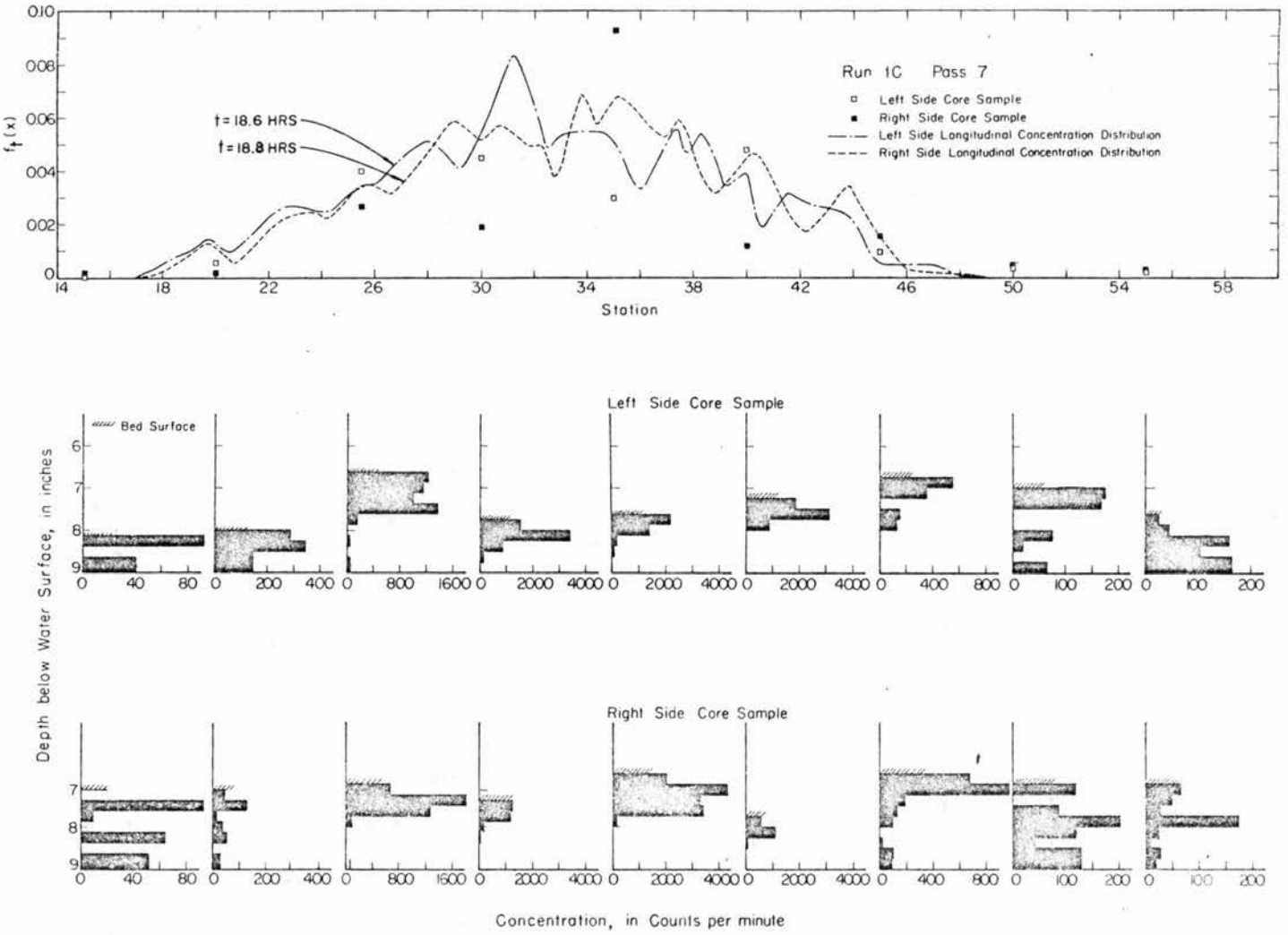

Figure C-2. Experimental longitudinal concentration distribution determined by scintillation detector and core sample results for Run 1C Pass 7

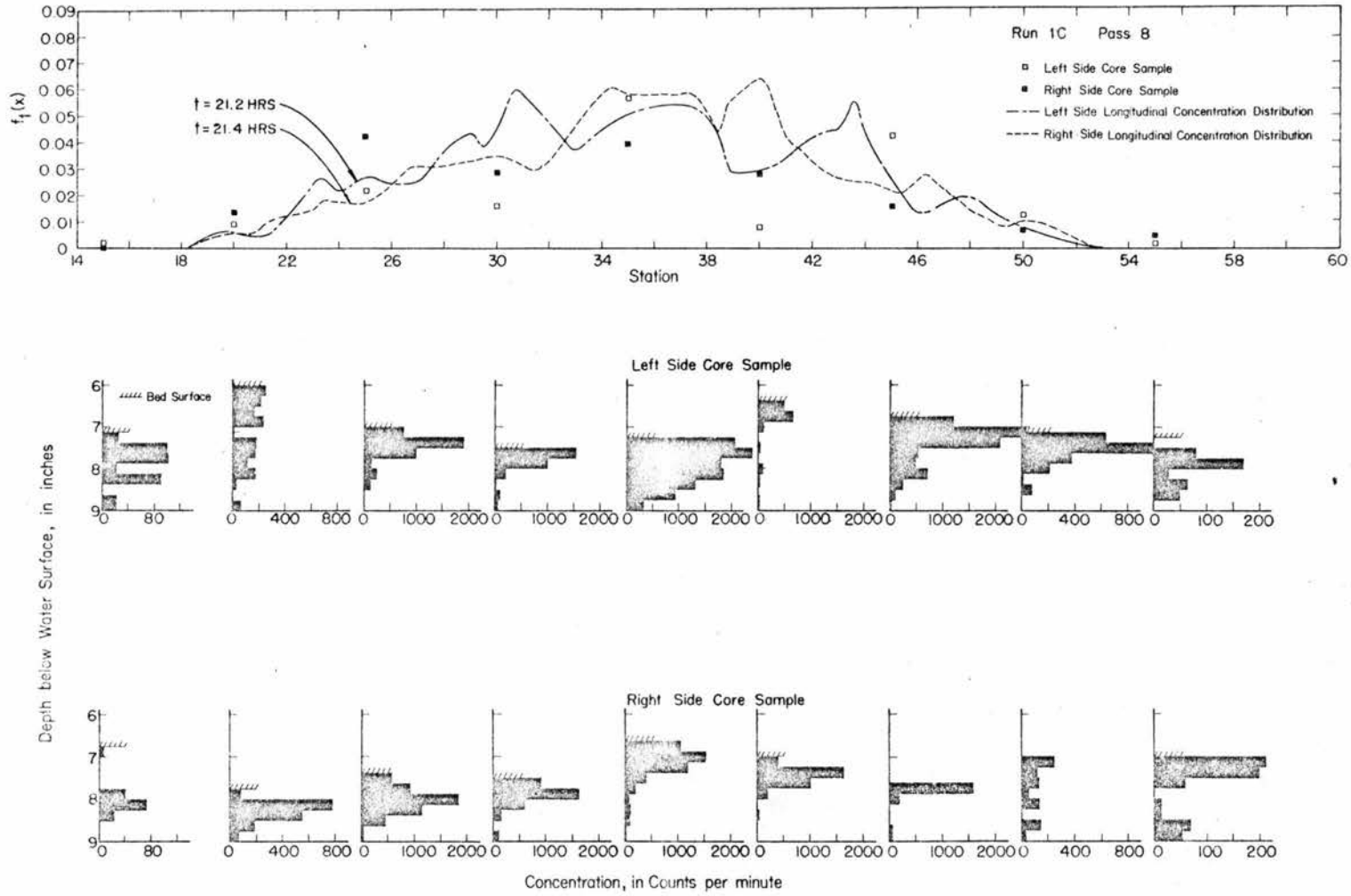

Figure C-3. Comparison between experimental longitudinal concentration distribution and core sample results for Run 1C Pass 8

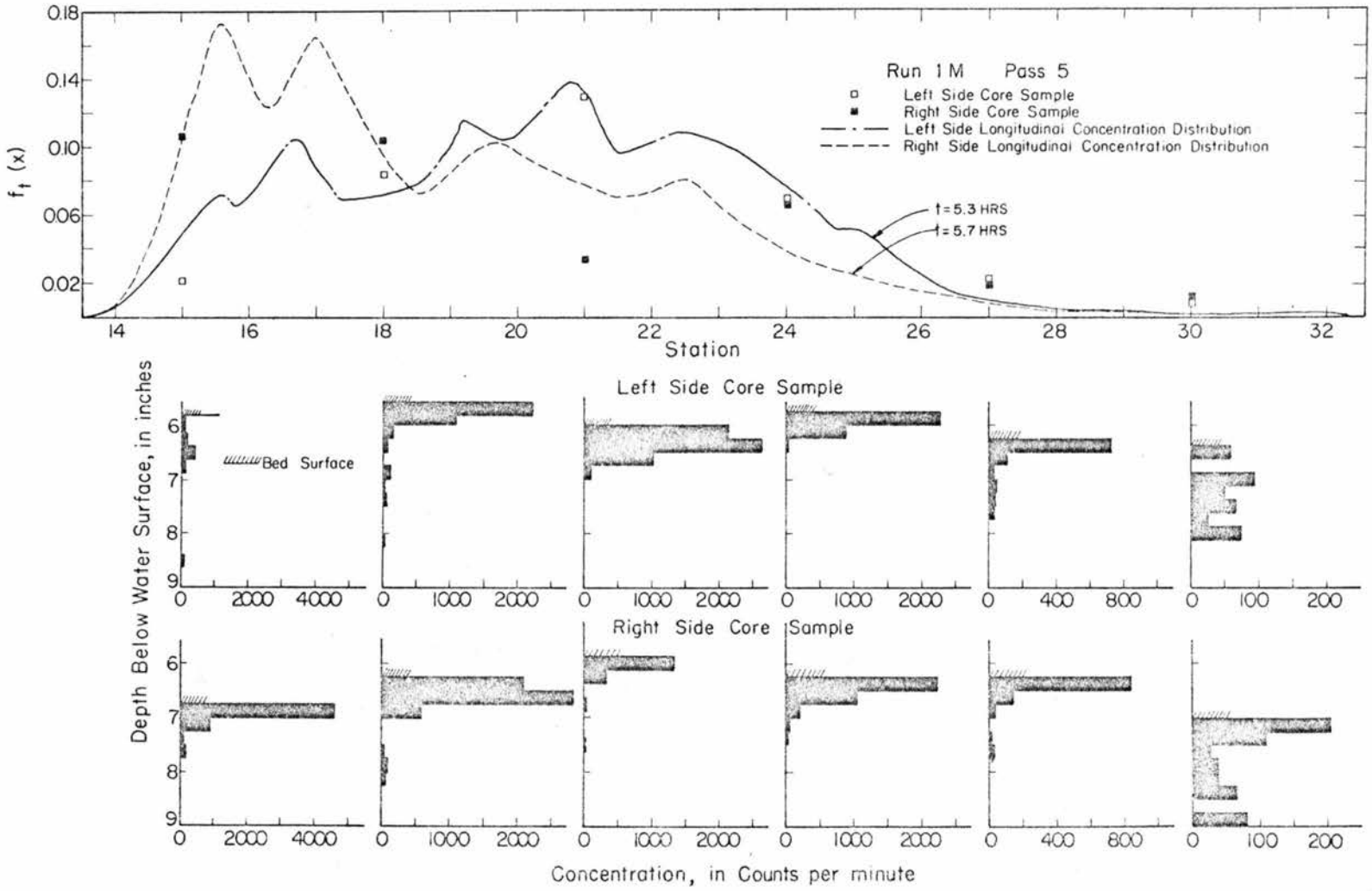

Figure C-4. Comparison between experimental longitudinal concentration distribution and core sample results for Run 1M Pass 5

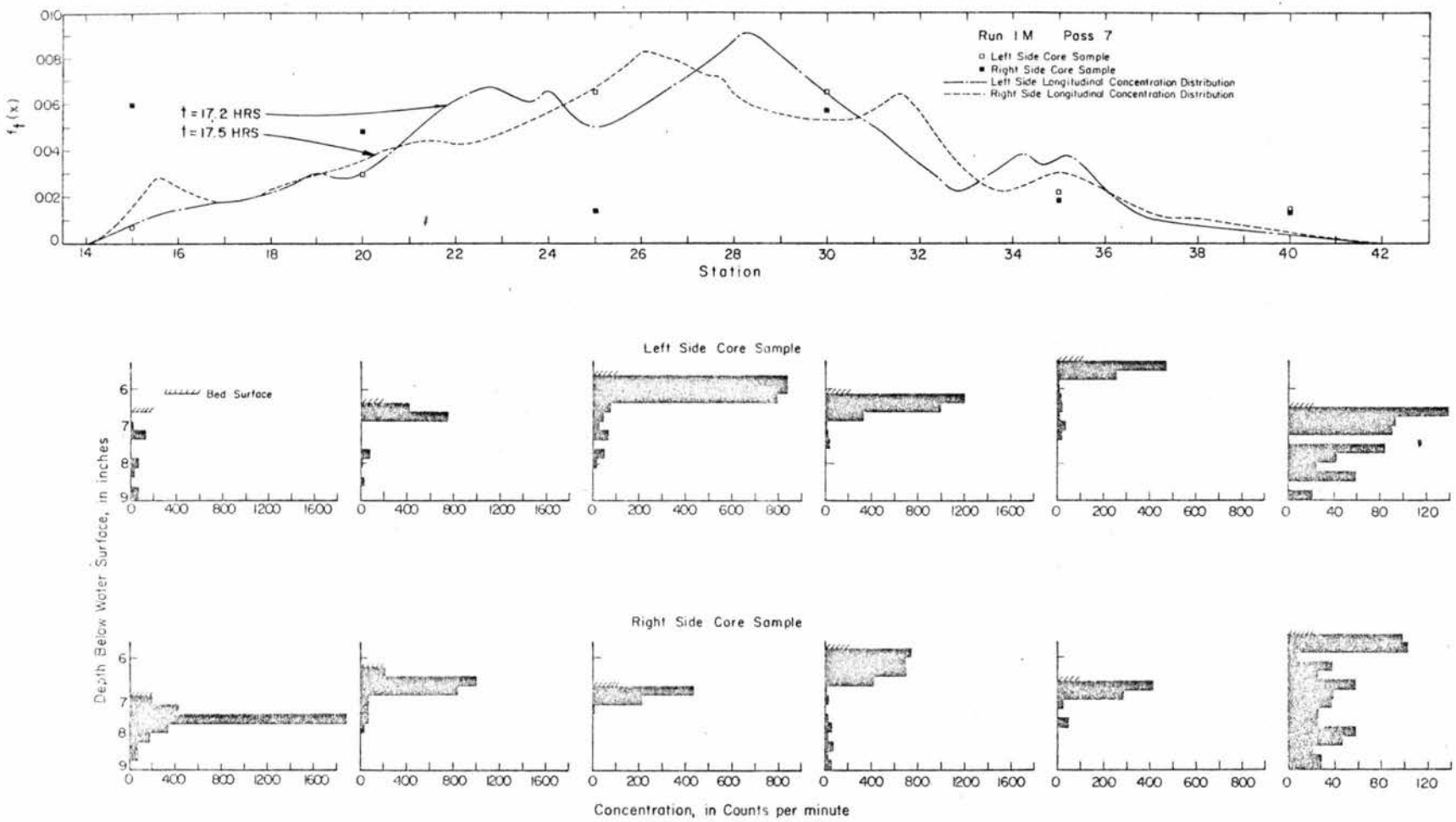

Figure C-5. Comparison between experimental longitudinal concentration distribution and core sample results for Run 1M Pass 7

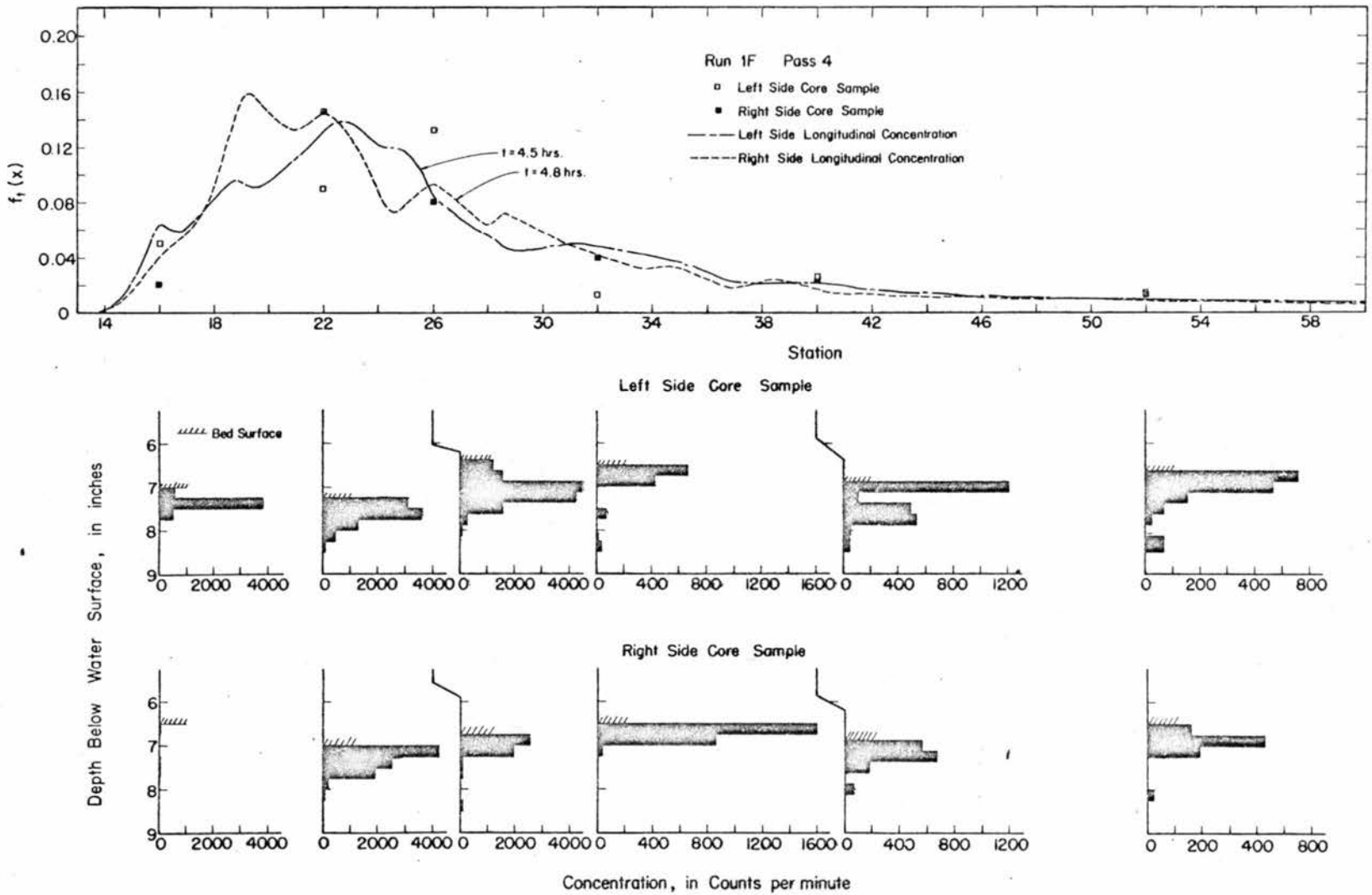

Figure C-6. Comparison between experimental longitudinal concentration distribution and core sample results for Run 1M Pass 7.

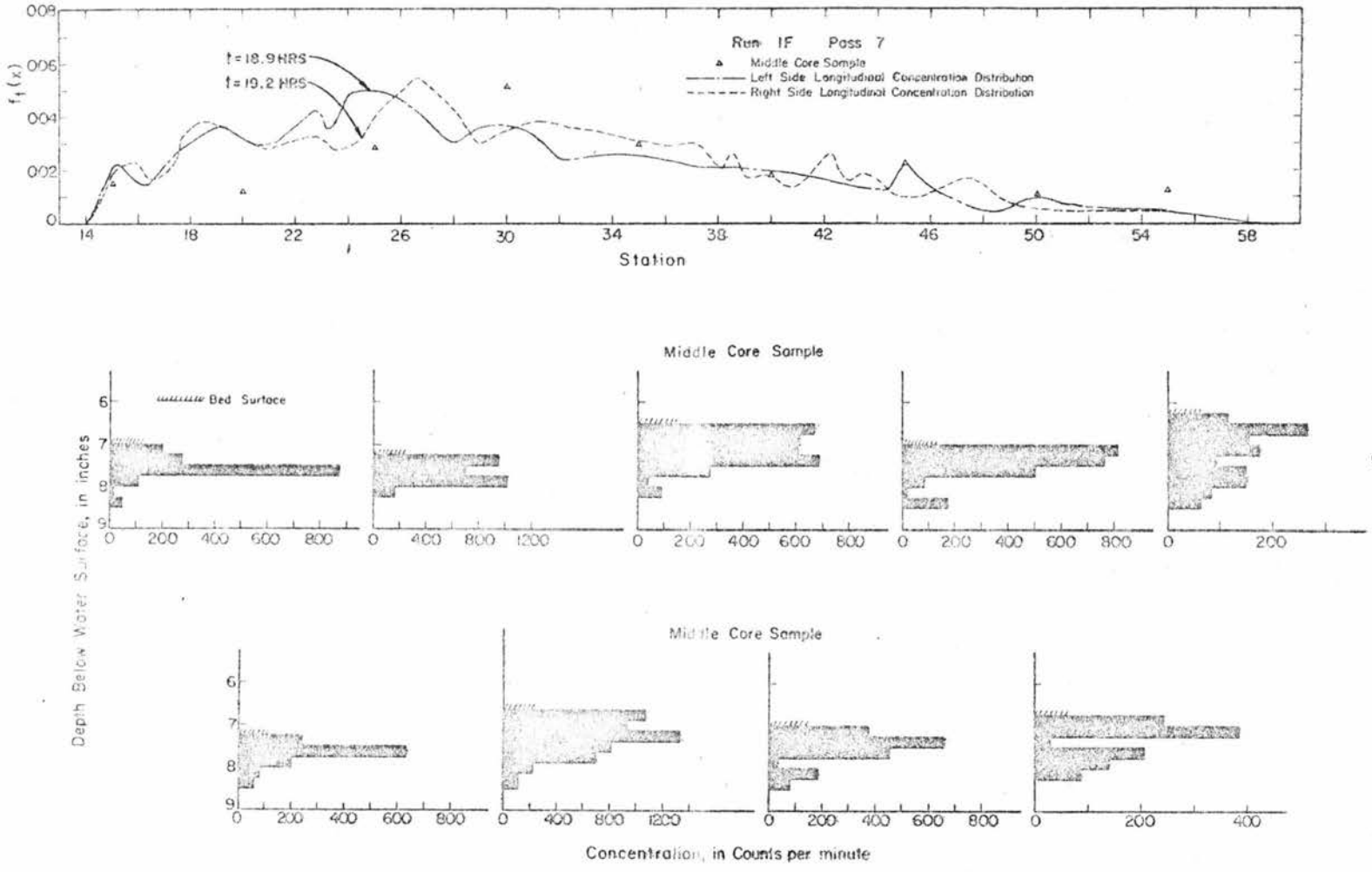

Figure C-7. Comparison between experimental longitudinal concentration distribution and core sample results for Run 1F Pass 7

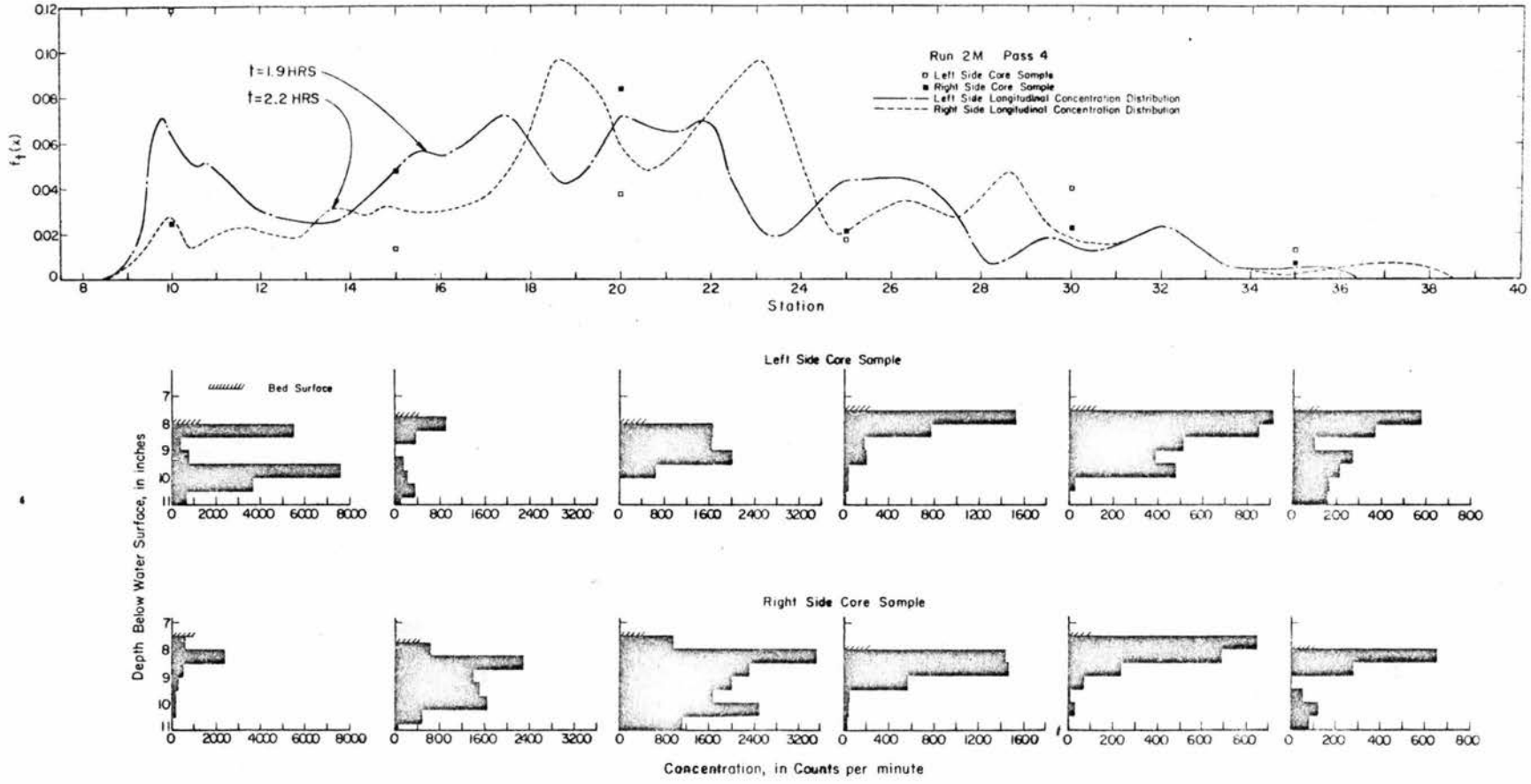

Figure C-8. Comparison between experimental longitudinal concentration distribution and core sample results for Run 2M Pass 4

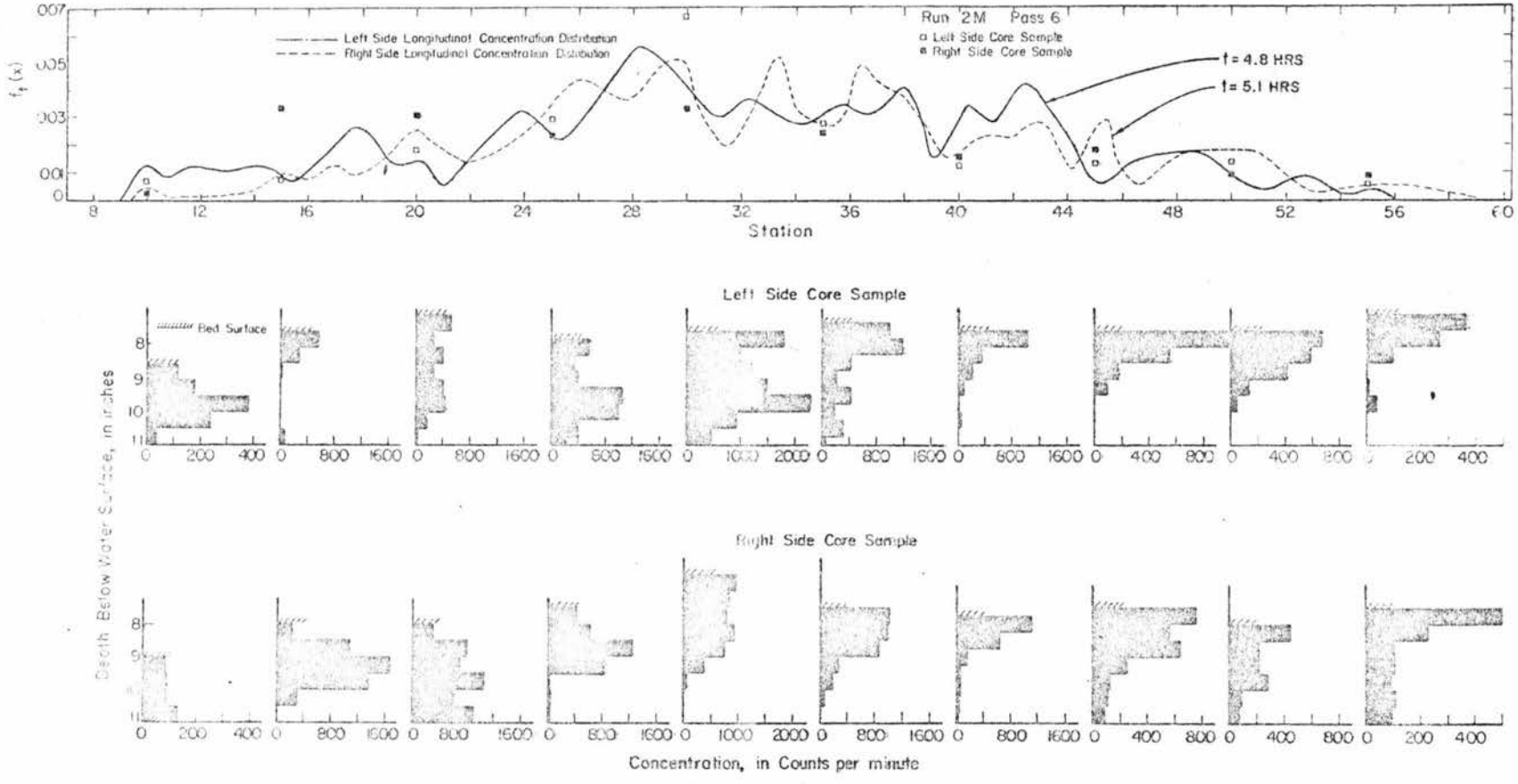

Figure C-9. Comparison between experimental longitudinal concentration distribution and core sample results for Run 2M Pass 6

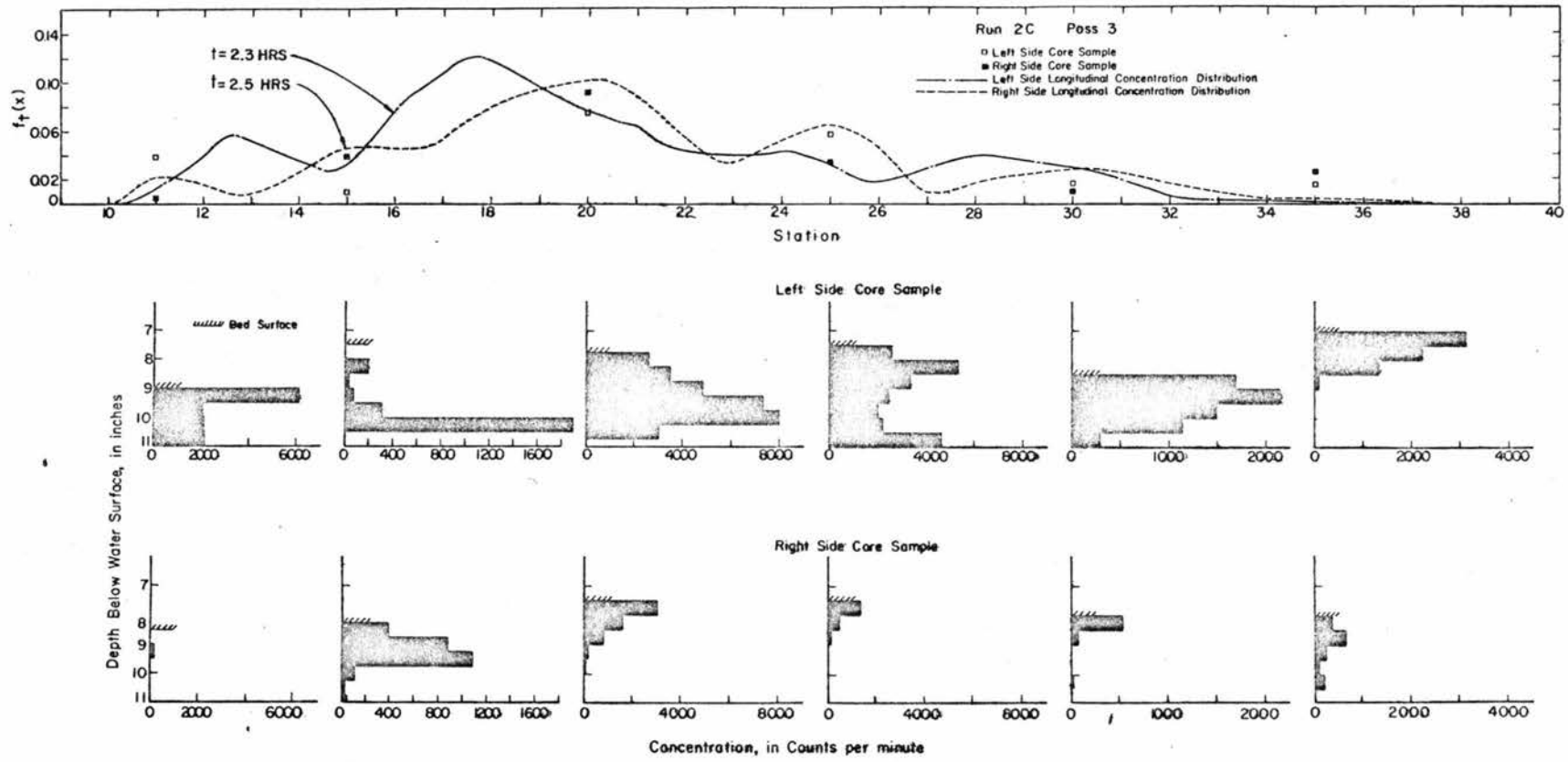

Figure C-10. Comparison between experimental longitudinal concentration distribution and core sample results for Run 2C Pass 3

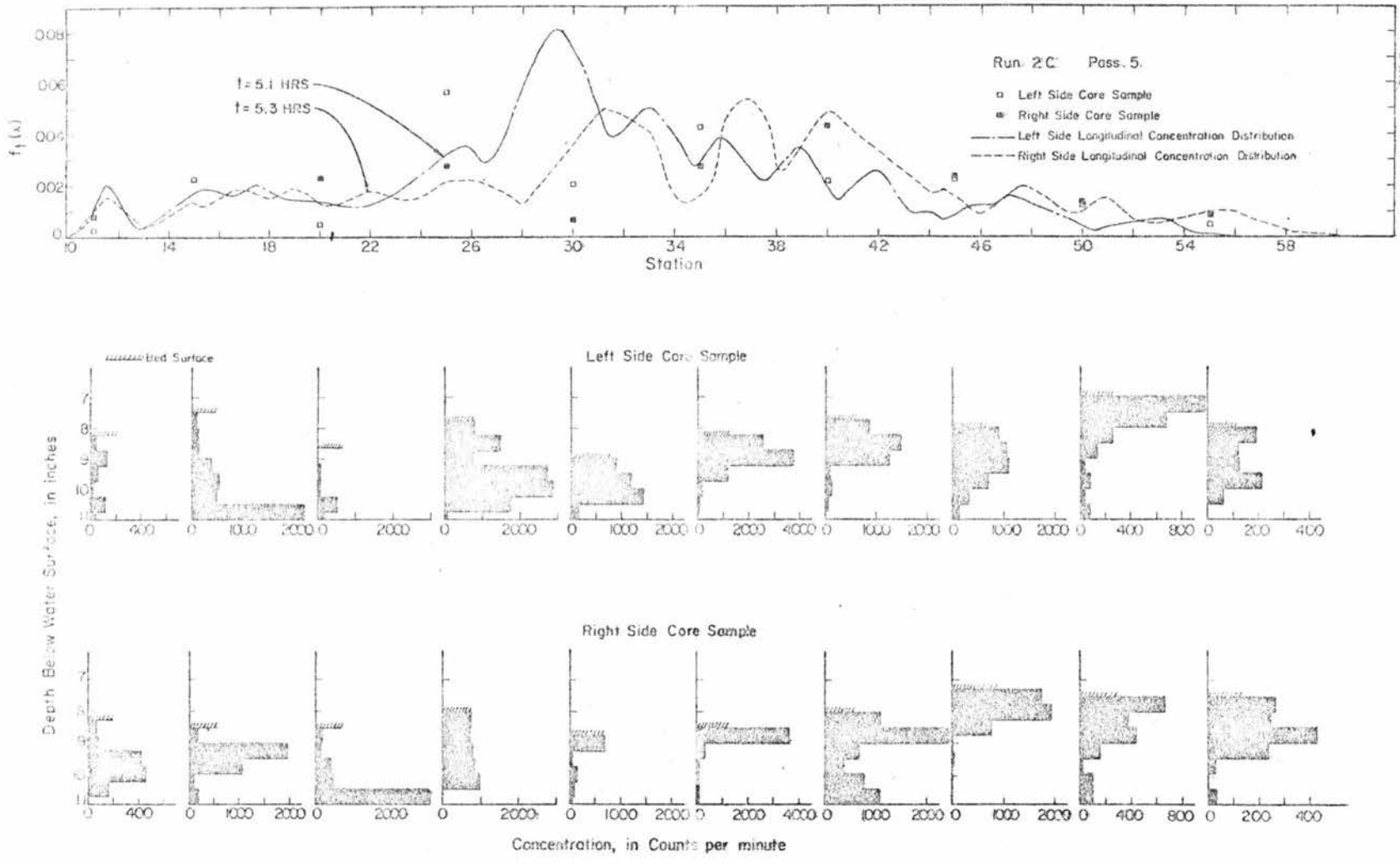

Figure C-11. Comparison between experimental longitudinal concentration distribution and core sample results for Run 2C Pass 5

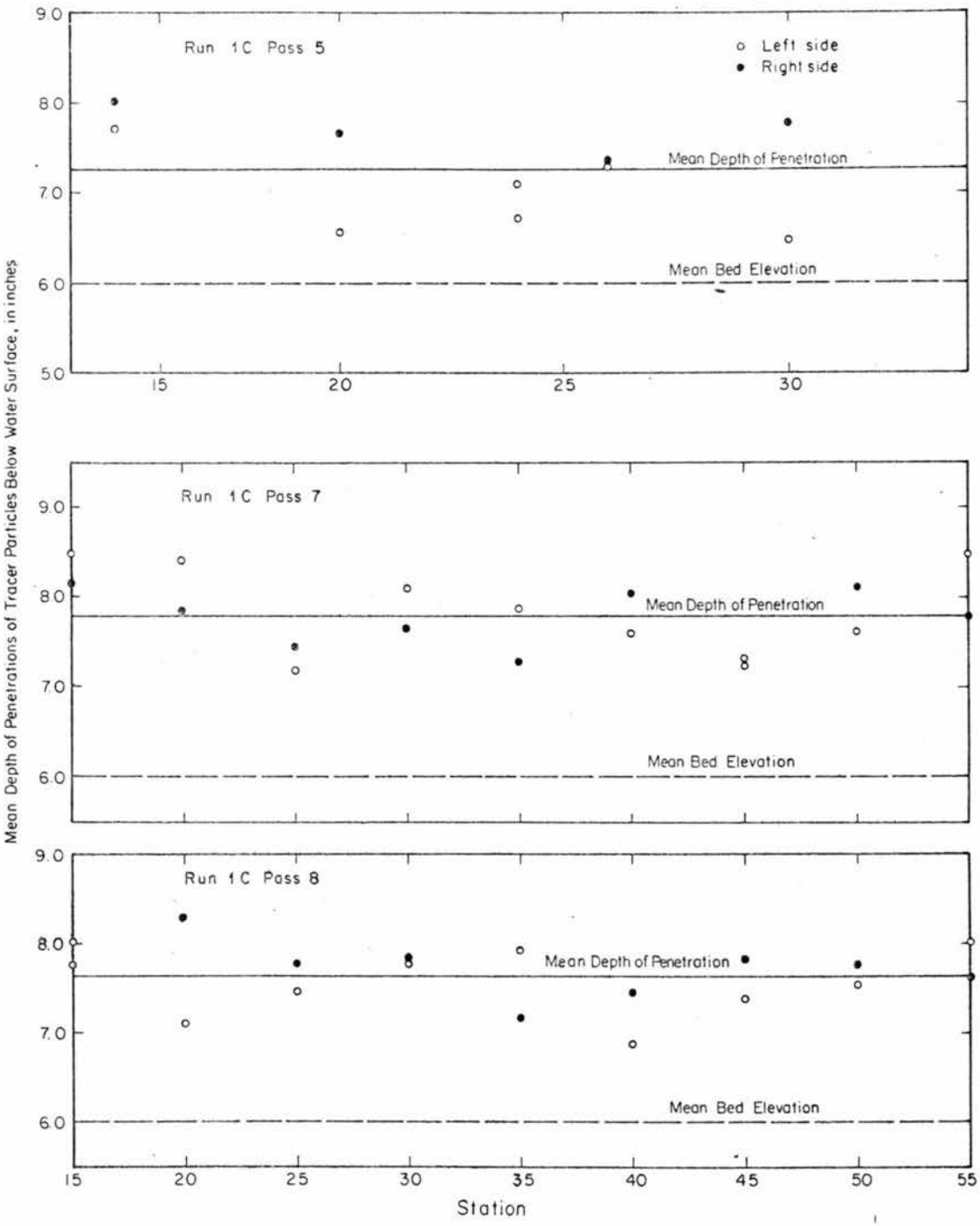

Figure C-12. Core sample results of the mean depth of penetration of tracer particles in the sand bed along the flume for Run 1C.

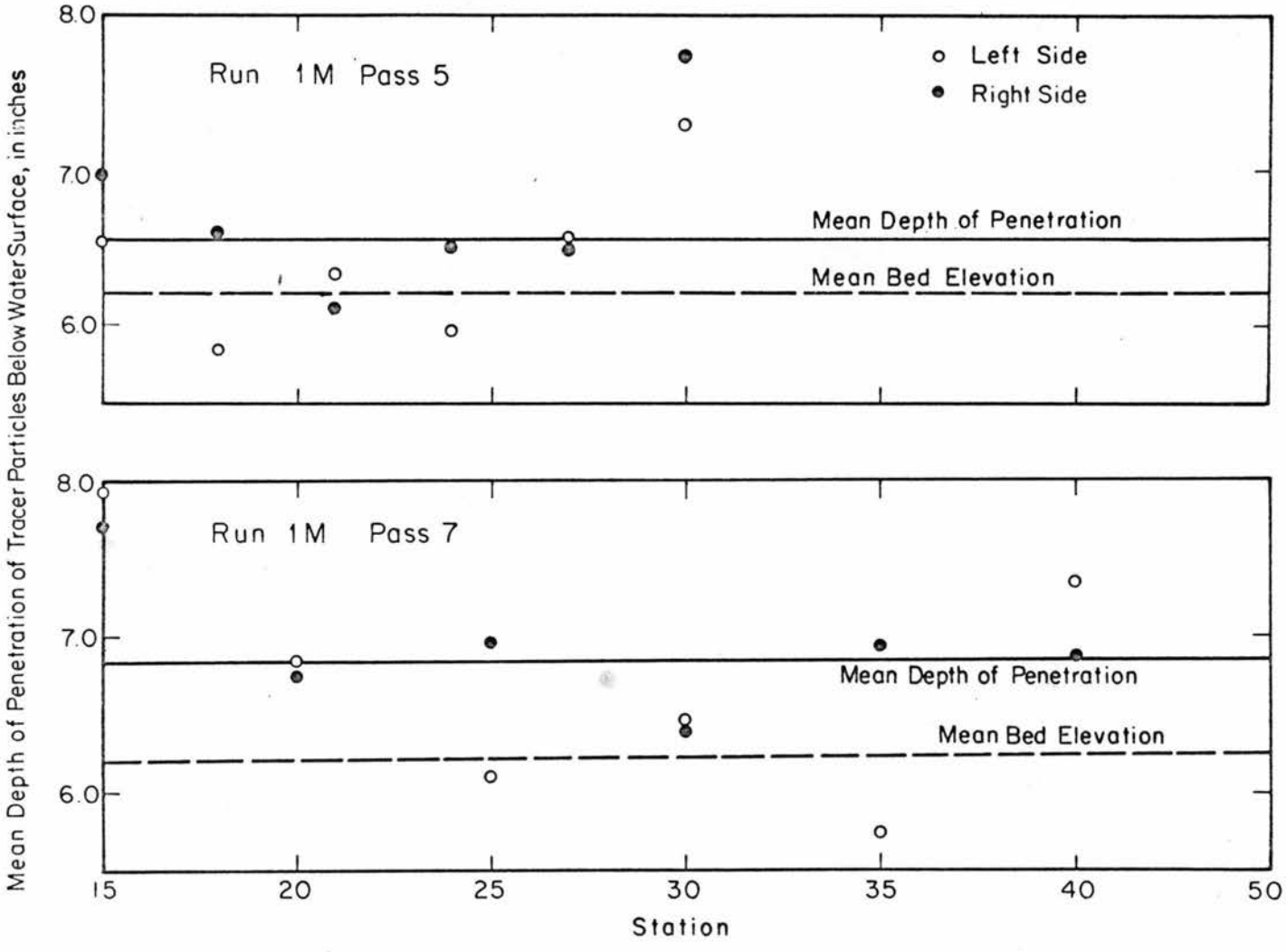

Figure C-13. Core sample results of the mean depth of penetration of tracer particles in the sand bed along the flume for Run 1M

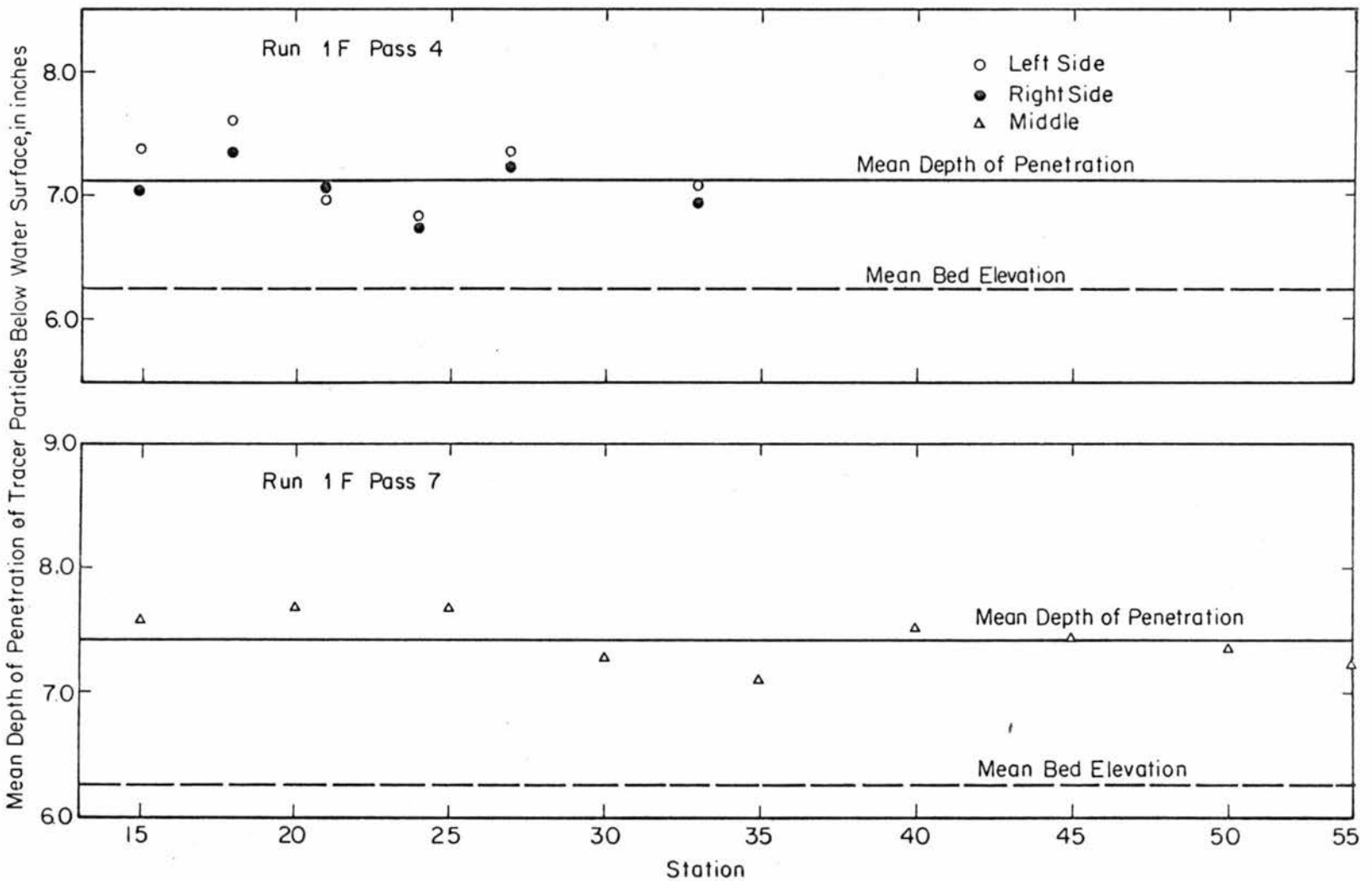

Figure C-14. Core sample results of the mean depth of penetration of tracer particles in the sand bed along the flume for Run 1F

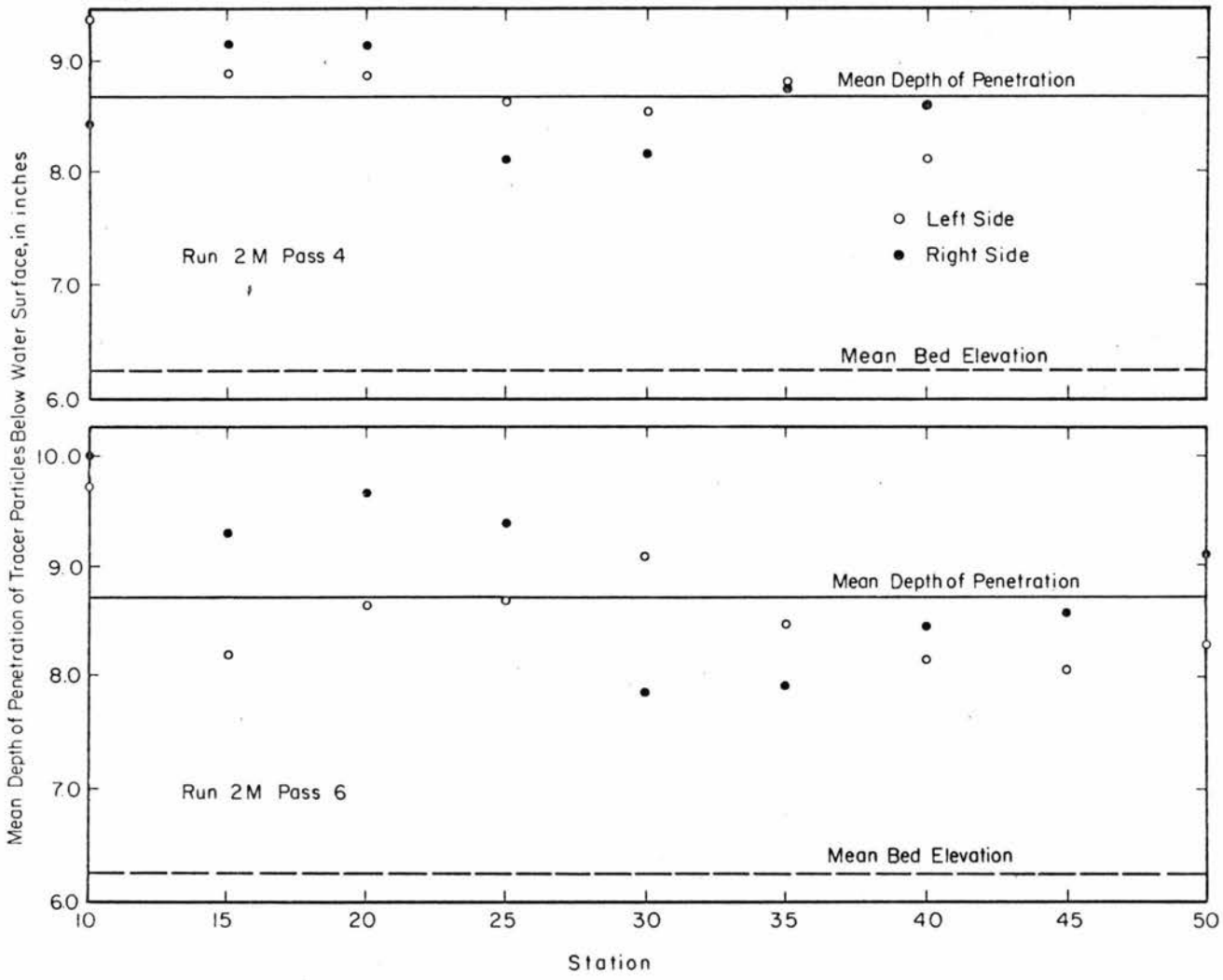

Figure C-15. Core sample results of the mean depth of penetration of tracer particles in the sand bed along the flume for Run 2M

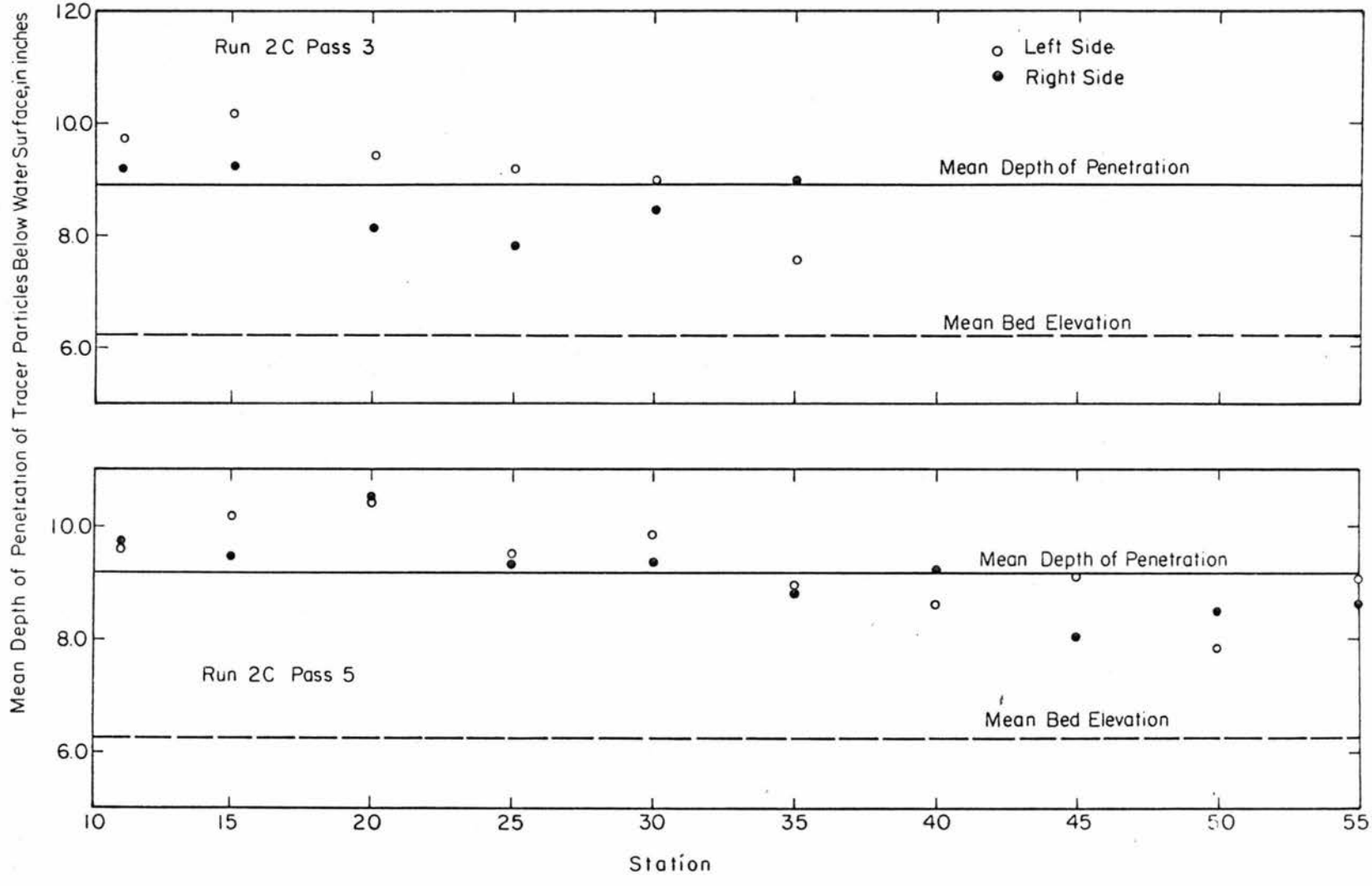

Figure C-16. Core sample results of the mean depth of penetration of tracer particles in the sand bed along the flume for Run 2C

APPENDIX D

COMPUTER PROGRAM AND SUPPLEMENTARY INFORMATION FOR THE VARIATION OF BED ELEVATION

SELECTED VARIABLE NAMES USED IN THE
PROGRAM FOR THE DISTRIBUTION OF BED ELEVATION

Variable Name	Term Represented
Program	
ID	Identification number
N	Number of data
Y	Original data of bed elevation y
X	Data of negative slope bed elevation
SD(I)	Sum of original data to i^{th} power $= \sum_{j=0}^{N} y_j^i$
ST(I)	Sum of data after trend line removed to i^{th} power $= \sum_{j=0}^{N} y_j^i$
SS(I)	Sum of data after standardized and trend line removed to the i^{th} power $= \sum_{j=0}^{N} y_j^i$
JJ	Number of negative slope data
SDX(I)	$= \sum_{k=0}^{JJ} x_k^i$
FJJ	Number of x's (negative slope data)

Variable Name	Term Represented
STX(I)	$\sum_{j=1}^{FJJ} x_j^i$ after trend line removed
SSX(I)	$\sum_{j=1}^{FJJ} x_j^i$ after trend line removed and standardized
Subroutine trend 2	
SY	$\sum_{j=1}^{N} y_j$ where y is the ordinate
SXY	$\sum_{j=1}^{N} x_i y_j$ where x is abscissa (same as distance)
SY2	$\sum_{j=1}^{N} y_j^2$
SX	$\sum_{j=1}^{N} x_j$
SX2	$\sum_{j=1}^{N} x_j^2$
B	Slope of trend line
A	Intercept of trend line
Y1	Computed Y on trend line

Variable Name	Term Represented
Subroutine MOM2	
XMO(I)	i^{th} moment about origin
XMM(I)	i^{th} moment about mean
VAR	Variance
STD	Standard deviation
COV	Coefficient of variation
CON	Constant
CSKEW	Coefficient of skewness
CKUR	Coefficient of kurtosis
Subroutine FREQ3	
CL	Lower class limit
PROB	Probability
Sum(J)	$\sum_{k=1}^{N} x_k^j$ where x = bed elevation
Subroutine STD2	
YBAR	$\overline{Y}$
S	Standard deviation of Y's

```
*FORTRAN
      PROGRAM YANG2
      COMMON DX,CUA,NCL,M
      DIMENSION X(1000),Y(1000),SD(4),ST(4),SS(4),SDX(4),STX(4),SSX(4)
      READ (5,99)DX,CUA,NCL,M
   99 FORMAT(2F10.2,2I10)
C     ZERO OUT SUMMATIONS
    2 DO 1 I=1,4
      SD(I)=0.0
      ST(I)=0.0
      SS(I)=0.0
      SDX(I)=0.0
      STX(I)=0.0
    1 SSX(I)=0.0
      READ(5,100)ID,N
  100 FORMAT(I9,4X,I3)
      IF (ID.EQ.111111111)4,3
    3 WRITE(6,102)ID,N
  102 FORMAT(*1*,I10,10X,*N =*,I5,10X,*ALL DATA*)
      READ(5,101)(Y(I),I=1,N)
  101 FORMAT(16(F4.2,1X))
      JJ=0
      N1=N-1
      DO 50 I=1,N1
      IF(Y(I+1).LT.Y(I))51,50
   51 JJ=JJ+1
      X(JJ)=Y(I)
   50 CONTINUE
      DO 5 I=1,N
      DO 5 IJ=1,4
    5 SD(IJ)=SD(IJ)+Y(I)**IJ
      FN=N
      WRITE (6,103)
  103 FORMAT(//* STATISTICS OF RAW DATA*)
      CALL MOM2(SD,FN)
      CALL TREND2(Y,N,FN)
      J=1
      DO 6 I=1,N
      DO 6 IJ=1,4
    6 ST(IJ)=ST(IJ)+Y(I)**IJ
      WRITE(6,104)
  104 FORMAT(//* STATISTICS OF DATA WITH TREND LINE REMOVED*)
      CALL MOM2(ST,FN)
      CALL STD2(Y,N,FN)
      K=1
      DO 7 I=1,N
      DO 7 IJ=1,4
    7 SS(IJ)=SS(IJ)+Y(I)**IJ
      WRITE (6,105)
  105 FORMAT(//* STATISTICS OF STANDARDIZED DATA WITH TREND LINE  REMOVE
     1D*)
      CALL MOM2(SS,FN)
      WRITE (6,108)
  108 FORMAT( *1DISTRIBUTION OF ELEVATIONS USING ALL DATA*)
      CALL FREQD3(Y,N)
      WRITE (6,106)ID,JJ
```

```
  106 FORMAT(*1*,I10,10X,*N =*,I5,10X,*DOWNSTREAM DATA ONLY*)
      DO 8 I=1,JJ
      DO 8 IJ=1,4
    8 SDX(IJ)=SDX(IJ)+X(I)**IJ
      FJJ=JJ
      WRITE(6,103)
      CALL MOM2(SDX,FJJ)
      CALL TREND2(X,JJ,FJJ)
      DO 9 I=1,JJ
      DO 9 IJ=1,4
    9 STX(IJ)=STX(IJ)+X(I)**IJ
      WRITE(6,104)
      CALL MOM2(STX,FJJ)
      CALL STD2(X,JJ,FJJ)
      DO 10 I=1,JJ
      DO 10 IJ=1,4
   10 SSX(IJ)=SSX(IJ)+X(I)**IJ
      WRITE(6,105)
      CALL MOM2(SSX,FJJ)
      WRITE (6,107)
  107 FORMAT( *1DISTRIBUTION OF ELEVATIONS USING DOWNSTREAM DATA ONLY*)
      CALL FREQD3(X,JJ)
      GO TO 2
    4 CALL EXIT
      END


      SUBROUTINE MOM2(SUMX,FNX)
      DIMENSION XMO(4),XMM(4),SUMX(4)
      IF (FNX .GT. 3.1) GO TO 8049
      WRITE (6,100) FNX
  100 FORMAT (*0FNX = *,F3.1/)
      GO TO 8000
 8049 DO 8050 I=1,4
 8050 XMO(I)=SUMX(I)/FNX
      XMM(2)=XMO(2)-XMO(1)**2
      XMM(3)=XMO(3)-3.0*XMO(2)*XMO(1)+2.0*XMO(1)**3
      XMM(4)=XMO(4)-4.0*XMO(3)*XMO(1)+6.0*XMO(2)*XMO(1)**2-3.0*XMO(1)**4
      XMM(1)=0.0
      VAR=FNX*XMM(2)/(FNX-1.0)
      STD=SQRTF(VAR)
      WRITE OUTPUT TAPE 6,8054,XMO(1),VAR,STD
 8054 FORMAT(7HOMEAN =,E15.8,5X,10HVARIANCE =,E15.8,5X,20HSTANDARD DEVIA
     1TION =,E15.8)
      IF(ABSF(XMO(1))-.0001)8056,8056,8057
 8056 COV=999999.99
 8057 COV=STD/XMO(1)
      CON =FNX**2/((FNX-1.0)*(FNX-2.0))
      CSKEW=CON*XMM(3)/(VAR*STD)
      CKUR=CON*((FNX+1.0)*XMM(4)-3.0*(FNX-1.0)*XMM(2)**2)/((FNX-3.0)*VAR
     1**2)
      WRITE OUTPUT TAPE 6,8055,COV,CSKEW,CKUR
 8055 FORMAT(27H COEFFICIENT OF VARIATION =,E15.8,5X,10HSKEWNESS =,E15.8
     1,5X,8HEXCESS =,E15.8)
 8000 RETURN
      END
```

```
      SUBROUTINE TREND2(Y,N,FN)
      COMMON DX,CUA,NCL,M
      DIMENSION Y(1000)
      SY=0.0
      SXY=0.0
      SY2=0.0
      DO 20 I=1,N
      FI=I
      SY=SY+Y(I)
      SY2=SY2+Y(I)**2
   20 SXY=SXY+Y(I)*FI
      SX=FN*(FN+1.0)/2.0
      SX2=FN*(FN+1.0)*(2.*FN+1.0)/6.0
      W=FN*SXY-SX*SY
      U=FN*SX2-(SX)**2
      B=W/U
      A=(SY-B*SX)/FN
      WRITE(6,200)B,A
  200 FORMAT(///* TREND LINE IS Y =*,F8.3,*X + *,F8.3)
      DO 12 I=1,N
      FI=I
      Y1=B*FI+A
   12 Y(I)=Y(I)-Y1
      RETURN
      END


      SUBROUTINE STD2(Y,N,FN)
      COMMON DX,CUA,NCL,M
      DIMENSION Y(1000)
      SUM=0.0
      SUM2=0.0
      DO 1 I=1,N
    1 SUM=SUM+Y(I)
      DO 3 I=1,N
    3 SUM2=SUM2+Y(I)*Y(I)
      YBAR=SUM/FN
      S=SQRT((SUM2-(SUM**2)/FN)/(FN-1.0))
      DO 2 I=1,N
    2 Y(I)=(Y(I)-YBAR)/S
      RETURN
      END
```

```
      SUBROUTINE FREQD3(X,N)
      COMMON DX,CUA,NCL,M
      DIMENSION X(1000),FD(150),SUM(4)
C
C     THIS SUBROUTINE COMPUTES AND PRINTS A PROBABILITY DISTRIBUTION.
C     DATA CAN BE BOTH POSITIVE AND NEGATIVE
C
C     LIST OF VARIABLES
C     DX=CLASS WIDTH
C     CU=UPPER CLASS LIMIT
C     NCL=NUMBER OF CLASSES
C     M=SEQUENCE NUMBER OF FIRST CLASS CONTAINING POSITIVE NUMBERS
C     JX=SEQUENCE NUMBER OF CLASS
C     X=DATA
C     SUM(J)=SUM OF X-S TO JTH POWER
C
      CU=CUA
      DO 10 I=1,150
   10 FD(I)=0.0
C     PLACE DATA IN THE PROPER CLASS
      DO 40 I=1,N
      IF(X(I))21,22,23
   21 JX=X(I)/DX
      JX=M-1+JX
      IF(JX)31,31,24
   31 JX=1
      GO TO 24
   22 JX=M
      GO TO 24
   23 JX=X(I)/DX
      JX=M+JX
      IF(JX-NCL)24,24,32
   32 JX=NCL
   24 FD(JX)=FD(JX)+1.0
   40 CONTINUE
C     PRINT FREQ DISTRIBUTION-THE TITLE OF THE DISTRIBUTION MUST BE
C     PRINTED BEFORE CALLING THIS SUBROUTINE
      WRITE (6,110)
  110 FORMAT(5X,*CLASS*,10X,*PROB.*)
      FN=N
      PROB=FD(1)/FN
      WRITE(6,111)CU,PROB
  111 FORMAT(2X,*BELOW*,3X,F5.2,5X,F5.3)
      N1=NCL-1
      DO 30 I=2,N1
      CL=CU
      CU=CU+DX
      PROB=FD(I)/FN
   30 WRITE(6,112)CL,CU,PROB
  112 FORMAT(1X,F5.2,* TO *,F5.2,5X,F5.3)
      PROB=FD(NCL)/FN
      WRITE(6,113)CU,PROB
  113 FORMAT(2X,*ABOVE*,3X,F5.2,5X,F5.3)
C
      RETURN
      END
```